THE LICENSING PROTEIN ORC4 IS REQUIRED FOR POLAR BODY EXTRUSION DURING MURINE MEIOSIS

A DISSERTATION SUBMITTED TO THE GRADUATE DIVISION OF THE UNIVERSITY OF HAWAIʻI AT MĀNOA IN PARTIAL FULFILLMENT OF THE REQUIREMENTS FOR THE DEGREE OF

DOCTORAL OF PHILOSOPHY

IN

DEVELOPMENTAL AND REPRODUCTIVE BIOLOGY

DECEMBER 2017

By

Hieu Thi Nguyen

Dissertation Committee:
David M. Jameson, Ph.D., University Representative
W. Steven Ward, Ph.D., Chairperson
Monika Ward, Ph.D.
Yusuke Marikawa, Ph.D.
Yukiko Yamazaki, Ph.D.

Keywords: DNA replication, chromosomes, embryo development, ORC4, Polar body extrusion

DEDICATION

I dedicate this dissertation to my mom (My Thu), my dad (Nguyen Van Ngu), Tu, Lam, Gieng, Thao, Van, Hanh and to the rest of the members of the Nguyen family past and future, and especially to my husband (Nick James) whom provided me with guidance through the hardest times of graduate school.

ACKNOWLEDGEMENTS

I would firstly like to express my sincere gratitude to my advisor Dr. W. Steven Ward who has provided strong support of my dissertation and helped me through this process with patience, intellectual support, motivating me to take questions further, and his caring nature. There was never a time that I could not ask Dr. Ward for his assistance, whether for research or life questions, and for that I will forever be grateful. I could not image having a better advisor for my Ph.D. research.

I would also like to thank my dissertation committee: Dr. Monika Ward, Dr. Yusuke Marikawa, Dr. Yukiko Yamazaki, and Dr. David Jameson for their time, effort, insightful comments, and encouragement during my Ph.D. journey. I also thank Institute for Biogenesis Research (IBR) colleagues and friends in Hawaii for helping with techniques, useful discussions, and having fun for the last 5 years.

ABSTRACT

Six proteins, ORC1-6, make up the origin recognition complex (ORC) that initiates licensing of the DNA replication origin. We have previously shown that subunit ORC1, ORC2, ORC3, and ORC5 are localized between the separating maternal chromosomes at anaphase II just after fertilization. During investigation, we identified ORC4 as having an unexpected localization in the polar body wherein ORC4 surrounds one set of chromosomes during both female meiotic divisions. The ORC4 structure, or ORC4 cage as we have termed it, eventually is discarded in the polar bodies while the chromosome set that does not interact with ORC4 segregate into the oocyte. Interestingly, none of the other five ORC proteins were found to be involved in this structure. In Zygotic G1, ORC4 surrounds the nuclei of the polar bodies, but was not detectable in the pronuclei. When the zygote entered mitosis, ORC4 was only detected in the polar body. At this point, the ORC4 that was in the polar body also migrated into the nuclei, suggesting that ORC4 or an associated protein is modified during the first embryonic cell cycle to allow it to bind DNA. We experimentally forced oocytes to extrude sperm chromatin as a pseudo-polar body and found that under these conditions, the sperm chromatin did become enclosed in an ORC4 cage. Next, we attempted to prevent the formation of the ORC4 cage by injecting peptides that contained sequences of different ORC4 protein domains into metaphase II oocytes just before typical cage formation. Our rationale was that the ORC4 peptides would block protein-protein interactions required for cage formation. Two out of six tested peptides prevented the ORC4 cage formation and simultaneously inhibited polar body extrusion, resulting in the formation of two pronuclei that were retained in the oocyte. Our previous results demonstrated that recombinantly expressed ORC4, which contained histidine tag at the C terminus, could be utilized by oocytes to form the ORC4 cage at one set of chromosomes. Using immunocytochemistry (ICC), we were able to show that ORC4-His tags incorporated with endogenous ORC4. However, we could not use these tags to study on live cells because they required cell fixation to identify by ICC. To test the localization of ORC4 in live cells, we generate a fusion ORC4-eGFP and ORC4 labeling with FlAsH. These constructs were then used to synthesize mRNA and microinjected into MII oocyte. Through confocal fluorescence fluctuation spectroscopy (FFS) measurements, we are able to record the movement of ORC4 signals moving forward to form a cage or PB. This work provides the first evidence that the ORC4 plays a necessary role for polar body extrusion.

CITATIONS

Material from this dissertation has been published in the following form:

Nguyen H, James NG, Nguyen L, Nguyen TP, Vuong C, Ortega M, Jameson, DM, and Ward WS. (2017) Higher order oligomerization of the listening ORC4 protein is required for polar body extrusion in murine meiosis. J Cell Biochem. 118(9):2941-2949

Nguyen H, Ortega MA, Ko M, Marh J, and Ward WS. (2015) ORC4 Surrounds Extruded Chromatin in Female Meiosis. J Cell Biochem. 116(5):778-86

Ortega MA, **Nguyen H**, and Ward WS. (2016) ORC proteins in mammalian zygote. Cell Tissue Res. 63(1):195-200.

Gawecka JE, Boaz S, Kasperson K, **Nguyen H**, Evenson DP, and Ward WS. (2015) Luminal fluid of epididymis and vas deferens contributes to sperm chromatin fragmentation. Hum Reprod. 30(12):2725-36

Le Saux CJ, Davy P, Brampton C, Ahuja SS, Fauce S, Shivshankar P, **Nguyen H**, Ramaseshan M, Tressler R, Pirot Z, Harley CB, Allsopp R. (2013) A Novel Telomerase Activator Suppresses Lung Damage in a Murine Model of Idiopathic Pulmonary Fibrosis. PLoS ONE 8(3): e58423.

PRESENTATIONS

I) Oral presentations:

Nguyen H, Ortega A. M, Marh J, and Ward WS. ORC4 plays another role in polar body extrusion in mouse oocyte and zygote. Short talk to be delivered at the Society for the Study of Reproduction (SSR) meeting, Puerto Rico, USA. June 2015.

Nguyen H, Ortega A. M, Marh J, and Ward WS. The DNA licensing protein ORC4 that surrounded chromatin is required for polar body extrusion. An hour speech to be delivered at the Institute for Biogenesis Research (IBR) Annual seminar, the University of Hawaii School Of Medicine, USA. February 22, 2015.

Nguyen H, Nicholas James. M, Vuong C, Nguyen L, Nguyen PT, Ortega A. M, and Ward WS. The DNA licensing protein ORC4 that surrounded chromatin is required for polar body extrusion. Short talk to be delivered at Tester Symposium, The University of Hawaii at Manoa, USA. April 8, 2016.

Nguyen H, Nicholas James. M, Vuong C, Nguyen L, Nguyen PT, Ortega A. M, and Ward WS. The DNA licensing protein ORC4 is required for polar body extrusion. An hour speech to be delivered at American Association for Laboratory Animal Science (AALAS) meeting, the University of Hawaii School of Medicine, USA. April 27, 2016.

Nguyen H, Nicholas James. M, Vuong C, Nguyen L, Nguyen PT, Ortega A. M, and Ward WS. The DNA licensing protein ORC4 is required for polar body extrusion. Short talk to be delivered at Gordon Research Conference (GRC) meeting. Waterville Valley, New Hampshire, USA. August 2016.

II) Poster presentations:

Nguyen H, Ortega A. M, Marh J, and Ward WS. ORC4 plays another role in polar body extrusion in mouse oocyte and zygote. Poster presentation to be delivered at Biomedical Sciences and Health Disparities Symposium, the University of Hawaii School Of Medicine, USA. April 2014.

Nguyen H, Ortega A. M, Marh J, and Ward WS. ORC4 plays another role in polar body extrusion in mouse oocyte and zygote. Poster presentation to be delivered at American Society of Reproductive Medicine conference, Honolulu Convention Center, USA. October 2014.

Nguyen H, Ortega A. M, Marh J, and Ward WS. ORC4 plays another role in polar body extrusion in mouse oocyte and zygote. Poster presentation to be delivered at Biomedical Sciences and Health Disparities Symposium, the University of Hawaii School Of Medicine, USA. April 2015.

Nguyen H, Nicholas James. M, Vuong C, Nguyen L, Nguyen PT, Ortega A. M, and Ward WS. The DNA licensing protein ORC4 is required for polar body extrusion. Poster presentation to be delivered at Vietnamese Education Foundation conference (VEF) meeting, Washington DC, USA. March 2016.

Nguyen H, Nicholas James. M, Vuong C, Nguyen L, Nguyen PT, Ortega A. M, and Ward WS. The DNA licensing protein ORC4 is required for polar body extrusion. Poster presentation to be delivered at Biomedical Sciences and Health Disparities Symposium, the University of Hawaii School of Medicine, USA. April 2016.

Nguyen H, Nicholas James. M, Vuong C, Nguyen L, Nguyen PT, Ortega A. M, and Ward WS. The DNA licensing protein ORC4 is required for polar body extrusion. Poster presentation to be delivered at the Society of Study for Reproduction (SSR), San Diego, California, USA. July 2016.

TABLE OF CONTENTS

LIST OF TABLES

CHAPTER 3

CHAPTER 4

LIST OF FIGURES

CHAPTER 1

CHAPTER 2

CHAPTER 3

CHAPTER 4

CHAPTER 5

LIST OF ABBREVIATIONS

GV	Germinal vesicle
AI	Anaphase I
MI	Metaphase I
AII	Anaphase II
G1	Gap 1 Phase
G2	Gap 2 phase 2
S-phase	Synthesis phase
CDK	Cyclin dependent kinase
DAPI	4', 6-diamidino-2-phenylindole
eGFP	Enhanced green florescent protein
PMSG	Pregnant mare serum gonadotropin
hCG	Human chorionic gonadotropin
Amp	Ampicillin
Kan	Kanamycin
ICSI	Intra-cytoplasmic sperm injection
ICC	Immunocytochemistry
ORC	Origin recognition complex
PBE	Polar body extrusion
ORC4	Origin recognition complex subunit 4
PBS	Phosphate buffered saline
Pre-RC	Pre-recognition complex
RT	Room temperature
Sec	Seconds
BFA	Brefelin A
Arp2/3	Actin-related protein 2/3
Cdc42	Cell division cycle 42
FLIM	Fluorescent live image microscopy

CHAPTER 1. INTRODUCTION

1.1 DNA replication:

The process of cellular division is an essential event for all living organisms whereby a cell splits into identical cells. Production and replication of cellular components is required during this event as the daughter cell gains genetic identity. DNA is a molecule consisting of a double helix of two DNA strands composing of four types of nucleotide subunits. When DNA replicates, these strands are separated and each strand of the original DNA serves as a template for producing a replica strand. In eukaryotic cells, the mechanisms that control DNA replication evolved to contain stringent regulations thus ensuring the maintenance of genome integrity (1). DNA replication is initiated at origin sites (i.e., specific sites wherein DNA replication initiates) in the chromosomes which serve to recruit essential protein components for initiation of DNA replication. The first known complex to bind to DNA replication initiation sites is the origin recognition complex (ORC), which functions by binding to chromosome origin sites in an ATP-dependent manner. ORC consists of six subunits (ORC1, ORC2, ORC3, ORC4, ORC5, and ORC6) that play an essential role in the initiation of DNA replication by identifying the DNA sequences that will serve as origins. The ORC serves to bind an unlicensed origin and to recruit Cdc6 and Cdt1 to chromatin sites generating the pre-replication complex (pre-RC). This pre-RC allows the bound DNA site to transition from unlicensed to a licensed origin by loading of the Mcm2-7 double hexamer. The binding of Mcm2-7 destabilizes and releases ORC, Cdc6, and Cdt1 at that site in the interphase nucleus. The ORC, Cdc6, and Cdt1 can then be exposed to a new origin site on the chromosome (2). The pre-RC assembly is required for replication licensing of chromosomes prior to DNA synthesis during S phase of meiosis. While this simplified description can serve as a general model for the initiation of DNA replication, origin licensing is actually rather complex and can have variations depending on the cell type (Fig. 1.1). In Eukaryotic cells, DNA replication initiates at multiple origins distributed throughout the entire genome. This process is a necessary event in evolution allowing the genome to increase in complexity and size (3). The initial regulation of DNA replication occurs at two different time points. The first-time point is called “Origin licensing” in which proteins essential for replication assemble unto DNA and form pre-RC complexes. The second-time point is called “Origin firing” in which the DNA is involved in the subsequent activation of helicases. Both Origin licensing and firing occur separately during the cell cycle to ensure that these events occur once per cell

cycle (4). The origin licensing occurs at mitosis and G1 phase. The process begins with the loading of pre-RC, which consists of proteins ORC1-6, Cdc6, and Cdc1 bound to chromatin sites. It is then followed by the loading of the Mcm2-7 double hexamer. The binding of Mcm2-7 destabilizes and releases ORC, Cdc6, and Cdt1 at that site in the interphase nucleus (2). After the release, the following proteins Sld5, Psf1, Psf2, and Psf3 bind and form the GINS complex. In association with the pre-RC, this complex helps to recruit Mcm10 and Cdc45 which starts the process of DNA replication (4). In reproduction, the replication of the mammalian zygote's DNA is the recombination of parental genomes (5), and this ensures the offspring inheritance of both paternal and maternal genetic phenotypes. Each genome is replicated independently in its pronuclei before the maternal and paternal pronuclei fuse together to become a single nucleus. This occurs just before zygotic mitosis and prepares DNA for replication at different stages of chromatin configuration (6). Maternal DNA exits from MII stage, but paternal DNA exits at G_0 and exchanges its protamines for histones (6) (7). DNA replication in mouse is potentially a good model to use and help us understand mammalian zygotic replication, because of their similarities in cell development. More specifically, somatic cells initiate licensing with five different proteins called ORC1L, ORC2L, ORC3L, ORC4L and ORC5L (2). In the first step, ORC2L-5L bind to many origins in the genome, which is followed by ORC1L binding to this complex (8). This initiates the recruitment of Cdc6 and Cdt1 to form pre-RC. This primes it and licensing can begin once of Mcm2-7 complexes to pre-RC. DNA replication is initiated following the recruitment of Mcm10, Cdc45, and DNA polymerase-α, and DNA primase (9).

Not only is the process complex but initiation is also varied. Analysis of ORC licensing in the mouse zygote revealed that ORC2 was localized at the metaphase II spindle poles 1-2 hours after fertilization and then between the separating chromosomes at anaphase II (10). Four hours after activation, ORC2 was bound on DNA and remained until S phase. This showed that the licensed origins occur at early anaphase II and G1 after fertilization or egg activation, but may continue during G1 phase. Licensing occurs in an environment of low cyclin-dependent protein kinase (CDK) activity. Prevention of DNA replication depends on CDKs activity during S, G2 and M phases, resulting in inactivation of replication licensing factors changes in gene of licensing factors, and expression of a repressor.

In addition to their roles in DNA replication, each protein of the ORC also plays a unique role in development: ORC1 in embryo growth (11); ORC2 in cell cycle regulation (12); ORC3 in

neuronal maturation (13); ORC5 in uterine leiomyomas and malignant myeloid diseases (14); ORC6 in chromosome condensation and segregation in Drosophila (15); and ORC4 in Meier-Gorlin syndrome in human (16). During my research to investigate the localization of the ORCs during the two meiotic divisions in mouse oocytes and in the first cell cycle of the zygote, we found that ORC1, ORC3, and ORC5 has similar patterns of localization to ORC2 at anaphase II (17). We do not detect ORC6 at metaphase or anaphase until early G1 of the mouse zygote by immunocytochemistry.

1.2 Mitosis and Meiosis

1.2.1 Mitosis

Mitosis is a process that follows the completion of S phase and transition through G2 in which a single cell with replicated chromosomes divides equally to form two new daughter cells containing identical cellular components, such as the cell membrane, cytoplasm, and organelles. The major purpose of mitosis is to induce cellular growth, repair, and reproduction to ensure that old, worn-out cells are replaced by new ones (18). Mitosis is divided into five phases: interphase, prophase, metaphase, anaphase, and telophase. 1) During interphase, the DNA has already been replicated into two identical full sets of chromosomes called sister chromatids in preparation for cell division. At this stage, the chromosomes cannot be seen very clearly because they exist in the de-condensed form. 2) During prophase, the chromosomes condense into X-shaped structures and can be easily seen under a microscope. This makes them easier to separate in the following phase. At the same time, the mitotic spindle a structure made of microtubules binding to the chromosome's kinetochore on the centromere of each sister chromatid begins to form. At this phase, we also see that the membrane around the nucleus disappears, indicating that the nucleus is preparing to break down in preparation for metaphase. 3) During metaphase, the spindle attaches to all the chromosomes and aligns them neatly (from end to end) along the center of the cell. The two kinetochores of each chromosome are attached to microtubules from opposite spindle poles. Before this occurs during metaphase, the cell must pass through the spindle checkpoint. During this time, the cell uses a check-pathway to ensure that all chromosomes are on the metaphase plate and that their kinetochores are correctly attached to microtubules. If the chromosome is not properly aligned or attached, the cell will pause division until the problem is resolved. 4) During anaphase, the sister chromatids are separated from each other by the mitotic spindle pulling one chromatid to one pole and the other chromatid to the opposite pole. This

results in one chromosome per cell, which has maximum condensation to help with segregation and reformation of the nucleus. 5) During telophase, the mitotic spindle breaks down, the chromosomes begin to de-condense, and the nuclear membranes and nucleoli re-form. The cytokinesis undergoes to overlap with the final stage of mitosis. This cytokinesis divides the cytoplasm to form two daughter cells. Each daughter cell contains the same number chromosomes as the mother cell (19) (Fig. 1.2).

The mitotic process occurs under cell-cycle control of a protein M-Cdk. In addition to triggering chromosome condensation, this protein also induces the assembly of the mitotic spindle. This ensures that each sister chromatid in a pair is attached to the opposite pole of the spindle. M-Cdk also plays a role in animal cells by promoting the breakdown of the nuclear envelop and rearrangement of the actin cytokinesis and the Golgi apparatus (19).

1.2.2 Meiosis

Meiosis, a process to create genetic diversity, is a specialized type of cell division in which a single cell divides twice to produce four haploid cells. Each haploid cell contains half the original amount of genetic information, which is distinct from the parent cell. The genetic differences of four haploid cells arise by two mechanisms (19). (1) Each gamete contains either the maternal or paternal form of each chromosome. Because the choice of maternal and paternal occurs independently and randomly for each pair of homologs, each daughter cell has a unique mixture of maternal and paternal origin chromosomes. (2) The maternal and paternal forms of each chromosome have similar DNA sequences, but they are not identical, and they undergo genetic recombination during meiosis, a process called crossing over to produce new hydride forms of each chromosome. Meiosis can be divided into meiosis I, including interphase, prophase I, metaphase I, anaphase I, and telophase I and cytokenesis and meiosis II, including prophase II, metaphase II, anaphase II, and telophase II and cytokinesis (Fig. 1.3). The process of cell division in meiosis is similar to mitosis. However, meiosis has to reduce the number of chromosomes by half as many chromosomes as their diploid precursor cells. During prophase I, the chromosomes have replicated and consists of two sister chromatids joined tightly together. These homolog then pairs up side by side and undergoes genetic recombination process forming crossovers, occurring at metaphase I. This process plays an important role in producing off-spring with genetic differences from each other. Like mitosis, the pair of crossover chromosome are pulled apart by the meiotic spindle, pulling each chromosome to one pole of the cell and

complete telophase and cytokinesis. After meiotic I, meiotic II occurs rapidly without DNA replication (Fig. 1.3). This process is resemble to mitosis (19).

1.3 Polar body Extrusion

During early embryogenesis, primordial germ cells migrate to the developing gonad. These cells proliferate through mitotic cell division before initiating symmetric cell division during Meiosis I and II. Two rounds of meiotic division generate a large haploid oocyte, which maintains most of the maternal stores in addition to two very small cells called polar bodies (20). During the first meiotic division, homologous chromosomes are segregated, and genetic diversity is created by crossing over at the chiasmata (21). When homologous chromosome separation is triggered, the Meiotic I (MI) spindle has reached a subcortical location. This results in the first asymmetric division the extrusion of one set of chromosomes in the first polar body (PB1). The remaining chromosomes in the oocyte then form the metaphase II (MII) plate. Upon fertilization, meiosis triggers and a second asymmetric cell division that leads to the formation of the second polar body (PB2) (22). During the second meiotic division, sister chromatids are segregated in a form that resembles mitotic cell division (23). Mouse oocytes are one of the best models for studying and understanding this meiotic process (Fig. 1.4).

Polar body extrusion is dependent on the positioning of the metaphase plate near the oocyte membrane, or cortex. Following germinal vesicle breakdown (GVBD), the meiotic I chromosome-spindle is aligned in the center of the oocyte, but shortly afterwards, the chromosome-spindle initiates a migration towards the nearest cortical region of one side of the cortex. This process establishes cortical polarity by an actin-enriched domain surrounded with a myosin ring (24). Actin is essential for the survival of most cells, and the protein actin forms filaments that provide cells with the internal mechanical support and driving force needed for movement to the cortex. Actin polymerization also contributes to the internalization of membrane vesicles to control the composition of the cell membrane and the interface of the cell with the environment. Interaction of actin filaments with myosin proteins yields two types of movements. First, myosin generates force between actin filaments, producing contractions that pull up the rear of moving cells, pinch these cells in two, and induce a change in cellular shapes to form tissue. Second, myosin associated with subcellular organelles and macromolecular complexes of proteins and RNA moves these cargos along actin filaments over short distances (25). During Anaphase II, coordinated protrusion of the actin-enriched domain and constriction

of the myosin ring lead to extrusion of the first polar body which contains one set of homologous chromosomes (22, 26). Following the first polar body extrusion, the oocytes proceed into metaphase of meiosis II (MII) where an MII spindle is assembled near the first division site beneath the cortex. A cortical actomyocin domain similar to that in MI is again established above the spindle. The oocyte is now fully mature and arrested in this stage, awaiting fertilization. Both spindle positioning and cortical polarization rely on actin filaments but not microtubules. The mechanism of this cortical polarization is poorly understood. Deng et al (27) reported that the role of the GTPase Ran involves chromatin signaling to control cortical polarity during polar body extrusion in mouse. Ran (RAs-related Nuclear protein), GTP-binding nuclear protein Ran, is a small G protein essential for translocation of RNA and proteins through the nuclear pore complex. The Ran protein is also involved in the control of DNA synthesis and cell cycle progression (27). Dehapiot et al, 2013 reported that generating mutations in Ran has been shown to disrupt DNA synthesis. The GTP/GDP activates Ran via exchanging factor RCC1 that is bound to chromatin. This results in the generation of a Ran-GTP gradient concentrated on the meiotic chromosomes in mouse oocytes. Disruption of Ran-GTP in mouse blocks chromatin-induced cortical polarization (28) . Moreover, Halet et al, 2007 found that the mechanism of the asymmetric meiotic divisions generating one large oocyte and two small polar bodies involves Rac. Polarization of Rac activation occurs during spindle migration and is concentrated at the chromatin nearest to the cortex. Inhibition of Rac during oocyte maturation blocks pro-metaphase I and spindle migration. This inhibition also caused the spindle to detach from the cortex and prevented polar body extrusion in metaphase II arrested oocytes (29). In addition, Dehapiot et al, 2013 showed that polar body extrusion occurs via a functional Cdc42/N-WASP pathway. The activated Cdc42 (Cdc42-GTP) concentrates at restricted cortical regions on meiotic chromosomes. This activation form is required for recruitment of N-WASP and the formation of F-actin-rich extrusion during polar body formation. Inhibition of Cdc42 in MII oocytes caused the release of N-WASP into cytosol, a loss of the polarized F-actin cap, and a failure to form a second polar body. The inhibition of Cdc42 also results in defection of central spindle in activated MII oocytes (22). In mouse oocytes, activators Arp2/3, Cdc42 and Rac are essential for oocyte polarization, spindle formation and migration during meiosis (30). The Arp2/3 complex, upstream of N-WASP, has been shown to regulate actin nucleation and actin filament networks required for various cellular processes, including cell migration and adhesion,

endocytosis, and establishment of polarity during oocyte meiosis (30). Sun et al, 2011 demonstrated that disruption of Arp2/3 complex by a newly-found specific inhibitor CK666 as well as iRNA-Arpc2 and iRNA-Arpc2 resulted in the failure of asymmetric division, spindle migration, and the formation and completion of oocyte cytokinesis (31). Rohatgi et al, 1999 also demonstrated that the C terminus of N-WASP binds to Arp2/3 complex and stimulates its ability to nucleate actin polymerization therefore they contain a core mechanism that directly connects signal transduction pathways to the stimulation of actin polymerization (30). Moreover, Dynamin 2 is also involved in spindle migration and polar body extrusion (32). Dynamin 2, located at the cortex and around the spindles of the cell, is involved in actin recruitment and actin-based vesicle mobility. Wang and colleagues (32) showed that actin cap formation was disrupted using iRNA dynamin 2. In general, cortical structure is established depending on signals from chromosomes (Fig. 1.5). The cortical actomyosin cap is a structure necessary for polar body extrusion. When the spindle is located at the vicinity of the cortex, the chromatin-mediated Ran gradient activates N-WASP, the Arp2/3 complex, and dynamin 2 via Cdc42 at the cortex to nucleate actin polarization to suppress premature myosin II ring contraction and to drive cytoplasmic streaming keeping the chromosomes and spindle in place (24).

The result of two rounds of meiotic division generates two polar bodies. The first polar body contains two sets homologous chromosomes, whereas the second polar body contains a haploid set of chromatids. The two polar bodies are degraded shortly after formation, but they provide beneficial genetic information about the egg's genetic background. Therefore, many in vitro fertilization's clinics have used polar body biopsies in pre-implantation genetic diagnosis to detect genetic and chromosomes abnormalities, which may be inherited by the offspring (33). Moreover, the two polar bodies have also been applied in research to prevent transmission of inherited mitochondrial disease (34). In humans, the mutated mitochondrial DNA (mtDNA) may develop many severe diseases such as diabetes, heart disease, liver failure, infertility, deafness, blindness, and cancer, but the presentation and treatment of mtDNA are less efficient because of the genetic revolution, as the mutated mtDNA and normal mtDNA present on cell. The pre-implantation genetic diagnosis (PGD) can detect mutated mtDNA which may choose mtDNA with a low risk of mutation to transfer into the uterus (34). Another method is also applied on mouse model to eliminate mutated mtDNA using nuclear transfer. The first and the second polar bodies are used as donor genomes to replace the genome of the recipient oocytes which carried

mtDNA disease following two reasons. (1) The PB carries few mitochondrial, but it has the same genome as the oocyte. (2) The PB are also separated from the oocyte, which can be easier to manipulate. This method can reconstruct genetic of offspring from the first and the second PB (33).

We discovered that the DNA replication ORC4 forms a cage surrounding one set of chromosome which will be extruded in both polar bodies during anaphase and G1. This unique cage is necessary to help cells reduce the 4N meiotic genome to the haploid stage, which is necessary for normal fertilization. Understanding the role of ORC4 on PBE will provide us different aspects of PBE mechanism. Several mechanisms have been shown to be important for PBE, including Ran gradient, N-WASP (35), Cdc42 (22), Formin-2 (36), Arp2/3 (31), and actin polarization (37) and others, but none of these mechanisms is unique to PBE and to asymmetric cell division. In addition, our preliminary data showed that the ORC4 also surrounds extruded chromosomes in erythrocyte cells. This implies that ORC4 may play roles in other asymmetric cell divisions. In assisted reproductive technologies, it is possible that ORC4 deletion can cause the generation of aneuploidy. The PBE has clear significance on human assisted reproduction, but we cannot perform this study on human embryo because of ethical concerns. However, murine ORC4 protein has a high degree of homology with the human ORC4, so the mouse embryo may be a good model to study this aspect on human *in vitro* fertilization.

1.4 Project goals and hypotheses

In the initial work, we have shown that ORC4, a 45-kDa, is a member of origin recognition complex, localizes like a cage surrounding one set of chromosomes, which will extrude to become the first or second polar body, respectively, at both meiotic divisions. ORC4 remains in the polar body cytoplasm for a short time. Then, it translocates into the nucleus of the polar body during zygotic G1 and binds to the embryo chromatin at zygotic anaphase. This suggests that the function of ORC4 changes during zygotic G1 from a role in polar body segregation to its originally defined contribution to DNA synthesis initiation. Because ORC4 is associated with DNA replication (17), its asymmetrical positioning with the set of chromosomes that will be ejected suggests a potential relationship between the regulation of DNA synthesis and polar body emission. This is the first chromatin-associated protein that is asymmetrically associated with only the extruded set of chromosomes.

I therefore **hypothesized** that ORC4 forms a cage surrounding extruded chromosomes in both polar bodies during female meiosis. In chapter 2 of this dissertation I present the results obtained while testing this hypothesis. These data are published:

> **Nguyen H**, Ortega MA, Ko M, Marh J, and Ward WS. (2015) ORC4 Surrounds Extruded Chromatin in Female Meiosis. J Cell Biochem. 116(5):778-86

In this first page of the work, we found that ORC4 surrounds one set of chromosomes based on immunofluorescent localization. We next wanted to eliminate the possibility that our ORC4 antibodies cross reacted with a different protein. Our attempts to inhibit ORC4 production with siRNA failed, but this is not surprising since immunofluorescence demonstrated that even GV oocytes have a large store of ORC4 localized to just below the oolemma. We therefore generated His-tagged murine ORC4 protein to test whether His-ORC4 injected into oocytes could incorporate into the ORC4 cage. Since the ORC4 cage does not form until anaphase, we injected the His-ORC4 protein into MII oocytes and then activated the oocytes. Moreover, our previous work demonstrated that when PBE was disrupted with brefeldin, the ORC4 cage did not form. However, when sperm were induced to create ectopic sperm polar bodies by delayed activation, the ORC4 cage did form. These data suggested that the ORC4 cage was associated with PBE, but it was not clear whether it was required for PBE. To disrupt the ORC4 cage, we designed six 18-amino acid long peptides that represented parts of ORC4 that were on the exterior face of the protein, based on a predicted three-dimensional structure of ORC4. We reasoned that the ORC4 cage required some form of polymerization of ORC4, either with itself or with another protein(s), and the peptides that faced the exterior of the protein might disrupt the ORC4 cage by competitive binding with the polymerization sites.

I **hypothesized** that the higher order oligomerization of the licensing ORC4 protein is required for polar body extrusion in murine meiosis. Chapter 3 of this dissertation discusses the following results obtained during experimental analysis. These data are published:

> **Nguyen H**, James NG, Nguyen L, Nguyen TP, Vuong C, Ortega M, Jameson, DM, and Ward WS. (2017) Higher order oligomerization of the listening ORC4 protein is required for polar body extrusion in murine meiosis. J Cell Biochem. 118(9):2941-2949.

Our previous results demonstrated that recombinantly expressed ORC4, which contained histidine tag at C terminal of orc4 sequences, could be utilized by oocytes to form the ORC4 cage at one set of chromosomes or PB. Using ICC, we were able to show that ORC4-His tags

incorporated with endogenous ORC4. However, we could not use this tags to study on live cells because of fixed cell preparations. We wanted to test whether enhanced green fluorescent protein (eGFP) or FlAsH would have the best method for determining the self-associated of ORC4 protein to form a cage or polar body extrusion in living cells. Expanding upon this observation, we used mORC4 variant 1 plasmids (full length of orc4) to create two plasmids. (1) The first plasmid we created was ORC4 with GFP fused at the C-terminus, ORC4-GFP. (2) The second plasmid we created was a mutation of the ORC4 plasmid containing six-amino acids (Cys-Cys-Pro-Gly-Cys-Cys) that replaced six amino acids at 407- 412.The ORC4-GFP and ORC4 mutation plasmids were transcribed to mRNA and then microinjected into MII oocytes.

I **hypothesized** that spatial and temporal resolution of ORC4 fluorescent variants reveals structural requirements for maintaining higher order self-association and pronuclei entry. In **Chapter 4,** the results obtained from testing the hypothesis were presented. These results have not yet been published and the investigations are ongoing.

1.5 Contributions

Theoretical design: Hieu Nguyen

Contributed to writing: Hieu Nguyen

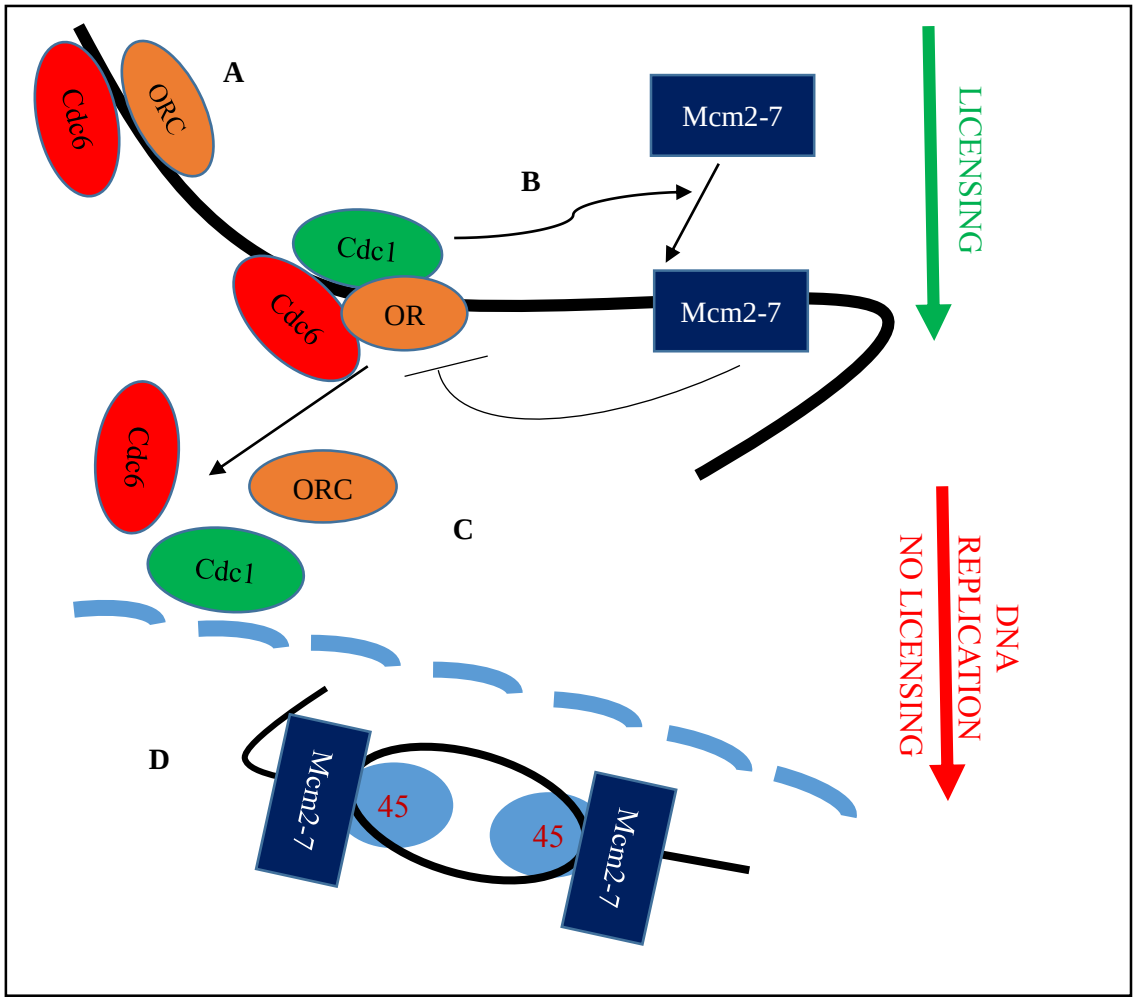

Figure 1.1: A model of replication licensing in live Caenorhabditis elegans embryos. The DNA licensing and replication occur during anaphase and S phase. (A) ORC complexes and cdc6 bind to unlicensed origin on DNA. (B) The origin is licensed by loading a Mcm2-7 double hexamer (M). (C) The ORC complexes, Cdc6, and Cdt1 are destabilized because of the binding of Mcm2-7. (D) The ORC complexes and Cdc6 are exported out of the interphase nucleus, whereas Cdc45 is recruited to Mcm2-7 when replication forks initiate.

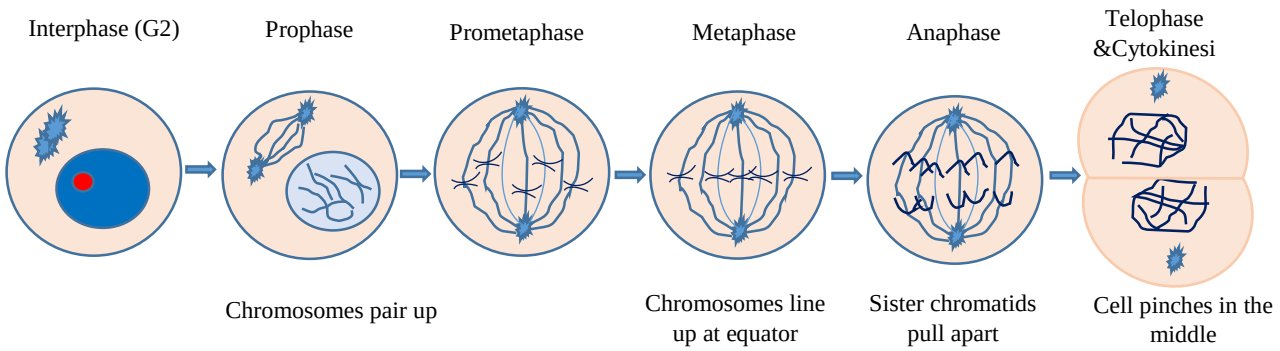

Figure 1.2: A diagram of mitosis stages: Prophase: the chromosomes pair up and each chromosome is consists of two identical sister chromatids. **Metaphase**: The chromosomes line up along the center of the cell. **Anaphase**: The sister chromatids pull apart by the mitotic spindle. **Telophase and cytokinesis**: Cell pinches in the middle to form two separate daughter cells each containing a full set of chromosomes.

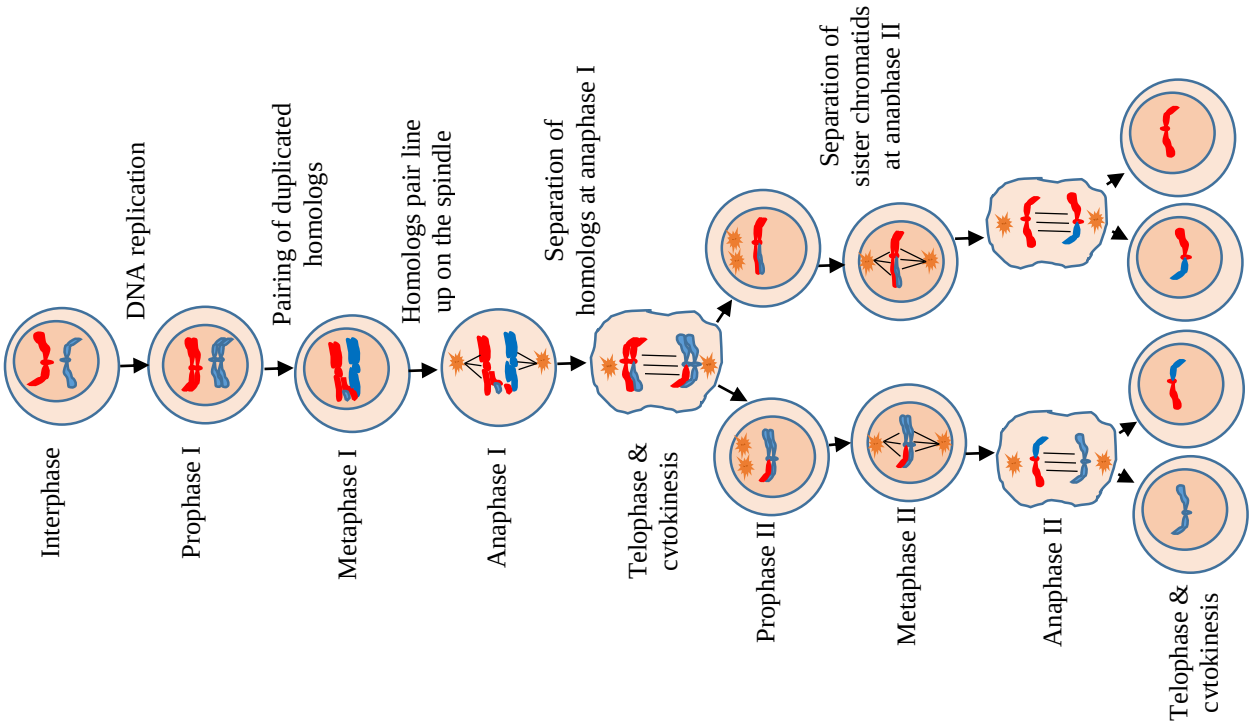

Figure 1.3: A diagram of meiotic stages. After DNA replication, cell is required to produce haploid gametes. The duplicated homologs pair up and are segregated into different daughter cells in meiosis I. At this stage, the homolog pairing leads to genetic recombination (crossing-over). The diploid cell enters the second meiotic II following with meiotic I. The final outcome is to produce four genetically different haploid.

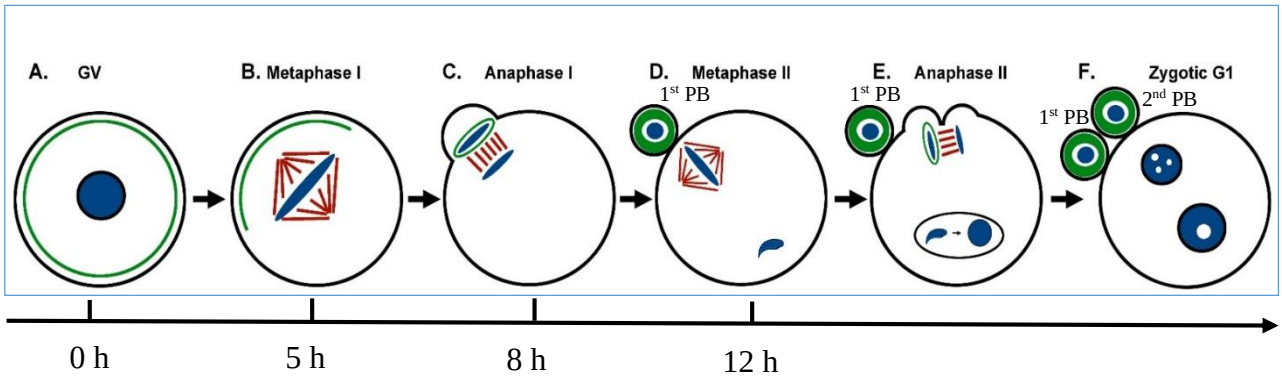

Figure 1.4: A model of meiotic maturation of a mouse oocyte. Meiotic maturation of a mouse oocyte. 5 hours after germinal vesicle breakdown (GVBD), the MI spindle is assembled and migrates towards one side of the cortex. Then, the MII spindle is formed beneath the cortex after a first polar body extrusion. Later, fertilization occurs to trigger meiosis II resulting a second polar body formation.

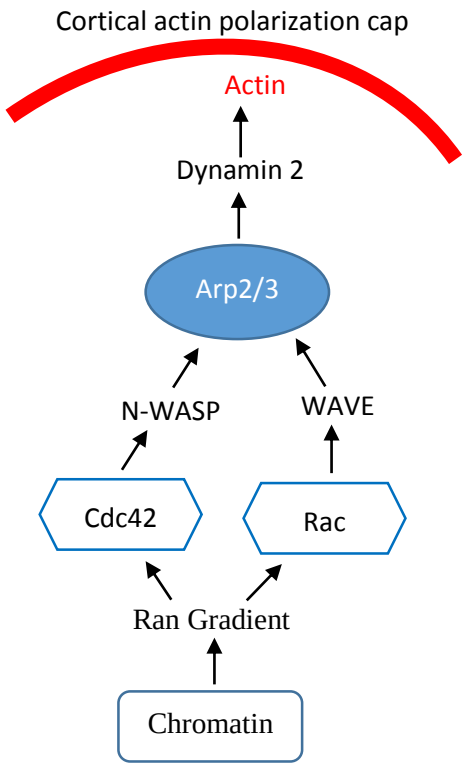

Figure 1.5: mechanism of polar body extrusion on mouse. The chromatin-mediated Ran^{GTP} gradient activates N-WASP and the Arp2/3 complex via Cdc42 at the cortex to nucleate actin polymerization.

CHAPTER 2. ORC4 SURROUND EXTRUDED CHROMATIN IN FEMALE MEIOSIS

2.1 Background

Origins are marked by ORC (origin recognition complex) proteins during the M-G1 transition to ensure all DNA is only replicated once during S-phase (38-41). This is the first step of a process called licensing that serves as a bookkeeping mechanism for the cell to monitor it progress in duplicating the chromosomes. The ORC is made up of six proteins, ORC1-6 ranging from 95 to 29 kD (NCBI database). The ORC complex proteins, which are found in all types of cells, from bacteria, in which DnaA is structurally and functionally homologous to ORC to mammals and are part of a group of proteins termed replication initiators (42). The six ORC proteins were originally discovered in yeast and named according to size, with ORC1 being the largest, and the subunits in other species names according to the homology with their yeast counterparts (43). More studies have been done on human ORC than mouse, but the close homology between these two species suggests that similar mechanisms are involved in both (44-46). Previous models for human ORC proposed that in actively dividing somatic mammalian cells, ORC2-5 remain associated with DNA replication origins throughout the cell cycle while ORC1 is recruited to the ORC complex only during G1 (38, 39, 47, 48). However, more recent work has suggested that it is possible all the ORC proteins are recruited to the origins during each cycle (49). Moreover, the DNA binding patterns of ORC to DNA vary during differentiation (50).

Licensing patterns during fertilization and subsequent early embryo development are particularly unique. Sonneville et al. (2) demonstrated that ORC2, one of the first ORC proteins to bind to naïve DNA origins in the C. elegans zygote, binds DNA only transiently, long enough to recruit the MCM7 helicases that represent the final step of licensing. We previously demonstrated that the maternal DNA is likely to be licensed before fertilization but the paternal DNA is licensed de novo in the embryo (10). We also identified unexpected roles for ORC2 in the first cell cycle. We demonstrated that ORC2 binds to the DNA in both pronuclei in late zygotic G1 as expected for its role in licensing. However, just after fertilization in anaphase II, ORC2 localized between the two separating sets of maternal chromosomes. While the original role of ORC proteins was to mark DNA replication origins, it has now been suggested that they also play more diverse roles that coordinate DNA replication with other cell division events (42, 51).

Here, we examined the roles of the other five ORC proteins in the first cell cycle. We found that ORC1, ORC3, and ORC5 had similar patterns of localization to ORC2 at anaphase II, but ORC6 and ORC4 exhibited surprisingly different patterns. In particular, the data suggest that ORC4 may play a role in polar body extrusion.

2.2 Materials and Methods

2.2.1 Animals

Eight-week old B6D2F1 (C57BL/6N X DBA/2) mice were used. Mice were obtained from National Cancer Institute (Raleigh, NC), and used at 8 – 12 weeks of age. Animal care and experimental protocols for handling and the treatment procedures were reviewed and approved by the Institutional Animal Care and Use Committee at the University of Hawai'i.

2.2.2 Preparation of Spermatozoa

Spermatozoa were obtained from B6D2F1 male mice (8- 12-week-old). A caudal epididymis was extracted, suspended in HEPES-CZB, and incubated for 45 minutes at 37°C under 5% CO_2 in air to allow the spermatozoa to disperse in the medium. The spermatozoa suspension for Intracytoplasmic sperm injection (ICSI) was mixed with PVP-saline (0.9% NaCl containing 12% w/v polyvinyl pyrolidone 360 kDa; ICN Biochemicals)

2.2.3 Preparation of Oocytes

To obtain mature metaphase II (MII) oocytes, mature female, 8 – 10-week-old, were induced to superovulate by injections of 5 IU PMSG and 5 IU hCG given 48h apart. Oviducts were removed 14 -15 hours after the injections of hCG and placed in CZB free Ca^{+2}. The cumulus cells were released from the oviducts into 0.1% bovine testicular hyaluronidase/CZB medium for 10 minutes to disperse cumulus cells. The cumulus-free oocytes were washed and kept in CZB at 37^o C under 5% CO_2 in air. These oocytes were used for immunocytochemistry and ICSI.

2.2.4 Intracytoplasmic Sperm Injection (ICSI)

ICSI was carried out as described by Kimura and Yanagimachi (52). ICSI was performed using Eppendorf Micromanipulators (Micromanipulator TransferMan, Eppendorf, Germany) with a piezoelectric actuator (PMM Controller, model PMAS-CT150; Prime Tech, Tsukuba, Japan). A single sperm head was sucked, tail first, into the injection pipette and moved back and forth until the head-mid piece junction (the neck) was at the opening of the injection pipette. The head was separated from the mid piece by applying one or more piezo pulses. An

oocyte was held to the holding pipette at the 9 o'clock position, and the sperm head was redrawn into the pipette and injected immediately into an oocyte. After discarding the mid piece and tail, the sperm head was redrawn into the pipette and injected immediately into an oocyte. After ICSI, oocytes were cultured in CZB at 37^{o} C under 5% CO_2 in air.

2.2.5 Preparation immature oocytes

To collect immature metaphase I and anaphase I oocytes, females were induced to super-ovulate by injections of 5 IU of PMSG. Oviducts were removed 48 hours after PMSG injections and placed in HEPES-CZB in a petri dish. The biggest follicles were break to release germinal vesicle stage (GV) oocytes. GV oocytes with surrounded cumulus cells were placed in CZB drops under mineral oil and cultured for 2 hours. After 2 hours, cumulus cells were removed by pipetting. The oocytes that underwent germinal vesicle breakdown were collected and cultured for 4 and 9 hours to reach metaphase I and anaphase I, respectively. Oocytes were then used for ICC.

2.2.6 Antibodies

Polyclonal goat anti-ORC1 (N-17, catalog no. sc-13231; Santa Cruz Biotechnology), polyclonal goat anti-ORC2 (C-18, catalog no. sc-13238; Santa Cruz Biotechnology), Polyclonal goat anti-ORC3 (K-17, catalog no. sc-21862; Santa Cruz Biotechnology), Polyclonal goat anti-ORC4 (C-15, catalog no. sc-19726; Santa Cruz Biotechnology), Polyclonal goat anti-ORC5 (T-15, catalog no. sc-19728; Santa Cruz Biotechnology), Polyclonal goat anti-ORC6 (2679C2b, catalog no. sc-81646; Santa Cruz Biotechnology) and monoclonal mouse-MCM7 (H-5, catalog no. sc-374403; Santa Cruz Biotechnology) primary antibodies were used. The Secondary antibodies included Alexa Fluor 488 rabbit anti-goat and Alexa Fluor 546 rabbit anti-mouse (Invitrogen, Grand Island, NY).

2.2.7 Immunocytochemistry (ICC)

Embryos were cultured in CZB until they reached the desired stage after ICSI, and fixed in 2% paraformaldehyde for 30 minutes at room temperature. After fixing, cells were washed three times with 0.1% Tween/PBS (PBSw) for 10 minutes. Cells were permeabilized in 0.5% Triton X-100 for 15 minutes, after that the cells were washed three times with PBSw contained 10% volume of 5% BSA. Cells were blocked with 5% BSA for 1 h at room temperature, then incubated in primary antibody at 1:50 dilution overnight at 4 o C. Again, the cells were washed three times with PBSw contained 10% volume of 5% BSA, then incubated in secondary antibody

at 1:1500 dilutions at room temperature for 45 minutes. Cells were again washed three times with PBSw contained 10% volume of 5% BSA then mounted with ProLong Gold antifade reagent with DAPI (catalog no. P-36931; Invitrogen). ICC was analyzed with an FV1000-IX81 confocal microscope from Olympus using Fluoview v. 2.1 software. For each stage of embryonic development, at least 20 embryos were examined by ICC, and the results were only reported if they were consistent in all embryos.

2.3 Results

2.3.1. ORC1, ORC3, ORC5 and ORC6 localize between the chromosomes at anaphase II similar to ORC2

We recently examined the expression pattern of ORC2 during the first two cell cycles of the mouse embryo. ORC2 localizes at the area between the separating chromosomes in anaphase II just after fertilization, then moves into the pronuclei where it becomes resistant to salt extraction, indicative of DNA binding (10). To complete the analysis of the expression patterns of all six ORC proteins, we examined ORC1, and ORC3-6 during the first cell cycle of the mouse zygote. We found that ORC1, ORC3, and ORC5 behave similarly to ORC2 in that they localized between the separating chromosomes at anaphase II (Fig. 2.1) and to the spindle poles zygotic metaphase. ORC1 surrounded the chromosomes at zygotic anaphase, but did not significantly overlap with the chromosomes, just as we had previously seen for ORC2 (10). This suggests that ORC1, ORC2, ORC3 and ORC5 may play structural roles during mitosis. ORC1, ORC3 and ORC5 could not be detected in the zygotoc pronuclei, however (data not shown). This differs from ORC2, which is easily detectable in the zygotic pronuclei at all stages (10). ORC6, on the other hand, was found only in the periphery of the nucleoli at all stages between zygotic G1 and 2-Cell G1 (Fig 2.2). During zygotic telephase, ORC6 was present around the nucleoli of the polar body, but was not detectable on the chromosomes (data not shown).

2.3.2 ORC4 surrounds the polar body chromatin at anaphase II

We were surprised to find that ORC4 behaves in a very different manner than the other ORC proteins. At anaphase II, ORC4 formed a ring, as visualized by confocal microscopy, around the set of chromosomes that would eventually segregate into the second polar body (Fig. 2.3B). Two different antibodies gave us the same result. This was a consistent finding in every zygote at anaphase II for which ORC4 staining was clear. ORC4 always surrounded the chromosomes that were nearest the zygotic membrane, and therefore presumed to be those

destined to segregate into the second polar body. This assumption is supported by the fact that in zygotic G1 after the polar body had been extruded, ORC4 was localized to the nuclear periphery of the polar body nucleus (Fig. 2.3L). ORC4 was not detectable in the pronuclei in the zygote at this stage. The decondensing sperm chromatin in the zygote after fertilization was initially not associated with ORC4 (Fig. 2.3B), but as decondensation progressed, ORC4 was found to be associated with sperm chromatin in a 3/12 zygotes (Fig. 3G, inset). At this point, ORC4 also bound to both sets of maternal chromatin, the one that would contribute to the maternal proncleus (Fig. 2.3G, arrow) and one that would be segregated into the polar body (Fig. 2.3G, arrowheads). The fact that so few zygotes had ORC4 bound to the sperm chromatin suggested that this binding seemed to be transient. Neither of the two pronuclei at zygotic G1 had detectable ORC4 (Fig. 2.3L).

2.3.3 ORC4 also surrounds first polar body chromatin

The results described above suggested that ORC4 may play a role in polar body extrusion. To test this, we examined whether ORC4 localized to the chromatin or perinuclear cytoplasm during the first division of female meiosis. We isolated oocytes at the germinal vesicle (GV) stage which is the point just before metaphase I, and cultured them for 8 to 9 hours until they reached metaphase I and anaphase I. At both the GV and GVBD (germinal vesicle breakdown) stages, ORC4 was present in a thin shell just below the cell membrane (Figs. 2.4A-D). At metaphase I, this layer became more diffuse (Figs. 2.4E and F). At anaphase I, ORC4 surrounded the polar body chromosomes, but not the oocyte chromosomes (Figs. 2.4G and H), just as in anaphase I (Fig. 2.3G). Because ORC4 seemed to play similar roles in anaphase I and anaphase II, we tested whether the same was true for ORC2. We found that ORC2 localized between the separating chromosomes of anaphase I, just as it does in anaphase II (10). Once the first polar body was extruded, at metaphase II, ORC4 surrounded the polar body nucleus (Figs. 4I and J). These data support the possibility that ORC4 plays a role in the extrusion of both polar bodies. Because the ring-like structures for the ORC4 complex were seen by confocal microscope sections, we tested whether the three dimensional structure was actually an ovoid sphere that completely enclosed the polar body chromatin. Figure 2.5 shows serial confocal sections of polar body chromatin in late anaphase I that clearly demonstrate that ORC4 forms a sphere that surrounds one set of chromosomes (Figs. 2.5C-G) but not the other (Figs. 2.5A-B).

2.4 Discussion

This work represents the completion of our study on the localization of the six ORC proteins during the first cell cycle of the mouse zygote. The data from this and our previous study (10) are summarized in Fig. 8.

2.4.1 ORC1-3, 5 and 6

In the zygote, perhaps more than in other cell types, ORC proteins seem to play roles in addition to their well-documented function in DNA replication. ORC1-3 and 5 all localize to the area between the separating chromosomes in anaphase II just after fertilization, and to the spindle poles in zygotic metaphase. It is not clear what role these four ORC proteins play in these structures, but it is intriguing that all four localize at both. A recent study has suggested that ORC2-5 assemble in the cytoplasm before being translocated to the nucleus (49). The co-localization of ORC1-3 and 5 at the mitotic spindle and between the separating chromosomes at anaphase II suggest that these are storage sites for the initial ORC complexes in close proximity to the newly forming nucleus. A similar localization of ORC2 between separating chromosomes at mitosis was previously noted in HeLa cells (53). Interestingly, ORC2 was also found at the spindle poles in the oocyte at metaphase I and between the separating chromosomes of anaphase I (10). Because both structures disappear and then re-establish in the second mitotic division of maternal meiosis, this suggests that ORC2 plays a role in mitosis other than licensing (54). We also demonstrated that ORC1 surrounded the separating chromosomes in zygotic metaphase (Fig 2.1) just as we had previously shown for ORC2 (10). ORC2 was constantly found around the DNA during telophase before it moved into the nucleus, and ORC1 seems to follow this pattern. We found that ORC6 was localized to the nucleoli of both pronuclei and the polar body, which agrees with studies in *Drosophila* (15) and human cells (39).

We were not able to visualize ORC1-3 or 5 co-localized with the DNA at any time. However, recent models for ORC suggest it might be more transiently associated with DNA than previously thought (43), so it is possible that we missed time points in which ORC subunits were associated with DNA. Our own data for ORC4 (discussed below) and ORC2 (discussed in ref. (10)) suggest that this is particularly true for the zygotes. Additionally, the fully formed ORC is a circular complex in which the six subunits are closely associated (55). This may provide steric hindrance from the other ORC subunits that prevents the antibodies from finding their epitopes.

2.4.2 ORC4 and the Polar Body

The most unexpected finding in our study was the association between ORC4 and the polar body chromatin. We have shown that ORC4 is part of a structure that surrounds the chromatin as an ovoid sphere that is destined to become the first and second polar bodies in both female meiotic divisions. It does not appear that any of the other ORC subunits are involved in this. ORC2 is located adjacent to the ORC4 sphere between the separating chromosomes in both divisions, and ORC1, ORC3, and ORC5 are similarly located there in anaphase II. This is consistent with the recent demonstration that in the first step of the formation of the ORC is the formation of the ORC2-5 complex, to which ORC4 binds before being transported into the nucleus (49). This suggests that ORC4 is capable of existing in the cytoplasm separately from the other ORC subunits as observed during polar body formation where an ORC4 sphere was present as soon as the chromosomes began to separate. In the first meiotic division, ORC4 was clearly present in a thin layer just below the oolemma then moved to the separating chromosomes in anaphase. In metaphase II, ORC4 was visible only in the cytoplasm of the first polar body, where it remained during anaphase II in those cases where the first polar body survived. These results raise the intriguing question that cytoplasmic ORC4 plays a role in the separation of the polar bodies from the oocyte.

Polar body extrusion is tightly coupled with the movement of the mitotic plate close to the oolemma during metaphase I and metaphase II in the maturing oocyte (56). A cortical domain forms over the spindle near the oolemma, and the mitotic plate is oriented perpendicular to the membrane (57, 58). Formin-2, a microfilament binding protein, directs the migration of the mitotic plate to the oolemma (59). A myosin ring helps to define the polar body cytoplasm, and the final emission (27). From these studies, it would appear that the chromatin that is destined to be extruded in the polar body is defined not by a molecular signal but by the orientation of the mitotic plate in the cytoplasm: the chromatin that is nearest to the oolemma will be extruded. The role that ORC4 may play in this, therefore, is not readily apparent. One possibility is that the ORC4 sphere stabilizes the polar body cytoplasm that will form the polar body. In support of this, it is interesting to note that the de-condensing sperm nucleus also forms a cone, similar to the polar body that is subsequently not extruded and reabsorbed back into the oocyte (27). It is not clear why the sperm cone is not extruded but the polar body cone is. We only found the ORC4 sphere around the polar body chromatin, and never around the sperm nucleus, and it is

possible that the ORC4 in the polar body cytoplasm plays a role in the eventual extrusion of the polar body cone. Another possibility is that it helps to segregate the polar body chromatin from nuclear factors that would activate genes inappropriately. We are currently testing whether ablation of ORC4 will prevent polar body formation.

2.4.3 ORC4 and Zygotic Chromatin

The role that ORC4 plays in polar body emission seems to be separate from its role in DNA replication. We have previously shown that the second polar body occasionally undergoes visible DNA replication (60) so it is likely that enough ORC4 binds to the DNA of the polar body to ensure at least partial licensing. We found that ORC4 undergoes two cytoplasmic to nuclear translocations in the first two embryonic cell cycles. We found three examples of ORC4 being associated with the sperm chromatin and both sets of separating maternal chromosomes at anaphase II (Fig. 2.3). In all three cases, ORC4 bound to the DNA of the chromatin at the same time in that it formed the ORC4 sphere that surrounded the chromosomes destined to become the polar body. Interestingly, at this point in fertilization, the maternal chromosomes are in anaphase and are not contained within a nuclear membrane therefore these chromosome sets are directly associated with the cytoplasm. It should be noted, the decondensing sperm nucleus also does not have a fully formed nuclear envelope (61). This association appeared to be short-lived, consistent with recent studies suggesting that the ORC complex forms transient structures in some cases (2, 43). Another possibility, mentioned above, is that ORC4 remains on the chromatin structures but is no longer available for antibody binding in the fully formed ORC. In this latter case, the data would suggest that ORC4 plays a role in establishing the fully formed ORC as observed in *S. pombe* (62).

The second obvious association of ORC4 with the chromatin was in late zygotic anaphase. The chromosomes became coated with ORC4 as they were separating from the mitotic plate (Fig. 2.6). This was preceded by a clear translocation of the cytoplasmic ORC4 in the second polar body into the nucleus just before zygotic metaphase (Figs. 2.6B and E). Interestingly, in those cases where the first polar body survived unit zygotic metaphase, ORC4 translocated into the nucleus of second polar body, but not the first (Fig. 2.6). In this case, the polar body DNA is sequestered inside nuclear envelope, but the zygotic anaphase chromosomes are not. The data suggest that the roles of ORC4 in the cytoplasm, within the nucleus, and in mitotic chromosomes are regulated both spatially and temporally. It is likely that the association

of ORC4 with the chromatin is related to licensing. ORC4 is the only ORC subunit that we have localized to the zygotic anaphase chromosomes. ORC1 (Fig 2.1) and ORC2 (10) surround the chromosomes but do not appear to bind directly to the DNA at this point. This raises the intriguing possibility that ORC4 directs the formation of ORC on the chromatin. Most current work on human ORC suggests that it is ORC1 that directs the binding of the final complex to DNA. However, in the yeast *S. pombe*, ORC4 has a unique domain that directs the binding of the ORC to the DNA (62). It is possible that mouse ORC4 plays a greater role in ORC binding to DNA that human ORC4.

2.4.4 Conclusions

Our data suggest that the ORC subunits play important roles in the mouse zygote other than licensing DNA replication origins. ORC1-3, 4 and 5 may all be involved in the separation of chromosomes during meiosis, and ORC4 may play a role in polar extrusion. Both functions are related to the proper segregation of the chromosomes just before and after fertilization.

2.5 Contributions

Research design: Hieu Nguyen and W. Steven Ward.

Conducted experiments: Hieu Nguyen, Michael A. Ortega, Myungjun Ko, Joel Marh.

Contributed to writing: Hieu Nguyen and W. Steven Ward

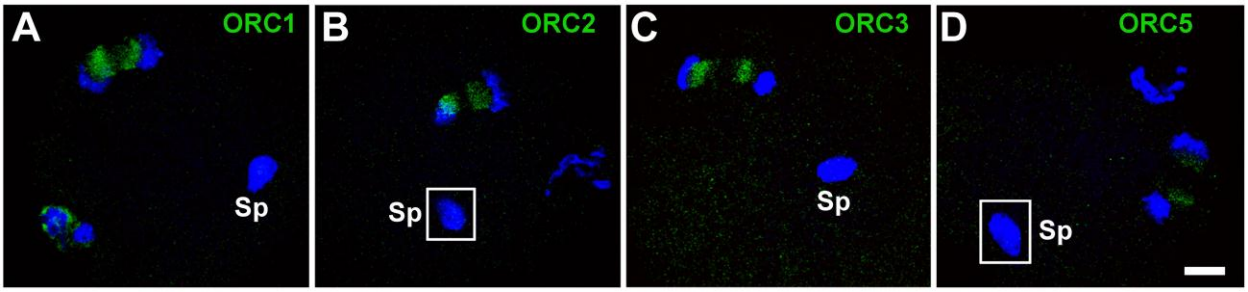

Figure 2.1. ORC1-3 and ORC5 are adjacent to the chromosomes at anaphase II. ICSI generated zygotes were fixed and stained for ORC1 (A), ORC2 (B), ORC3 (C) and ORC5 (D) and visualized by confocal microscopy. All four ORC subunits localize to the area between separating maternal chromosomes in anaphase II. The decondensing sperm nucleus had no visible staining in any oocyte. Insets in (B) and (D) represent areas in different confocal planes than the maternal chromatin. Sp, de-condensing sperm nucleus. All images are shown at the same magnification, bar = 10 μm.

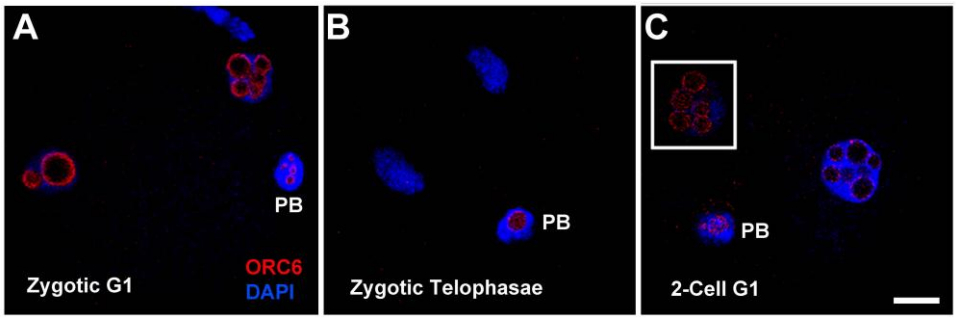

Figure 2.2. ORC6 in the first zygotic cell cycle. ICSI generated zygotes were fixed and stained for ORC6 at zygotic G1 (A), zygotic telophase (B), and 2-cell G1 (C) and visualized by confocal microscopy. Inset in (C) is the area in different confocal plane from the main image that contained the second nucleus. PB, second polar body. All images are shown at the same magnification, bar = 10 μm.

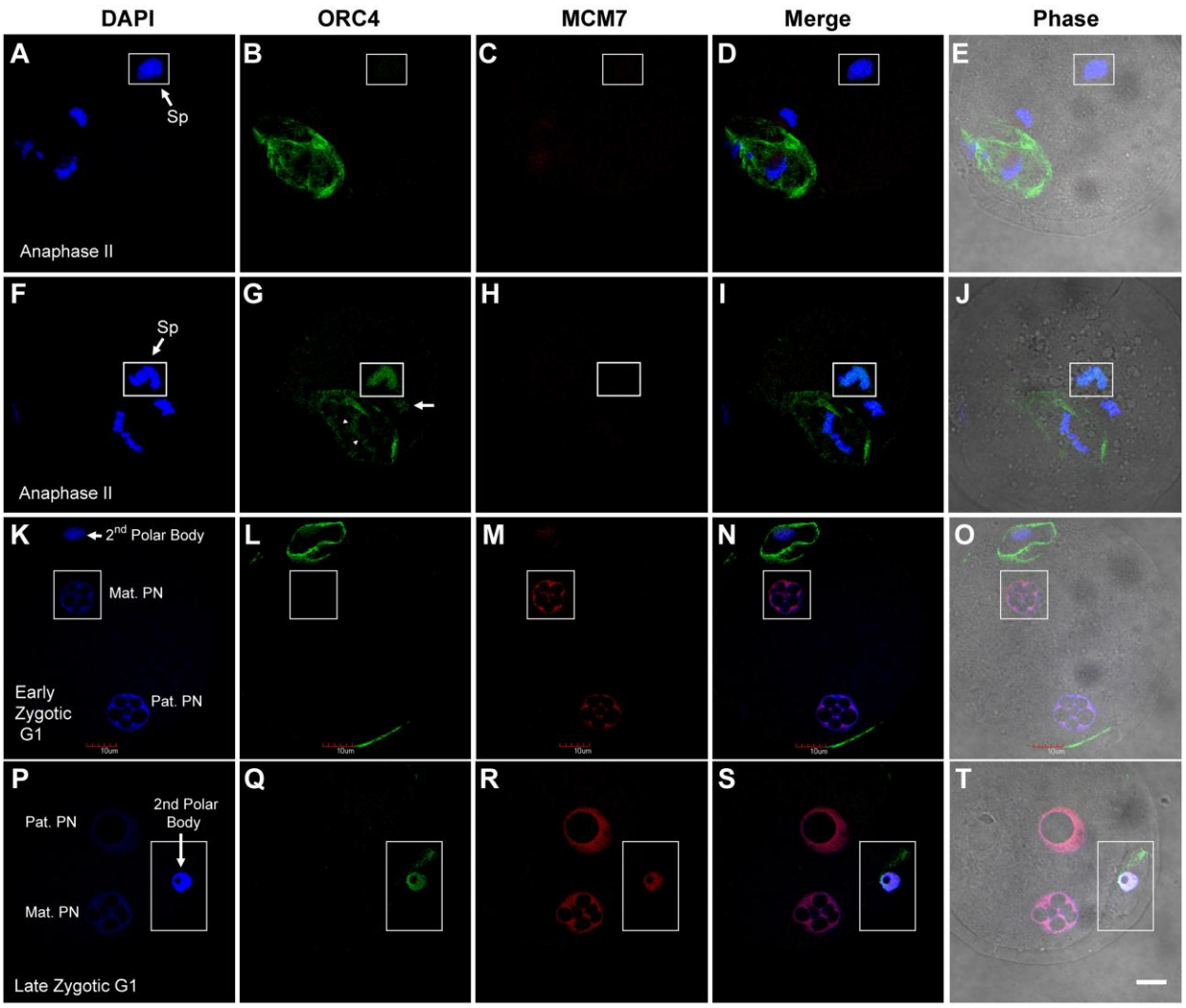

Figure 2.3. ORC4 surrounds the polar body chromatin during anaphase II. ICSI generated zygotes were fixed and stained for ORC4 at early anaphase II (A-J), early zygotic G1 (K-O) and late zygotic G1 (P-T), and visualized by confocal microscopy. ORC4 surrounds the chromatin that is closest to the oolemma (B and G), and the nucleus of the polar body at G1 (L). ORC4 was also visible in the decondensing sperm nucleus (G, inset) but not in a sperm that was less decondensed (B). ORC4 translocates to the nucleus of the second polar body in late G1 (Q). All insets show areas from different confocal planes than the rest of the figure. All images are shown at the same magnification, bar = 10 μm.

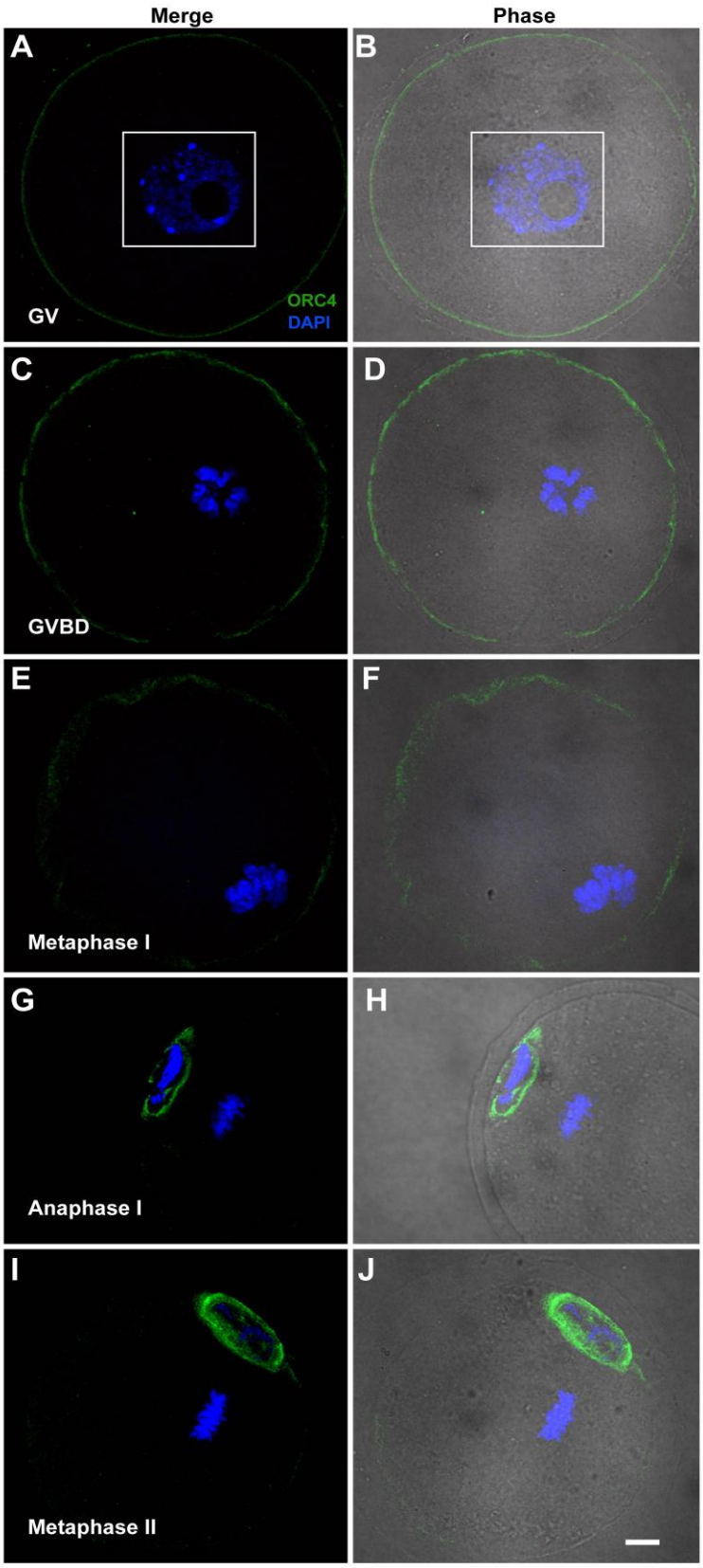

Figure 2.4. ORC4 in maturing oocytes. GV oocytes were isolated and cultured in vitro, then stained for ORC4 and visualized by confocal microscopy. GV (A and B), and GVBD oocytes (C and D) contained ORC4 in the cell periphery. Metaphase I oocytes (E and F) had more diffuse patterns of ORC4 distribution. At anaphase I (G and H), ORC4 surrounded the chromatin nearest the oolemma, and this was maintained in metaphase II (I and J). All images are shown at the same magnification, bar = 10 μm.

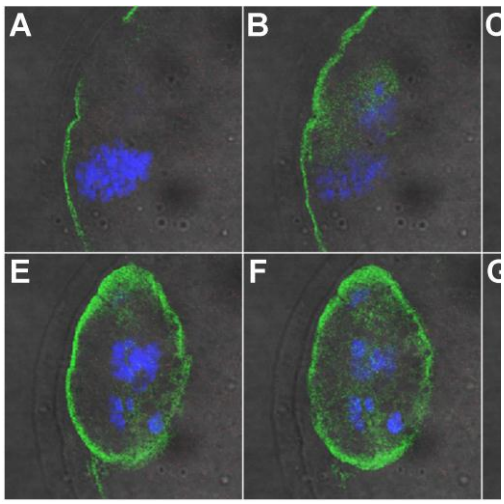

Figure 2.5. ORC4 forms an ovoid sphere around the polar body chromatin at anaphase. A GV oocyte was matured in vitro until it reached anaphase I and then fixed and stained for ORC4. The images are serial confocal planes starting at one chromosome set at anaphase I (A). The second set of chromosomes appears in (B). ORC4 begins as a small oval shape (B and C) then becomes a ring (D and E) then becomes a solid oval, again (F to G), indicating that ORC4 surrounds only one set of chromosomes as an ovoid sphere at anaphase I. All images are shown at the same magnification, bar = 10 μm.

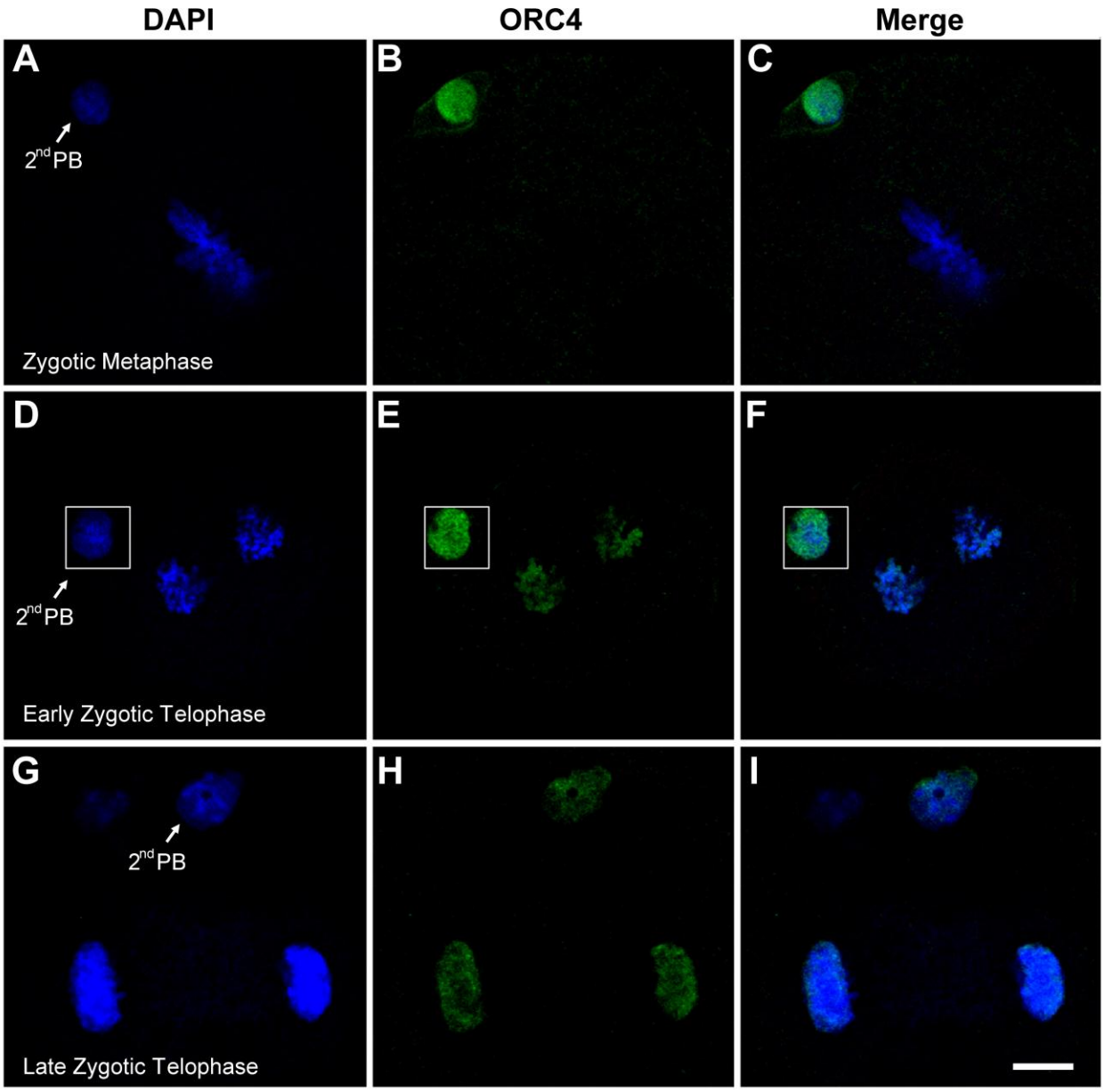

Figure 2.6. ORC4 translocates to the DNA during zygotic metaphase. ICSI generated zygotes were fixed and stained for ORC4 at different stages of zygotic metaphase. In zygotic metaphase, ORC4 is present in the nucleus of the second polar body (2^{nd} PB) but not on the zygotic metaphase chromosomes (A-C). By early telophase, both sets of chromosomes are coated with ORC4 (D-F), and this persists to late telophase (G-I). All images are shown at the same magnification, bar = 10 μm.

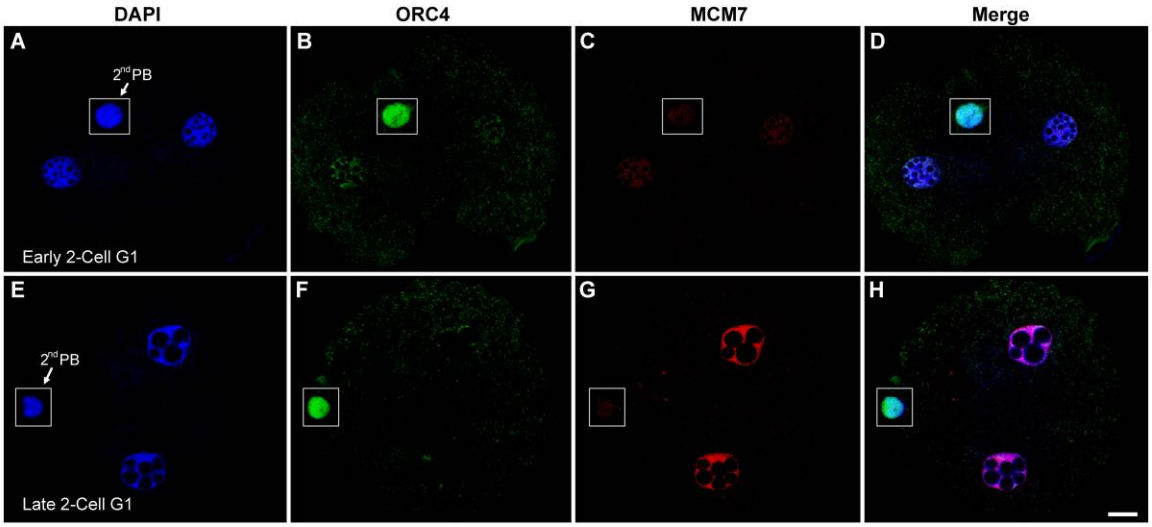

Figure 2.7. ORC4 is present in early G1 2-cell embryo nuclei. ICSI generated 2-cell G1 embryos were fixed and stained for ORC4 and MCM7. In early 2-cell G1, ORC4 is detectable in both nuclei (A-D). Later in G1, MCM-7 is visible in both pronuclei, but ORC4 is absent (E-H). The polar body (PB) retained ORC4, and did not accumulate MCM7. Insets show areas from different confocal planes than the rest of the figure. All images are shown at the same magnification, bar = 10 μm.

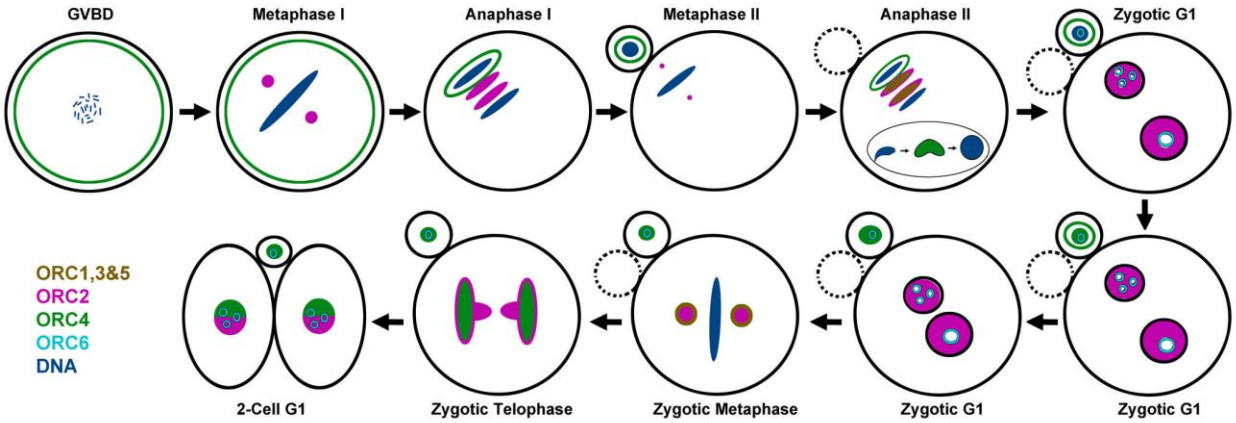

Figure 2.8. Diagram of ORC subunit distribution during the first two cell cycles of the mouse embryo. The distribution of the ORC subunits were determined in both this study and our previous publication for ORC2 (10).

CHAPTER 3. Higher Order Oligomerization of the Licensing ORC4 Protein is required for Polar Body Extrusion in Murine Meiosis

3.1 Introduction

During mammalian, female meiosis, developing oocytes reduce the number of chromosomes to 1N by ejecting them in two polar bodies in a process called polar body extrusion (PBE) (57, 63). Polar bodies arise from asymmetric divisions in which most of the cytoplasm is retained in the oocyte (Fig. 3.1-1). To achieve this unequal division, actin filaments associated with Rab11 containing vesicles reposition the germinal vesicle chromosome plate to the cortex of the oocyte before cytokinesis (64, 65). It is not clear how the set of chromosomes that will be ejected is chosen. In the first meiotic division, it could simply be the chromosomes that are more proximal to the cortex, but in the second division the metaphase plate is not originally aligned perpendicular to the oolema (56). Also, the oocyte is not simply discarding damaged DNA since it appears that the chromosomes in both the first or second polar body are intact because they can both be used to substitute for oocyte DNA and produce live pups in mice (66, 67).

We recently discovered an unexpected link between PBE and the DNA licensing protein ORC4 (17). ORC4 is one of six proteins that bind to DNA replication origins during the G1 stage of the cell cycle to establish the start sites for DNA synthesis (68). While the primary roles for the ORC proteins are well established to be in DNA replication, recent evidence suggests that many of them have additional functions that are related to the cell cycle, possibly to help coordinate the timing of DNA synthesis with other cellular processes (42, 51). While studying the roles of the six ORC proteins in early mammalian embryogenesis, we found that ORC4 forms a cage that surrounds the set of chromosomes that will be extruded during anaphase in both meiotic divisions of murine oogenesis, but not around the set of chromosomes that remains in the oocyte (17) (Fig.1-1C & E). We termed this structure the ORC4 cage. Here, we tested whether this ORC4 cage was required for PBE. We found that when the ORC4 cage formation was experimentally inhibited prior to second meiotic division, the oocytes did not extrude a second polar body.

3.2 Material and Methods

3.2.1 Animals

B6D2F1 mice obtained from National Cancer Institute (Raleigh, NC) were used as sperm and oocyte donors. Animal care and experimental protocols for handling and the treatment procedures were reviewed and approved by the Institutional Animal Care and Use Committee at the University of Hawai'i.

3.2.2 Preparation of Spermatozoa and Oocytes

Swim-up spermatozoa were prepared from the cauda epididymis as described (69). The spermatozoa suspension was used for intracytoplasmic sperm injection (ICSI). Metaphase II (MII) oocytes were prepared from superovulated mice as described previously (10). Briefly, oviducts were removed 14 -15 hours after the injections of hCG and and the cumulus cells were released from the oviducts into 0.1% bovine testicular hyaluronidase in CZB (70) medium for 10 minutes to disperse cumulus cells. The cumulus-free oocytes were washed and kept in CZB under a controlled environment (37ºC and 5% CO_2).

To collect immature metaphase I and anaphase I oocytes, females were induced to superovulate by injections of 5 IU of eCG, as described (71). Oviducts were removed 48 hours after eCG injection and placed in HEPES-CZB (52) medium in a petri dish at room temperature. Germinal vesicle (GV) oocytes with surrounding cumulus cells were placed in CZB drops under mineral oil and cultured for 2 hours. The oocytes that underwent germinal vesicle breakdown were collected and cultured for 4 and 9 hours to reach metaphase I and anaphase I, respectively.

3.2.3 Intracytoplasmic Sperm Injection (ICSI)

ICSI was carried out as described (52). Briefly, ICSI was performed using Eppendorf Micromanipulators (Micromanipulator TransferMan, Eppendorf, Germany) with a piezoelectric actuator (PMM Controller, model PMAS-CT150; Prime Tech, Tsukuba, Japan). After ICSI, oocytes were cultured in CZB at 37°C under 5% CO_2.

3.2.4 Immunocytochemistry (ICC)

ICC was performed as described previously (10). Embryos were cultured in CZB until they reached the desired stage after ICSI or parthenogenesis activation, and fixed in 2% paraformaldehyde for 30 minutes at room temperature. After fixing, cells were washed, blocked with 5% BSA for 1 h at room temperature, then incubated in primary antibody [Polyclonal goat

anti-ORC4 (L-15, catalog no. sc-19725 and C-15, catalog no. sc-19726; Santa Cruz Biotechnology, Santa Cruz, CA), monoclonal mouse anti-HIS (catalog no. CGAB-HIS-0050; Genecopoeia) at 1:50 dilution overnight at 4°C. The cells were washed again, then incubated in secondary antibody at 1:1500 dilutions at room temperature for 45 minutes. Cells were washed again, and mounted with ProLong Gold antifade reagent with DAPI (catalog no. P-36931; Invitrogen). Images were collected on an Olympus FV1000 confocal microscope using Fluoview v. 2.1 software.

3.2.5 mORC4-his tagged protein expression

Recombinant plasmid containing hexahistidine (His_6) tagged *mORC4* (Genecopiea), with a T7 promoter, was transformed into *E. coli* (BL21(DE3)pLysS; Inivtrogen) to induce protein overexpression. An individual colony of transformed *E. coli* plated on LB (containing 150 µg/mL ampicllin and 35 µg/mL chloramphenicol) was picked to inoculate a 50 mL overnight culture (TB + Amp and chloraphenicol). After 18 hours 5 mLs of the overnight culture were added to 1 L of Terrific Broth (+150 µg/mL ampicllin and 35 µg/mL chloramphenicol). Induction of ORC4-his expression was started when the OD_{600} reaches 0.8 – 1.0. To induce protein expression, bacteria was cooled to ~18°C, induced with 0.5 mM IPTG and incubated at room temp with 300 RPM shaking for 18h. Coomassie staining and western blot was used to monitor mORC4 expression and track purity of the sample following NiNTA and SEC purification.

3.2.6 Microinjection of mORC4-his tagged protein into oocyte

Recombinant mORC4-his_6 protein was microinjected into the cytoplasm of MII oocytes, as described (72). In all experiments 10 pl of 1.8 µg/ml of peptide was injected into each oocyte. Following microinjection for different times, the oocytes were incubated in CZB free calcium medium contained 10 mM of $SrCl_2$ with varying time points. ICC were used to visualize ORC4 cage formation and overlap between His_6 and endogenous ORC4 antibody staining.

3.2.7 Induction of ectopic sperm polar body formation

Sperm were washed with 0.5% SDS for 1 min, then heated at 95°C for 5 minutes, and finally incubated with Tx-100 for 10 minutes. A single SDS-washed, heated sperm head was picked up into the injection pipette. An oocyte will be held to the holding pipette at the 9 o'clock position and then rotated until it reaches the metaphase II spindle. The prepared sperm head was redrawn into the pipette and microinjected immediately into the oocyte in the vicinity of the

membrane. Following ICSI, injected oocytes were cultured in CZB 37°C under 5% CO_2 in air for three hours and then activated with $SrCl_2$ for desired time points (1h, 2h, and 3h, respectively). Phase microscopy and ICC were used to evaluate ORC4 cage formation.

3.2.8 Brefeldin treatment of oocytes and embryos

GV and MII oocytes were incubated with BFA (10 mM/ml) supplemented with 10 mM of $SrCl_2$ at desired time points (12h and 2h or 5h, respectively) to inhibit polar body formation. All oocytes and embryos were incubated at 37°C in a humidified atmosphere of 5% CO_2 in air.

3.2.9 Microinjection of Peptides into oocytes

Six different peptides were injected into the cytoplasm of MII oocytes 1 hr before activation. In all experiments, 10 pl of 2.0 µg/µl RNA was injected into each oocyte. Following microinjection, the oocytes were incubated in CZB free calcium medium containing 10 mM of $SrCl_2$ for one hour. Phase microscopy and ICC were used to evaluate polar body extrusion.

3.2.10 mORC4-his Fragment Deletions

mORC4-His_6 plasmids were used to create assembly vectors by using NdeI and AvaI enzymes. Fragmented inserts with desired sequences were amplified by PCR reactions. The primers used to amplify the desired sequences included homology arms at the beginning and at the end of the assembly vectors. Gibson assay was then used to join vector and fragmented inserts together and the Gibson products were electrophoresed into bacteria. Fragments were confirmed by single PCR colony and sequencing.

3.2.11 mRNA synthesis

Plasmids containing the mORC4- and ORC4-His_6 fragment mRNAs were linearized by an enzyme downstream of the *ORC4* gene. mMESSAGE mMACHINE T7 transcription kit from Thermo Scientific was used to synthesize mRNA ORC4-His_6 constructs. Agarose (1%) electrophoresis was used to confirm mRNA product, and isolate mRNA by Direct-zol RNA miniprep (Zymo Research). ORC4-His_6 mRNA constructs were stored at -20°C prior to microinjection.

3.2.12 Injection of mRNA

Each ORC4-His_6 mRNA constructs was used to microinject into the cytoplasm of MII oocytes. A microinjection volume of 10 pl/oocyte was used in all experiments. Following microinjection, the oocytes were incubated for 6 hours before parthenogenesis activation by

using CZB free calcium medium contained 10 mM of $SrCl_2$ for three hours. ICC and Phase microscopy were used to visualize polar body extrusion.

3.3 Results

3.3.1 HIS-ORC4 Integrates Into the ORC4 Cage.

We wished to first ascertain that the ORC4 cage, observed previously by our lab using ICC, truly contained ORC4 and was not an off-target effect of the antibodies (17). These experiments used two different commercial antibodies to identity ORC4 as a major component of the chromosome cage. We therefore made mouse ORC4 constructs with histidine tags for two variants of ORC4: variant 1 that represents the full length version of ORC4, 433 amino acids in length (*his-v1-mORC4*) and variant 2 (73) that encodes the first 121 amino acids of the full length ORC4 (*his-v2-mORC4*). Both *his-mORC4* transcripts were expressed in bacteria and the proteins isolated on a nickel column. The purified protein, HIS-v1-mORC4 was electrophoresed and assayed with the ORC4 antibody we used for ICC and with an antibody to the HIS tag (Fig.2). The antibody we used for ORC4 ICC recognized a protein at an identical molecular weight as the antiHis ab, verifying that our prior ICC experiments identified ORC4 (17).

We next attempted to inject each variant into MII oocytes to determine if they become incorporated into the ORC4 cage as it forms after MII oocytes are activated. Our previous results demonstrated that the ORC4 cage is formed after metaphase is completed, during anaphase of both meiotic divisions (17). Oocytes were injected with our recombinant ORC4-His_6 protein and stimulated to MII to examine if the His protein intergrates with native ORC4 in the cage structure. The full length, HIS-v1-ORC4 proved to be too difficult to solubilize for injections, but the smaller variant 2, HIS-v2-ORC4, could be injected. When oocytes were subsequently activated them with $SrCl_2$ then stained with an antibody to the HIS-tag, we found that HIS-v2-ORC4 did incorporate into the ORC4 cage (Fig. 3.3). This supported the conclusion that the DNA replication associated protein was part of the ORC4 cage that extruded chromosomes from the cytoplasm.

3.3.2 A New ORC4 Cage Is Formed when the Oocyte Expels Sperm Chromatin

The recruitment of ORC4-His_6 to chromosomes during anaphase in meiosis suggests that ORC4 has a novel function associated with PBE. If so, the ORC4 cage should not be formed when PBE was inhibited, and, conversely, a new ORC4 cage should form if chromatin that was normally retained in the zygote was extruded. When we inhibited PBE with brefeldin A (BFA)

(20) (Fig. 3.4) or cytochalasin B (Fig. 3.5), parthenogenetically activated oocytes divided into two equal sized cells and no ORC4 cage was formed. This suggested that the ORC4 cage was dependent on PBE. We then tested whether a second ORC4 cage formed if sperm chromatin was induced to be expelled at metaphase II. During normal fertilization the de-condensing sperm nucleus forms a "sperm cone" in which the oolemma around the sperm nucleus blebs outward in a manner similar to the initial stages of PBE (74,75)(Fig. 3.1-1E). This blebbing is normally resolved and the sperm chromatin is reabsorbed into the zygote. We never found an ORC4 cage around the sperm chromatin in normal fertilization (17) (Fig. 3.6A). The sperm cone, however, can be experimentally induced to form a complete vesicle that is ejected from the oocyte as an ectopic sperm pseudo polar body, similar to PBE (Fig. 3.6B&C). This occurs when sperm are washed with an ionic detergent and then injected into oocytes. These sperm fail to activate the oocyte to complete its second meiotic division, but do begin to de-condense. When these fertilized oocytes are allowed to incubate for 3 hrs, then activated with $SrCl_2$, the sperm chromatin is expelled as in a vesicle that resembles a polar body (26). We repeated this experiment and found that a new ORC4 cage formed around the extruded sperm chromatin. ORC4 first localized at the oolemma near the decondensing sperm chromatin (Fig. 3.6B), then an ORC4 cage formed around the sperm chromatin (Fig. 3.6C). At G1, the sperm chromatin has been ejected as a pseudo polar body with an ORC4 cage (Fig. 3.6D). The ORC4 cage formed normally around the maternal chromatin that was extruded in the polar body in these oocytes. These data suggested that a second ORC4 cage forms around sperm chromatin when it is induced to be expelled by experimental manipulation.

3.3.3 Disruption of the ORC4 Cage by ORC4 Peptides Prevents PBE

The experiments above suggested that ORC4 cage formation is disrupted when PBE is inhibited, and that a new ORC4 cage can be induced to form around sperm chromatin when it is extruded from the oocyte. This indicates that the ORC4 cage is associated with PBE, but does not prove it is necessary for PBE. We first attempted to test whether the ORC4 cage was required for PBE by disrupting it with siRNA to *Orc4* but this had no effect, presumably because there was sufficient ORC4 protein present in the GV oocyte to construct the cage (17). Therefore, we disrupted the cage more directly using ORC4 peptides. We reasoned that the ORC4 cage required oligomerization, either ORC4 self-association or ORC4 interacting with another protein. We generated a putative three-dimensional structure for the full-length mouse ORC4 protein

using Phyre II software (Fig. 3.7) and identified six, 18 amino acid peptides that represented sequences of the protein that faced external surfaces that could be involved in protein-protein interactions to form polymers. The six peptides are shown in relation to the full length, v1-ORC4 protein in Fig. 3.7. We note that no soluble peptides could be identified for one section of the ORC4 protein, between amino acids 210 and 340.

Individual peptides were synthesized and injected into MII oocytes 1 hr before parthenogenetic activation. Four of the peptides that we injected, 6, 9, 14 and 16, had no effect on either the ORC4 cage or the production of the polar body (Table 3.1, Fig. 3.9), and were used as negative control samples in progressive experiments. Peptides 1 and 10, however, disrupted the ORC4 cage in anaphase II (Fig. 3.9B) or not to form at all (Fig. 3.9C) in many of the oocytes injected. Injection of peptides 1 and 10 caused the parthenogenetically activated oocytes to produce two pronuclei (2 PN) within the oocyte rather than ejecting half of the chromosomes in a polar body in 27% and 13% of the oocytes, respectively (Table 3.1, Fig. 3.9D). Peptide 1 proved to be much less soluble than peptide 10, so we were not able to inject as many oocytes with peptide 1, even though it appeared to be more effective. In all cases of 2 PN oocytes, there was no evidence of the ORC4 cage (Fig. 3.9D). When the ORC4 cage was disrupted by peptide 1 or peptide 10 injection, DNA synthesis still occurred, demonstrating that only one function of ORC4 was inhibited. These data suggested that the binding sites for ORC4 polymerization are close to the amino acid sequences that were in peptides 1 and 10.

3.3.4 Disruption of the ORC4 Cage with ORC4 Fragments

Injecting small, ORC4 peptides proved to be limiting because of solubilization problems. The solutions were viscous and sticky causing many of the injected oocytes to die. Furthermore, it was possible that the sites on the ORC4 protein that were responsible for polymerization to form the ORC4 cage were larger than 18 amino acids, and larger peptides would have been more difficult to inject. We therefore created five ORC4 fragments that contained the gene sequences for ORC4 fragments that were 36 to 55 amino acids in length that included those of peptides 1, 10 and 16 (Table 3.2). This was done by deletion mutation of the original murine *v1-ORC4* plasmid. The ORC4 fragments were inserted into expression plasmids and mRNA for each was synthesized. We also created mRNA for the v2-ORC4. To test our ability to inject intact mRNA into oocytes and that oocytes would generate protein from our mRNA, we first prepared and injected mRNA for GFP into MII oocytes and examined the oocytes by fluorescent microscopy

before and after parthenogentic activation. All oocytes fluoresced green indicating that MII oocytes are capable of synthesizing protein from mRNA. Protein synthesis was evident before and after activation, and continued for up to 3 hrs after activation.

We next injected mRNA for the five ORC4 fragments we had created, and for the v2-ORC4 variant into MII oocytes, and then parthenogenetically activated them. We found that v2-ORC4, which was found to be incorporated into the ORC4 cage when injected as recombinant protein, caused the oocyte to produce two pronuclei instead of a polar body in 25.1% of oocytes (Table 3.2). Similar percentages of 2 PN oocytes resulted from the injection of the four ORC4 fragment mRNAs that contained peptides 1 and 10. Only 3.9% of the oocytes injected with the control ORC4 fragment mRNA that contained peptide 16 progressed to 2PN. These differences were highly statistically significant (Tables 3.1&3.2). As with the peptide injections, in all cases of 2PN oocytes, there was no visible ORC4 cage.

3.4 Discussion

Our previous work demonstrated that ORC4 forms a cage around the ejected chromosomes in both meiotic divisions (17). Here, we provide several lines of evidence to support our hypothesis that the ORC4 cage is required for polar body extrusion (PBE). First, when parthenogentically activated oocytes are induced to divide into two equal sized cells, rather than forming a polar body (Fig. 1-1B & D, Fig. 3.1-2), the ORC4 cage is no longer formed. More convincingly, when the sperm chromatin is induced to be extruded as pseudo-polar body, a new ORC4 cage is formed (Fig. 3.1-3E & F). Normally, the sperm chromatin which remains in the oocyte is not associated with an ORC4 cage (Fig. 3.1-3). The fact that the ORC4 cage forms around the sperm chromatin suggests that it is clearly associated with extrusion of the chromatin.

The most direct evidence that the ORC4 cage is required for PBE is that ORC4 peptides and ORC4 fragments that were injected into the oocyte prevented the formation of the ORC4 cage, and when this happened both maternal sets of chromatin were retained within the oocyte, rather than one being ejected in a polar body (Fig. 3.9, Tables 3.1&3.2). As discussed above, the premise for this experiment was that peptide fragments that contained ORC4 sequences would inhibit the polymerization of ORC4 that is required to form the cage. We focused on MII oocytes rather than GVBD oocytes because the ORC4 cage does not form until after activation, so we could inject the peptides before the cage was formed. MII oocytes are also stronger and survive injection more easily. The peptide sequences that were chosen were based on a putative ORC4

3D structure (Fig. 3.7), but the results do not depend on the accuracy of this particular structure. We found that of the six peptides we tested, only two prevented ORC4 formation and caused the oocyte to retain both sets of chromatin producing two pronuclei (2 PN) rather than the normal one pronucleus and one polar body (1PN + PB) (Table 3.1). Because the other four peptides were also ORC4 sequences, they served as good controls for this experiment. These experiments specifically targeted the ORC4 cage, and this disrupted PBE, demonstrating that the ORC4 cage is required for PBE.

Two areas of ORC4 appeared to be involved in oligomerization, as judged by their ability to prevent ORC4 cage formation, the sequences defined by peptides 1 and 10 (Fig. 3.8). Neither peptide, nor the larger versions of these sequences that were injected as mRNA, were able to inhibit PBE all of the time, but the percentages of 2PN parthenogenetically activated oocytes that were formed (13% to 27%) were all very statistically different from controls (Tables 3.1 & 3.2). There are many possible reasons for this, including the stability of the peptides injected, the limit on the amount of peptide or mRNA that could be injected, and the efficiency of the peptides and ORC4 fragments to inhibit the cage. When we attempted to lengthen the ORC4 domain that inhibited cage formation with mRNA, we did not increase the percentage of oocytes that developed to 2 PN for peptide 1. For peptide 10, however, increasing the number of amino acids from 18 to 46 increased the percentage of 2 PN oocytes from 13% to 25%, a statistically significant increase ($p = 0.005$, Table 3.1 & 3.2). This suggests that at least one of the putative polymerization domains for ORC4 is larger than 18 AA. It is clear that of the six areas of the ORC4 protein that were injected, two of them were able to prevent ORC4 cage formation and in every instance that the cage was inhibited, so was PBE.

One interesting apparent paradox in the data may provide some insight into how the ORC4 cage is formed. One would expect that the ORC4 cage which is a three dimensional sphere (17), would include not only simple polymerization but some kind of branching to link the polymers. We showed that HIS-v2-ORC4 becomes part of the ORC4 cage (Fig. 3.3) but excessive amounts of this ORC4 variant can also prevent its formation (Table 3.2). One explanation for these results is that v2-ORC4 plays a role in branching to form the cage, but too much will prevent the cage from forming by recruiting all the available full length v1-ORC4 for branching instead of polymerization.

The more usual function of ORC4 is to participate in the ORC complex that identifies origins of replication (14, 41). ORC4 is part of the core that forms the ORC (48), and it binds directly to DNA and can form non-canonical structures with DNA (16, 76). ORC4 exists in the cytoplasm before it forms the ORC (48), so its presence in the cytoplasm of the oocyte (17) is consistent with its behavior in somatic cells. It is possible that the sequestration of ORC4 in the ORC4 cage also functions to delay DNA replication during the two mitotic divisions of the meiotic oocyte. There is also an accrual of ORC1, ORC2, ORC3 and ORC5 in the area between the separating chromosomes at anaphase I and anaphase II in oogenesis (10, 17) that may serve a similar function. The ability of ORC4 to bind directly to DNA, itself, may contribute to the formation of the ORC4 cage that coats the extruded chromatin. It is also possible that ORC4 cage formation participates in asymmetric divisions of other cell types and in the extrusion of chromatin from developing erythroblasts (77, 78).

This work demonstrates that the DNA licensing protein ORC4 forms a large cytoplasmic structure, the ORC4 cage that is required for PBE. This is the first example of a functional structure formed by the ORC proteins. Current work is focused on understanding the mechanisms of how the ORC4 cage coordinates PBE and DNA replication.

3.5 Contributions

Research design: Hieu Nguyen, Nicholas Grant James, David M. Jameson, Michael A. Ortega, and W. Steven Ward.

Conducted experiments: Hieu Nguyen, Nicholas G. James, Lynn Nguyen, Thien P. Nguyen, and Cindy Vuong.

Contributed to writing: Hieu Nguyen, Nicholas G. James and W. Steven Ward.

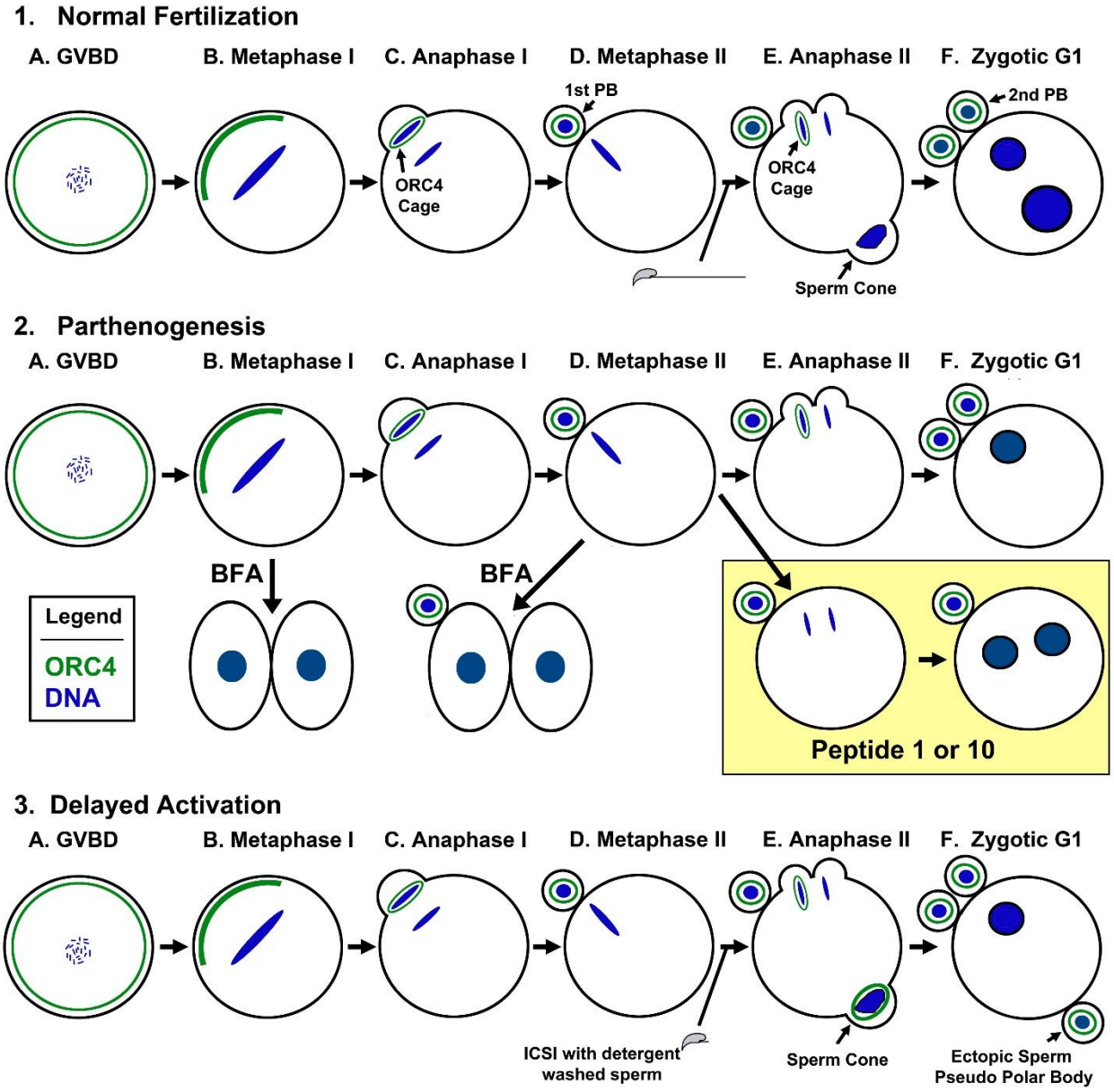

Figure 3.1: Diagram of ORC4 in mouse early embryonic development. (1) Normal fertilization: ORC4 is present in the cortex of GVBD oocytes (A), and coalesces near the chromosomes in metaphase I (B). ORC4 forms a cage around the chromosomes that are ejected in the first (C, D) and second (E, F) polar bodies. (E) The sperm chromatin forms a "sperm cone" which can be thought of as an abortive polar body that is reabsorbed by the oocyte by G1. (2) parthenogenesis: ORC4 behaves the same way in parthenogenetically activated oocytes. BFA treatment of metaphase I (B) and metaphase II (D) oocytes results in the oocytes dividing into two equal sized cells and no polar body. The effects of BFA and Peptide injection are also shown. (3) Delayed activation: Detergent washed sperm do not activate oocytes when injected. If activation by $SrCl_2$ is delayed, the sperm chromatin is surrounded by ORC4 and ejected as a pseudo-polar body (F).

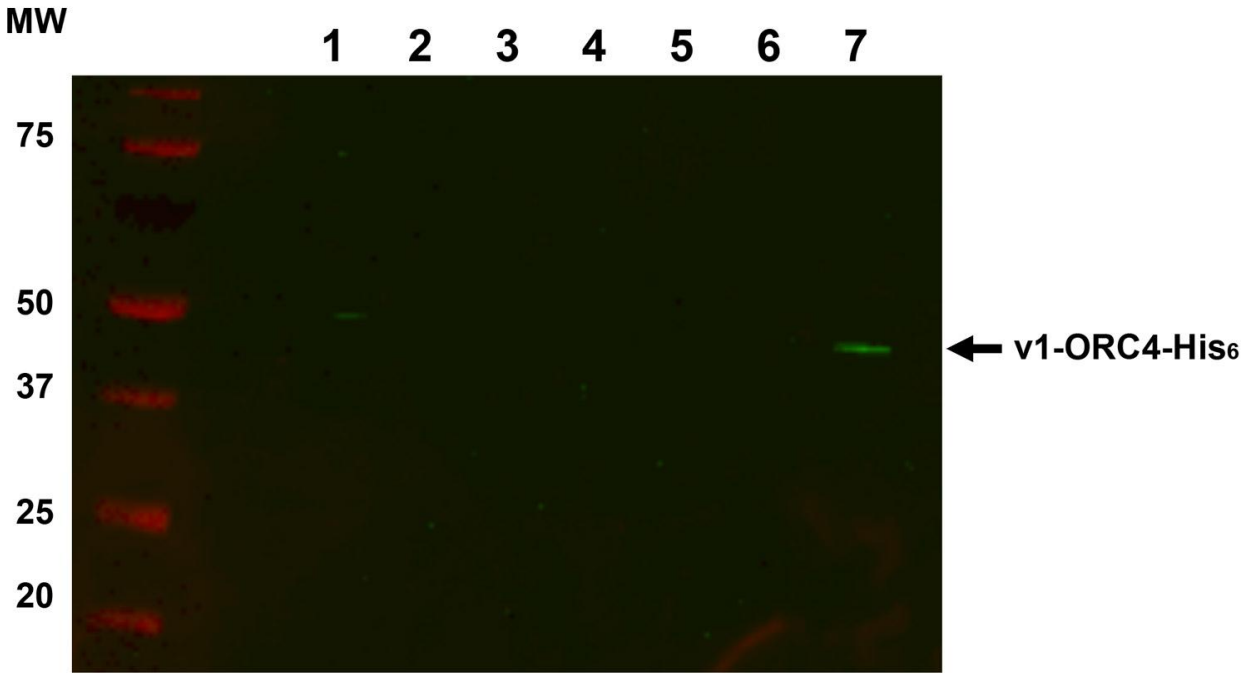

Figure 3.2: Confirmation of Antibody Recognition of ORC4. The *his-v1-mORC4* transcript was expressed in bacteria and the protein isolated on a nickel column, then by size exclusion chromatography (SEC). Fractions from the final SEC column are shown below. The isolated HIS-v1-ORC4 was analyzed by western blot using the antibody for ORC4 (C-15 from Santa Cruz Biotechnology) used in this study. The isolated HIS-v1-ORC4 was recognized by the antibody (lane 7). Lane 1, post induction fraction; lane 2, void volume (~90 mLs); lane 3, peak at 120 mLs; lane 4, peak at 130 mLs; lane 5, peak at 150 mLs; lane 6, peak 170 mLs; lane 7, 205 mLs (~ 47 kDa MW based on calibration of the column).

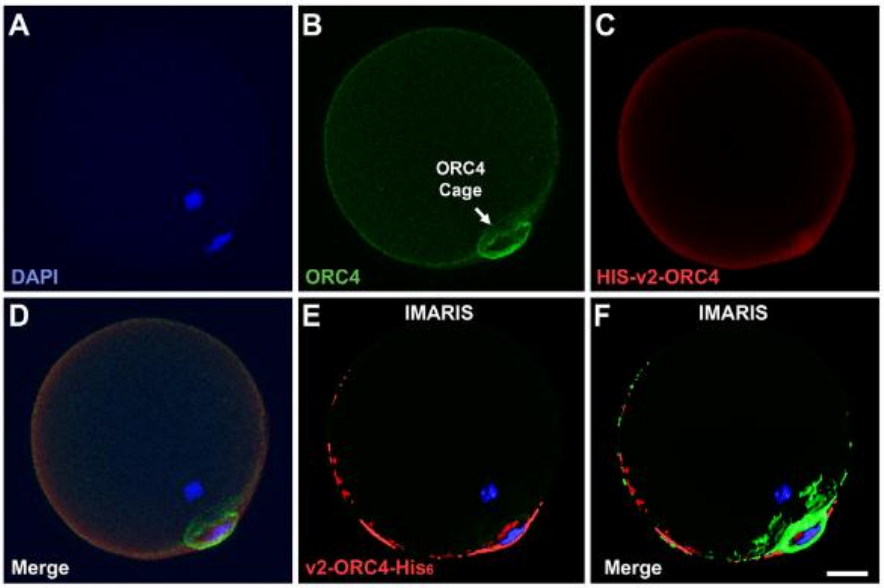

Figure 3.3. Incorporation of v2-ORC4-HIS$_6$ into the ORC4 cage. Purified v2-ORC4-HIS$_6$ protein was injected MII oocytes prior to activation. The oocytes were developed to G1 with the second polar body, then fixed and immunostained for ORC4 (green), and for the Histidine tag (red). The figure showed confocal sections of one oocytes with filters for DAPI (A), ORC4 (B), His-tag (C), and merge (D). Imaris software was used to identify where the v2-ORC4-HIS$_6$ was localized (E and F). Bar =10 um.

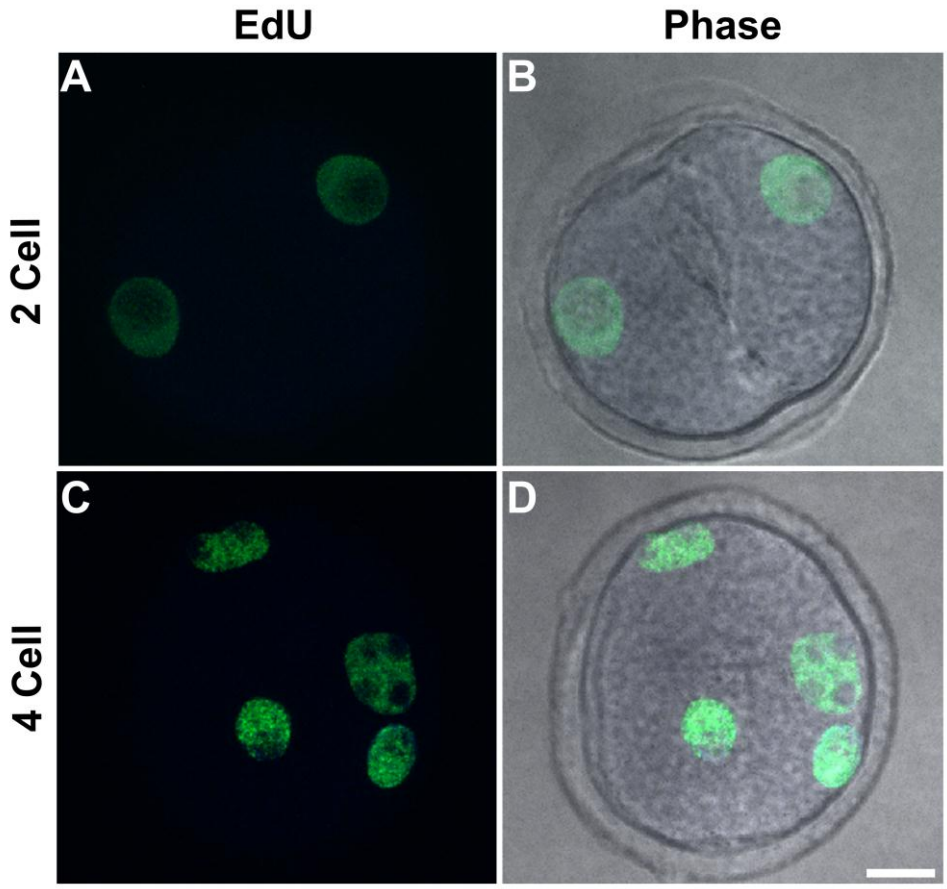

Figure 3.4. Effect of Brefildin A (BFA) on Polar Body Extrusion and ORC4 Cage Formation. MII oocytes were treated with Cytochalasin B (10 µg/ml) for 2 hrs, then activated with $SrCl_2$ in the presence of 10 µM EdU. The parthenogenetically activated oocytes were then incubated for up to 24 hrs, then stained for ORC4 and EdU incorporation. No ORC4 cages were formed (data not shown). At 8 hrs post activation, two pronuclei were formed inside the oocyte (A, B) and EdU staining indicated that DNA synthesis was not inhibited. By 24 hrs, the oocyte had four pronuclei that were all positive for EdU staining, suggesting that even though cytochalasin B inhibited polar body extrusion and oocyte cytokinesis, DNA synthesis and nuclear division was not. This supports the different roles of ORC4, one in DNA synthesis and one for DNA replication.

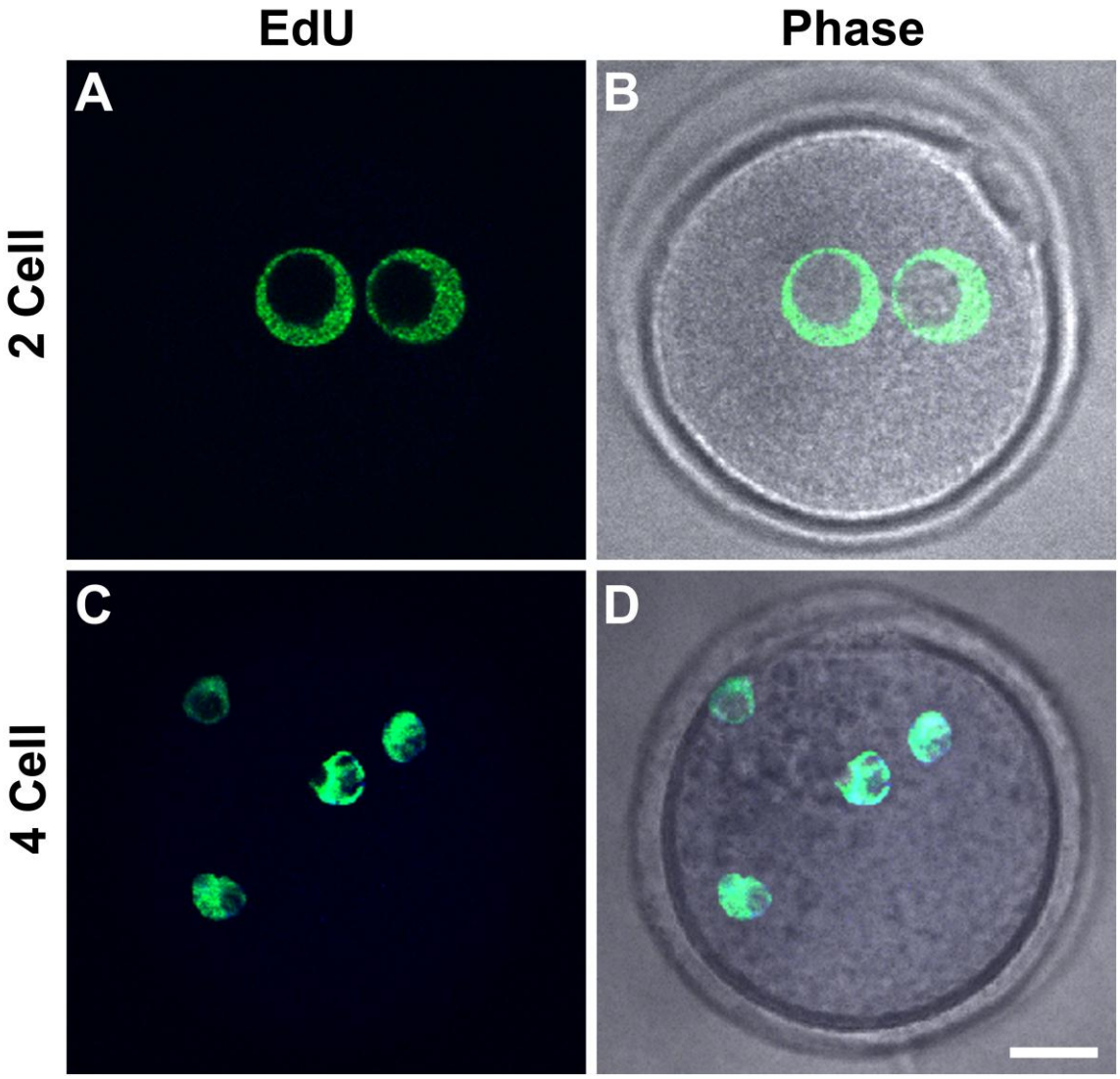

Figure 3.5. Effect of Cytochalasin B on Polar Body Extrusion and ORC4 Cage Formation. MII oocytes were treated with Cytochalasin B (10 µg/ml) for 2 hrs, then activated with $SrCl_2$ in the presence of 10 µM EdU. The parthenogenetically activated oocytes were then incubated for up to 24 hrs, then stained for ORC4 and EdU incorporation. No ORC4 cages were formed (data not shown). At 8 hrs post activation, two pronuclei were formed inside the oocyte (A, B) and EdU staining indicated that DNA synthesis was not inhibited. By 24 hrs, the oocyte had four pronuclei that were all positive for EdU staining, suggesting that even though cytochalasin B inhibited polar body extrusion and oocyte cytokinesis, DNA synthesis and nuclear division was not. This supports the different roles of ORC4, one in DNA synthesis and one for DNA replication.

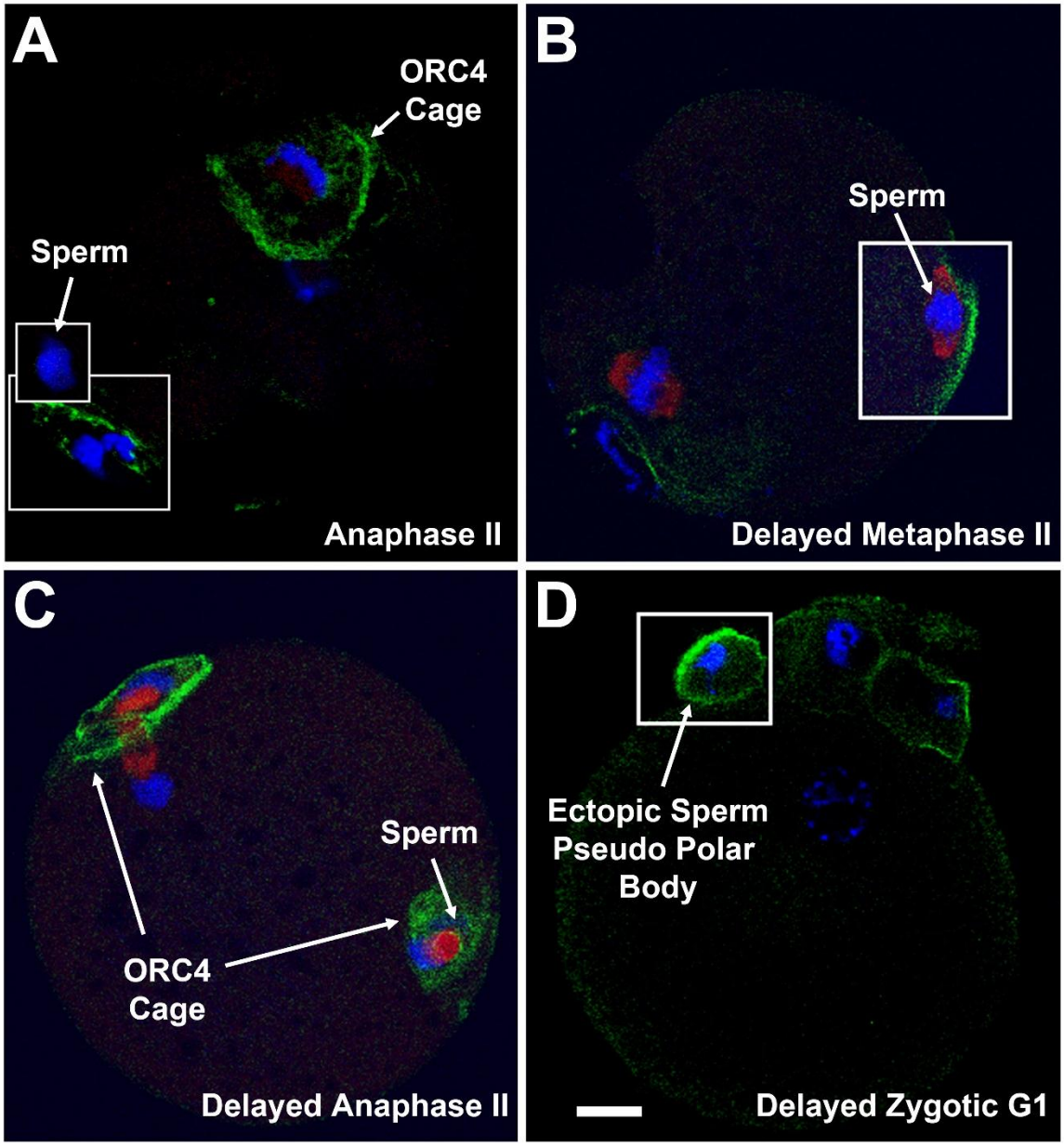

Figure 3.6. A New ORC4 Cage Forms with Ectopic Sperm Pseudo Polar Bodies. (A) Confocal image of a normal ICSI fertilized oocyte at anaphase II. The ORC4 cage surrounds the maternal chromosomes that will be extruded, and the DNA in the first polar body (lower inset). The sperm chromatin is devoid of ORC4 cage (upper inset). (B-D) An embryo injected with a detergent washed spermatozoa and activated 2 hrs later. (B) The delayed embryo in metaphase II before activation. ORC4 begins to accumulate at the oolemma new the decondensing nucleus. Tubulin (red) accumulates around the poles of the chromatin mass. (C) By anaphase II, ORC4 has completely surrounded the sperm chromatin. (D) At G1, the sperm of the delayed activated zygote has been ejected into an ectopic pseudo polar body in which the chromatin is surrounded by an ORC4 cage. Bar = 10 μm.

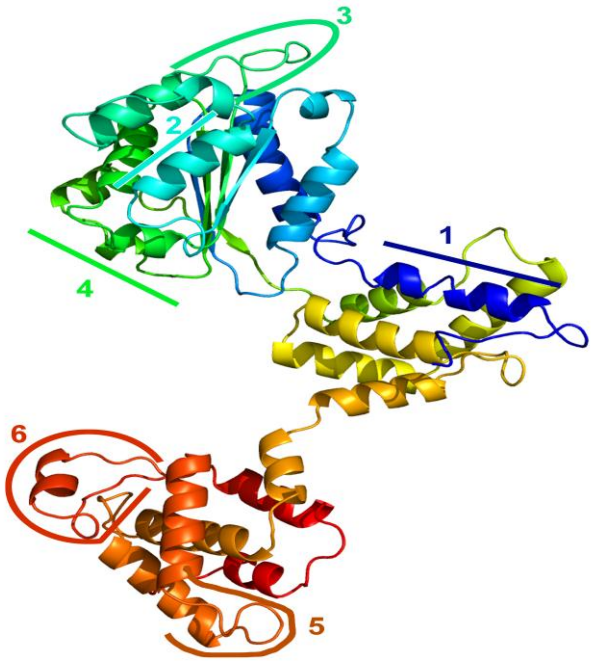

Figure 3.7. Putative 3D Structure of Murine ORC4. Using the Phyre[2] software (http://www.sbg.bio.ic.ac.uk/phyre2/html/page.cgi?id=index) we generated a predicted 3D model for the full length murine v1-ORC4 protein. The position of the six peptides used in this study are shown.

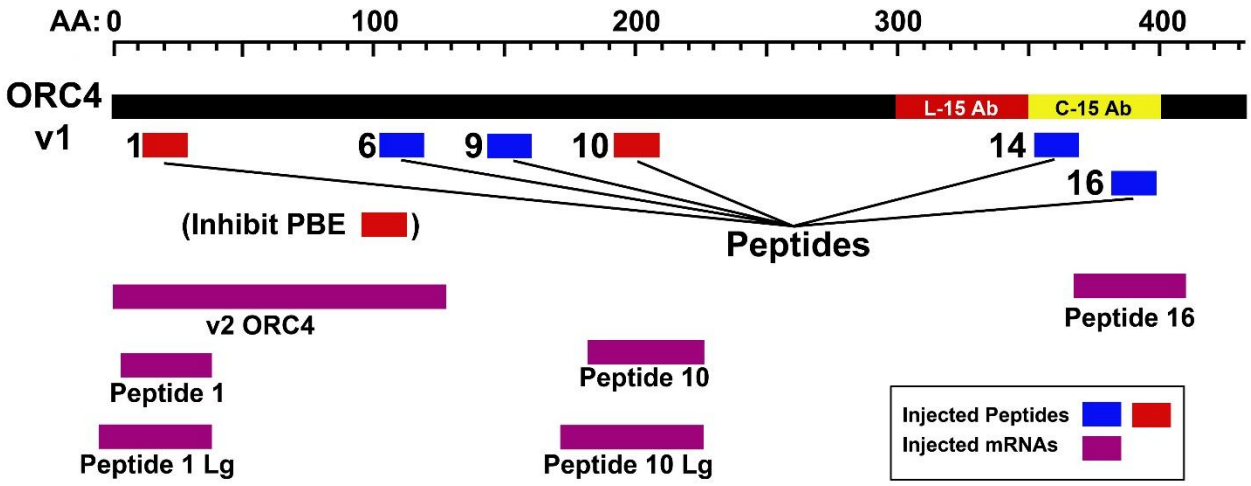

Figure 3.8. ORC4 peptides and fragments. The full-length version 1 ORC4 with 433 amino acids is shown in relation to the six peptides and five ORC4 fragments used in this study. The peptides are shown in blue (peptides with no effect on PBE) and red (the two peptides that prevented PBE). The positions of the five ORC4 fragments that mRNA sequences used in this study coded for are shown in purple.

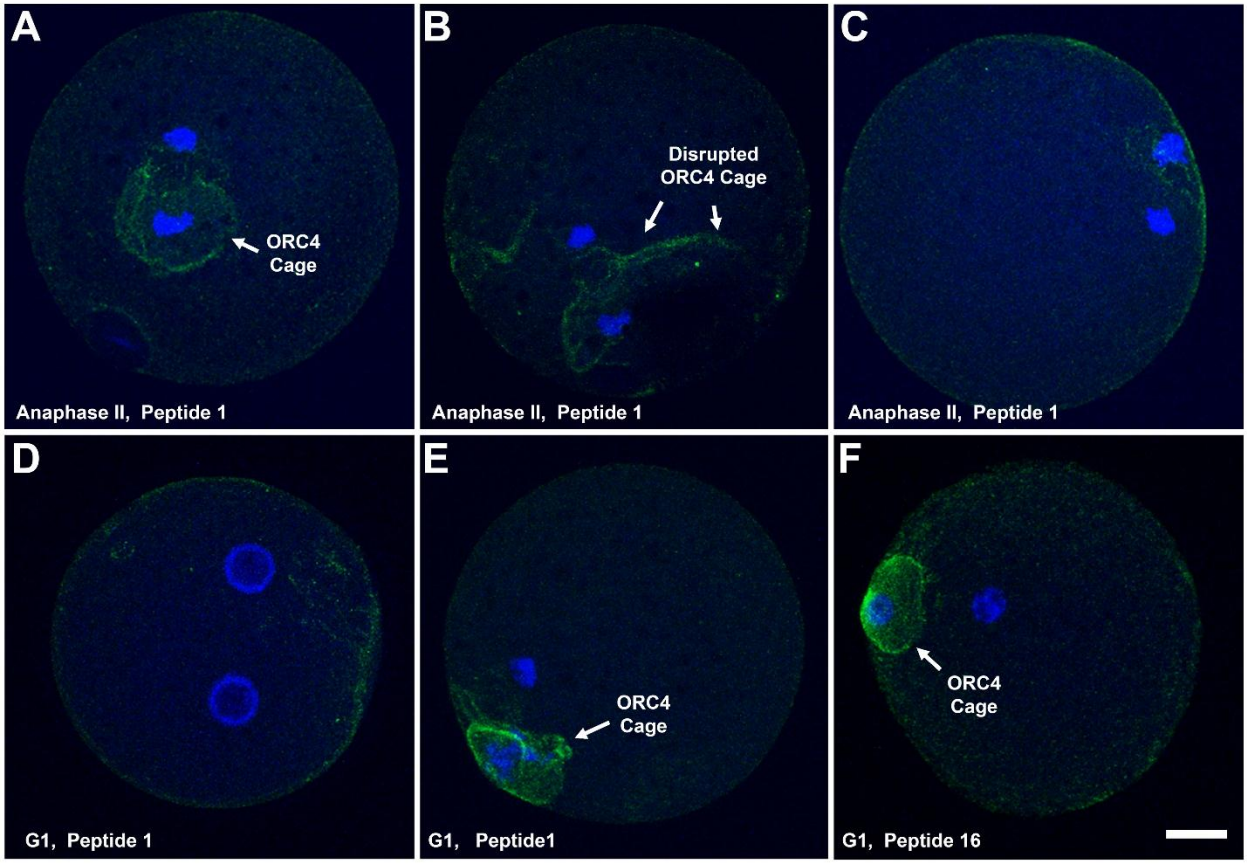

Figure 3.9. Injection of ORC4 peptides disrupts ORC4 cage and inhibits PBE. MII oocytes were injected with ORC4 peptides 1 hr before parthenogenetic activation. The oocytes were stained at anaphase II or G1 for ORC4. (A) An oocyte with peptide 1 that formed a normal ORC4 cage at anaphase II. (B) An oocyte with the ORC4 cage didrupted at anaphase II. (C) An oocyte with peptide 1 with no visible ORC4 cage. (D) An oocyte injected with peptide 1 that did not extrude a polar body. Both maternal sets of chromosomes formed pronuclei. Some ORC4 staining was visible at the cortex. (E) An oocyte injected with peptide 1 that formed a normal polar body with an ORC4 cage. (F) An oocyte injected with control peptide 16 that progressed to PBE. Oocytes were stained with an antibody for ORC4 (green) and DAPI (blue. Bar=10mM).

Peptide	AA Position in ORC4	No. Oocytes	2 PN
1	12 to 29	68	15 (22.1%)*
6	102 to 119	122	0
9	138 to 155	96	0
10	191 to 208	139	16 (11.5%)
14	352 to 369	123	2 (1.6%)
16	382 to 399	88	2 (2.3%)

Table 3.1. Injection of ORC4 Peptides. Peptides were injected into MII oocytes before parthenogenetic activation. The percentages of oocytes that progressed to having two pronuclei (2 PN) instead of the normal development to one PN and a polar body, are shown. For each peptide, at least two independent experiments were performed. There was no statistically significant difference between the individual experiments within each peptide, or between peptides 6, 9, 14 and 16 using, using the Fisher's Exact Test ($p < 0.05$). There was no statistical difference between peptides 1 and 10, but both were statistically different from all other peptides. All p values are listed in Table 1.

ORC4 Frag	AA Position in ORC4	No. AAs	No. Oocytes	2 PN
v2-ORC4	1 to 121	121	128	32 (25%)*
Peptide 1	12 to 47	36	120	32 (26.7%)
Peptide 1 Lg	2 to 47	46	152	40 (26.3%)
Peptide 10	190 to 235	46	158	29 (18.4%)
Peptide 10 Lg	180 to 235	55	140	35 (25.0%)
Peptide 16	374 to 413	40	127	5 (3.9%)

Table 3.2. Injection of mRNA for ORC4 Fragments. mRNA for five different ORC4 fragments were injected into oocytes before parthenogenetic activation, and the progression to 2 PN was assessed. For each ORC4 fragment mRNA that was injected, two experiments were performed. There was no statistical significantly difference between experiments for each peptide, or between v2-ORC4, Peptide 1, Peptide 1 Lg, Peptide 10, or Peptide 10 Lg. Peptide 16 was highly statistically significant for all other peptides. All p values are listed in Table 2.

CHAPTER 4: Spatial and Temporal Resolution of ORC4 Fluorescent Variants Reveals Structural Requirements for Maintaining Higher Order Self-association and Pronuclei Entry

4.1 Introduction

The combined results from Chapters 2 and 3 provide evidence that ORC4 has a role outside of DNA licensing, namely that ORC4 undergoes large scale reorganization from the plasma membrane to self-association into a cage-like structure that surrounds chromosomes destined for extrusion. The essential regions required for higher order cage formation were identified as the N-terminus and the middle domain through injection of peptides designed to occupy surface exposed regions of ORC4 (Chapter 3). Injection of embryos with peptide sequences from amino acids 12 - 29 and 191 - 208 were found, via immunocytochemistry, to prevent ORC4 cage formation whereas peptides designed from other regions (such as 102 - 119 and 138 - 155) failed to prevent ORC4 self-association. Inhibiting the higher order assembly of ORC4 was found to prevent PBE resulting in injected embryos forming 2 pronuclei (PN) during maturation instead of dividing into two cells (79). Interestingly, prevention of higher order ORC4 complex formation did not disrupt licensing for DNA replication. This demonstrates that the dichotomy functions ascribed to ORC4 within embryos are not mutually exclusive and, thus, likely involve interactions within different regions of the protein.

While our results have provided a unique look at ORC4 activity during oocyte development and identified its role in PBE, we are still missing critical events associated with the dynamic switch in function of ORC4 during oocyte activation. Advance fluorescence methodology like Fluorescence Lifetime Imaging (FLIM) has been previously utilized to track the activity of proteins down to the low nanomolar concentration and, therefore, could be utilized for providing methods to track ORC4 dynamics in live embryos (80), (81), (82). Fluorescence is a process whereby light is emitted from a molecule subsequent to absorption of light. Absorption of a photon promotes a ground-state electron, typically from a π orbital, to an excited state wherein it will relax down to the lowest vibrational level within the lowest excited state. The electron will then remain in the excited state for a period of time, at which point it will return to the ground state and emit a photon of light (i.e. fluorescence). The average time in which the electron remains within the excited state is called the lifetime (83). This property is unique among each fluorophore and is often times obtained using time- or frequency domain measurements.

Excited state lifetime measurements are powerful as they can provide unique information about the molecular environment that is not observed from intensity measurements. To obtain a quantitative lifetime values requires fitting the time-resolved data, obtained using the methods mentioned above, to a model until the best is obtained as determined via reduced χ^2 value. Simple decay, such as obtained for the fluorophore fluorescein in a basic solution, is straight forward and can often times be modeled using a single exponential decay. Heterogeneous emission requires more complex analysis, such as multiple exponential models. However, this type of analysis is only able to resolve multiple components when your sample has high emission (<2000 counts). The lifetime data was converted to a phasor plot to determine temporal property of each fluorophore tested. Lifetime measurements have become popular in microscopy as it can provide a spatial and temporal map thus detailing organization of fluorophores within a cell and alterations in microenvironment. One difficulty in this is the lack of counts per pixel. Therefore, extraction of lifetimes requires significant statistical analysis to obtain average lifetime values. In 1984, a model-less method of analysis was introduced, called the phasor plot, which has gained popularity among microscopist as it only requires the raw data. The phasor analysis graphical representation where the modulation is a vector with an angle equal to the phase delay (83). The x and y coordinates of the vector derive from: $x = G = M\cos\phi$; $y = S = M\sin\phi$. For a single exponential decay, this vector describes a semicircle which is referred to as the universal circle. Single fall on it. Complex decays fall inside the universal circle. Thus able to graphically represent complex decay emission and spatially separate components within a sample on the phasor plot (Fig. 4.1). In this section of the dissertation, we constructed fluorescent variants of ORC4 generated by fusing it to a fluorescent protein (FP), enhanced green fluorescence protein (eGFP), as well as a variant containing a unique amino acid sequence for site-specific labeling. eGFP is a ~ 26 kDa protein that displays green fluorescence when it is excited with blue light (84). It has been shown that ORC fusion with GFP at either N- or C-termini, retain their DNA replication function (2). However, we cannot predict how fusion of eGFP onto ORC4 will affect its function(s) in oocytes as the addition of this protein will increase the total mass to 158% of the original construct. We have also generated an ORC4 containing a FlAsH sequence inserted within the C-termini as a means to circumvent these potential issues from the eGFP fusion construct. FlAsH-EDT_2 is a derivative of fluorescein and used in site-specific labeling of proteins in live cells wherein it binds with high affinity to proteins containing the tetra-cysteine

motif cys-cys-pro-gly-cys-cys (85), (86) (Fig. 4.5). FlAsH-EDT_2 is cell membrane permeable and is smaller than 1 kDa (87) compared to eGFP (26 kDa) and would therefore not be expected to cause large perturbations within the protein due to the significantly smaller mass increase. Herein we demonstrate the injection of mRNA of each fluorescent variant of ORC4 can provide a unique signal allowing for the quantification of ORC4 dynamics at different stages of oocyte activation. Lifetime imaging indicates the licensing function has probably not been altered for both constructs as each variant could be spatially resolved within the PN. Furthermore, we provide compelling evidence that the ORC4-FlAsH variant can be recruited to the ORC4 cage during PBE and was shown to be consistently associated with PB. These results demonstrate that fluorescent variants of ORC4, specifically those labeled with small molecules, could be useful for future single molecule dynamic studies for ORC4.

4.2 Materials and Methods

4.2.1 Animals

Eight-week of age mice, B6D2F1 (C57BL/6N X DBA/2), were used. Mice were obtained from National Cancer Institute (Raleigh, NC), and used at 8 – 12 weeks of age. Animal care and experimental protocols for handling and the treatment procedures were reviewed and approved by the Institutional Animal Care and Use Committee at the University of Hawai'i.

4.2.2 Creating the orc4-egfp construct

mORC4 variant 1 plasmids (full length of orc4) bought from genecopoeia were used to create assembly vectors by using AvaI enzyme. eGFP sequences was amplified by PCR reactions. The primers used to amplify the eGFP sequences included homology arms at the beginning and at the end of the assembly vectors. Gibson assembly was then used to join vector and eGFP together and the Gibson products were electrophoresed into bacteria. The orc4-egfp constructs were confirmed by single PCR colony and sequencing.

4.2.3 Creating the construct of orc4 for FlAsH labeling

mORC4 variant 1 plasmids (full length of orc4) bought from genecopoeia were used to create a mutation construct containing six-amino acid sequences (Cys-Cys-Pro-Gly-Cys-Cys). First, we deleted six amino acids at amino acid number 407- 412 and replaced them with Cys-Cys-Pro-Gly-Cys-Cys sequences by using Gibson. The mutation products were confirmed by a single PCR colony and sequencing.

4.2.4 mRNA-ORC4-eGFP synthesis

Plasmids containing the mORC4- eGFP and ORC4-FlAsH mutation constructs were linearized by an enzyme downstream of the *ORC4* gene. mMESSAGE mMACHINE T7 transcription kit from Thermo Scientific was used to synthesize mRNA ORC4-eGFP constructs. Agarose (1%) electrophoresis was used to confirm mRNA product, and isolate mRNA by Direct-zol RNA miniprep (Zymo Research). ORC4-eGFP mRNA constructs were stored at -20°C prior to microinjection.

4.2.5 Injection of mRNA-eGFP

Each ORC4-eGFP mRNA and ORC4-FlAsH mutation constructs were used to microinject into the cytoplasm of MII oocytes. A microinjection volume of 10 pl/oocyte was used in all experiments. Following microinjection, the oocytes were incubated for at least 4 hours and checked for eGFP signal under microscope. When eGFP signal expressed on oocytes, we activated oocyte development via parthenogenesis activation by using CZB free calcium medium contained 10 mM of $SrCl_2$ for two hours (AII) and three hours (G1). These AII and G1 embryos were imaged and tracked eGFP movement by using fluorescence microscopy.

4.2.6. FlAsH labeling

After microinject mRNA-ORC4 mutation containing of the Cys-Cys-Pro-Gly-Cys-Cys amino acids for at least 4 hours before parthenogenesis activation injected oocytes to develop AII and G1 stages. Solid FlAsH-EDT_2 was provided by Dr. Nicholas James. Following microinjection, the oocytes were incubated with $SrCl_2$ 2 hours and 3 hours for anaphase II and G1, respectively. Activated oocytes were then incubated with FlasH-EDT_2 for 30 minutes. Next, the activated oocytes were washed with EDT + DMSO and PBS + glucose to remove FlAsH. The activated oocytes labeled with FlAsH were analyzed with a confocal fluorescence fluctuation spectroscopy.

4.2.7. Dynamics of fluorescent ORC4 in Oocytes

Confocal fluorescence fluctuation spectroscopy (FFS) measurements were recorded on an Alba fluorescence correlation spectrometer (ISS, Champaign, IL), equipped with x-y scanning mirror, connected to a Nikon TE2000-U inverted microscope (Nikon, Melville, NY) with a PlanApo VC 60 x 1.2 NA water objective. Two-photon excitation of enhanced eGFP was provided by a Chameleon Ultra (Coherent, Santa Clara, CA) tuned to 920 nm with < 1 mM laser power. Fluorescence emission was collected through a 535/50M bandpass filter (Chroma,

Bellows Falls, VT) in front of a photo multiplier detector (H7422P-40, Hamamastu, Hamamastu City, Japan). Cells were imaged in a humidified enclosed chamber kept at 37ºC (Tokai Hit, Fujinomiya, Sizuoka, Japan). An objective heater wrapped round the neck of the objective was used to minimize temperature drifts (with a 20 minute delay to equilibrate the temperature prior to imaging) and the collar of the objective was adjusted to compensate for temperature and thickness of the coverslip.

Diffusion and concentration of ORC4 constructs was determined using Raster Imaging Correlation Spectroscopy (RICS) (85). Briefly, 12.8 micron (50 nm pixels) regions of interest were selected from the fluorescence image. The pixel sampling time was 12.5 μs, each frame had 256 x 256 pixels, and each measurement lasted ~ 1 min (100 frames). The beam waist (ω_0) calibration was achieved by measuring the autocorrelation curve of fluorescein (~ 20 nM) in 0.01 M NaOH, and fitted with a diffusion rate of 430 μm^2/sec, which were performed before each day's measurement (85). The typical values of ω_0 were at the range of 0.35 – 0.4 μm.

FLIM (Fluorescence-lifetime imaging microscopy) measurements were recorded through an ISS A320 Fast FLIM box coupled to the Ti:Sapphire laser, which produces 80-fs pulses at a repetition rate of 80 MHz, and photo multiplier detector (H7422P-40, Hamamastu, Hamamastu City, Japan). Fluorescein, which was used as the lifetime reference (4.0 ns), and FlAsH was excited at 780 nm and the fluorescence signal was filtered away from excitation light through a 520 nm bandpass filter (FF01-520/35; Semrock Rochester, NY) mounted in front of the detector.

4.3. Results:

4.3.1 Biophysical Characterization of ORC4-eGFP

Oocytes injected with mRNA ORC4-eGFP were observed to have a homogenous distribution, including in the PB, of fluorescence during all activation stages imaged (Fig. 4.2). The movement of ORC4-eGFP was analyzed using a technique called fluorescence-lifetime imaging microscopy, or FLIM. FLIM provides a pixel analysis on the lifetime of the fluorescing species; thus allowing for the resolution of pixels that contained eGFP versus autofluorescence. FLIM was recorded for each oocyte. FLIM data were analyzed by a mathematical process termed FLIM-phasor, which calculates the shift in wavelength between the excitation and emission signals, and the intensity of the fluorescent signal. FLIM-phasor is a modeless plot wherein the phase shift and demodulation (raw data) are plotted on X (G) and Y (S) coordinate system. Signals from eGFP have a known phasor point based on the lifetime of the fluorophore

(~ 3 ns), while background "autofluorescence" is composed of a more complex mixture of molecules. As such, eGFP phasor points should lie near the arc, or universal circle, of the FLIM-phasor analysis (Fig. 4.2D; Table 4.1).

FLIM-Phasor analysis of ORC4-eGFP injected oocytes showed phasor points that were shifted inside the universal circle indicating a more complex lifetime compared to non-fused eGFP injected into oocytes (Fig. 4.2D). This suggests that ORC4 alters eGFP fluorescence or that the fusion proteins interact with the same result. Nearly all images collected contained a large number of pixels within the autofluorescence region when injected with the ORC4-eGFP variant. The majority of oocytes analyzed (No 6/10) were found to have pixels within their PBs that corresponded to the autofluorescence region (Fig. 4.3). Essentially, ORC4-eGFP was prevelant throughout the oocyte with no visible accumulation at any site. The phasor points of ORC4-eGFP showed no major changes in location at different stages of oocyte activation. However, phasor points associated with the PN at zygotic G1, though very low in intensity, were found to be shifted more towards the universal circle than ORC4-eGFP throughout the embryo, suggesting that PN ORC4-eGFP was closer to that of free eGFP. This suggests that ORC4 proteins in the PN have a different protein-protein interaction than those in the cytoplasm (Fig. 4.3).

The dynamics of ORC4-eGFP were determined by analyzing fluctuation data collected from oocytes containing a strong signal from eGFP. RICS (Raster imaging correlation spectroscopy) analysis, which allows for a spatial observation of molecular fluctuations, produced an average diffusion of ORC4-eGFP of 5.0 ± 0.5 μm^2/sec. This rapid speed usually indicates untethered, soluble proteins. Visual inspection of the collected frames indicated that the diffusion might be more complex as we observed areas containing large fluorescent spots (Fig. 4.5A and 4.5B). Analysis of regions containing these spots produced diffusion values that were ~ 10x slower than regions containing no spots (0.8 ± 0.3 vs. 7.5 ± 1.0 μm^2/sec). These data suggest that there are two populations of ORC4-eGFP in the cytoplasm, a rapidly moving, untethered population and another one that is self-associated, moving more slowly. These results are in line with our observation that ORC4 can self-associate. However, we were unable to observe large self-association, like cage formation, from the fluorescence signal during PB formation and the FLIM-phasor analysis did not identify spatially resolved structures for ORC4-eGFP.

4.3.2 Biophysical Characterization of ORC4-FlAsH

The lack of ORC4 cage appearance from our eGFP fusion construct suggests that this modification may have limited ORC's ability to self-associate; potentially inhibiting it from recruitment during cage formation. Therefore, we created a mutated protein, ORC4-FlAsH, that has no additional amino acids and only has six amino acids substituted in an alpha-helix portion of the protein. These include four cysteine residues that interact with a compound, EDT_2, to generate a fluorescent signal in cells (Fig. 4.6). We characterized the dynamics of ORC4-FlAsH, which was fluorescently labeled after the protein was produced by the embryo using the site-specific FlAsH-EDT_2 compound, to determine if we could obtain better spatial resolution of ORC4. Non-mRNA injected embryos that were treated with FlAsH-EDT_2 showed a high number of pixels with phasor points similar to the unbound fluorophore (Fig. 4.7A and B). Nevertheless, we were able to detect some accumulation of ORC4 in the area where we expected to see the ORC4 cage (Fig. 4.7C). Note the total fluorescence was low, but the excited state properties that were determined by FLIM were indicative of FlAsH as compared to autofluorescence. This indicated that our washing protocol was not fully effective at removing non-specific bound FlAsH-EDT_2; however, we were unable to modify the current protocol due to the sensitivity of the embryos to the wash conditions. FLIM-phasor analysis of embryos injected with ORC4-FlAsH mRNA, and treated with the FlAsH-EDT_2 compound, produced phasor points that were shifted away from the non-specific bound phasor points (Fig. 4.8B). These results are in line with previous reports that observed modified fluorescent properties of this fluorophore when bound to the FlAsH sequence (86). Even though they were off the universal circle, they appear closer to the expected FlAsH phasor point than autofluorescence signal. Therefore, the use of FLIM-phasor analysis allowed us to resolve non-specific versus specific binding of FlAsH-EDT_2 within the embryos. For our experiments we only used embryos with the majority of their phasor points associated with ORC4-FlAsH. We also note that there were fewer phasor points in the autofluorescent region when working with ORC4-FlAsH compared to ORC4-eGFP.

Intensity images of ORC4-FlAsH (Fig. 4.7A) showed non-homogenous emission distribution throughout the embryo, unlike ORC4-eGFP, with intensity patterns also being observed in the PB (Fig. 4.5B and C). Images appeared to have bright decorations along the plasma membrane and distinct circular, or cage like, structures near the plasma membrane during PBE (Fig. 4.7C), which is in line with previously characterized spatial organization of ORC4

(79). Fluctuation analysis produced nearly identical diffusion properties as our ORC4-eGFP construct (average diffusion 6.0 ± 1.0 μm^2/sec; individual components 7.0 ± 0.8 and 0.6 ± 0.2 μm^2/sec). The concentration of ORC4-FlAsH, which was determined by analysis of the autocorrelation function was found to be higher (160 ± 50 nM) than the eGFP variant (40 ± 10 nM) from our sampled embryos (n = 10). This variation might be caused from alterations in the actual amount of mRNA injected into each oocyte or might indicate alterations in protein production/degradation for each construct. Much like ORC4-eGFP, the phasor points of ORC4-FlAsH were slightly shifted within the PN, as well as around the PM, compared to the points that resolved ORC4-FlAsH with the embryo. These correlated results are indicative that these constructs are not excluded from the PN and that licensing from both variants likely still occurs.

4.4 Discussion

Herein we present a study aimed at characterizing the dynamics of ORC4, following cage formation up to PBE, in live, activated oocytes using advance fluorescence microscopy. Fluorescence methodologies are extremely sensitive which can allow for the examination of target molecules down to the single molecule level (87), (88). However, this sensitivity can only be achieved in systems that contain a bright signal above the background. In the case of cells there is always contaminating emission from the system, or autofluorescence, and it is critical to not only minimize this signal but also to confirm that the origin of emission being reported is in fact associated with the molecule of interest (89), (90). Our system, activated oocytes, are highly dynamic cellular systems that undergo large fluctuations in proteins and membranes (79). As expected from such a complex system, we observe a large amount of autofluorescence signal even when exciting with an infrared laser. Therefore, time resolved measurements were prioritized over intensity-based measurements as we were uncertain to the amount of signal that would be originating from ORC4-eGFP or ORC4-FlAsH compared to the embryo autofluorescence. Using FLIM-phasor analysis we were able to spatially resolve the lifetime of our fluorescent markers, both eGFP and FlAsH, from the autofluorescence signal thus allowing for the resolution of ORC4 protein in live oocytes during different states of maturation (Fig. 4.2A and 4.7A). To simplify our interpretation, sample analysis was constrained to embryos wherein the majority of phasor points (> 90) were originating from our fluorescent molecule.

The essential questions that we sought to address within this study were: 1) does modification of ORC4 at the C-terminus, with eGFP or the FlAsH sequence, alter its activity?

and 2) could we observe cage formation and PBE with either of these constructs? Our experiments demonstrated that activated embryos that were injected with our mRNA could still undergo PBE and division. Each embryo tested contained endogenous ORC4 which makes it difficult to make any conclusive statements regarding the functionality of these variants towards development. As such, we focused on known biophysical properties and qualitative characterization from confocal imaging. For example, our model of ORC4 cage formation predicts higher order self-association of ORC4 and we should be able to quantify this via diffusion characteristics of labeled ORC4. Our fluctuation data yielded multiple rate constants: ~ 6 and ~ 0.5 μm^2/sec to which we assign the monomer form and to a self-associated state of ORC4, respectively; demonstrating self-association can occur with both variants. The lack of spatial resolution of higher order self-association of ORC4-eGFP (i.e. no visualization of a cage at any stage of activation) is indicative that this variant is not recruited for chromosome selection nor involved in PBE. Further evidence of this lack of higher order assembly for ORC4-eGFPs is the non-essential requirement of eGFP and lack of structured emission from within the PB whereby only 40% of cells examined contained eGFP within the PB (Fig. 4.1C and D). Therefore, we speculate that the addition of eGFP at the C-termini introduces steric hindrance on higher order ORC4 structure formation thus preventing this variant from being tightly associated for cage formation during chromosome selection or PBE. Comparison with the ORC4-FlAsH produced in embryos provided us a means to test our hypothetical model as this construct contains only minor perturbation within the C-termini. Images from this variant were drastically different whereby distinct concentration patterns of ORC4 where observed under intensity measurements, unlike ORC4-eGFP, indicating that this variant can be segregated to unique areas of the embryo (Fig. 4.4B and C). Likewise, the majority (>90%) of PBs imaged had phasor points corresponding to bound FlAsH, they presented with unique structures (Fig. 4.7C and 4.8C). This comparison provides more support that ORC4-eGFP is not used by embryos for PBE and that the phasor points observed inside PB likely originate from stochastic diffusion of the construct. It is our conclusion then that the addition of eGFP causes disruption of higher order self-association of ORC4 that is required for cage formation. This model also states that the lack of significant modifications of the ORC4-FlAsH variant would cause minimal, if any, alterations in structure or energy of interaction; thus allowing for it to be integrated with endogenous protein during activity.

The most characterized function of ORC4 is DNA licensing which occurs inside the PN during cell division (17). We interrogated the lifetime of our constructs at different points during embryo maturation to see if our constructs could be found within the PN (Fig. 4.3 and 4.8). Phasor points corresponding to ORC4-eGFP and ORC4-FlAsH were spatially resolved within the PN, however, the points from both variants were not identical to the points found inside the embryo. The lifetime, which is being represented by the phasor points, is a measurement of the time it takes for the excited electron to return to the ground state in the presence of all the deactivation rates acting on the fluorescent molecule at that time. Phasor point differences observed for both eGFP and FlAsH indicates that the environment around the fluorescent molecule, which can be inferred to ORC4 as well, is not identical when located between the PN and embryo. Also, the phasor points that spatially and temporally resolve for the PN was also found to highlight regions around the PM (Fig. 4.8). FLIM-phasor analysis establishes that not only can both constructs enter the PN but the forces acting upon ORC4 within the embryo is not identical to when bound to the PM or within the PN. The requirements for binding to the PM or complex formation during licensing within the PN are likely different.

This work demonstrates that the addition of a large polypeptide to the C-termini negatively impacts higher order self-association of ORC4, specifically affecting structured organization required for cage formation, and ORC4 activity in PBE. Our ultimate goal is to use single particle tracking and nano-imaging to provide a detailed molecular mechanism of ORC4 dynamics beginning with activation of the oocyte up to cell division. Fluorescent tracking of ORC4 will, therefore, require the use of constructs that do not significantly alter the mass of the protein to ensure the dual functions assigned to ORC4, PBE and DNA licensing, are not altered during embryo maturation. Herein we describe a possible ORC4 construct, namely ORC4 with a FlAsH sequence at site Cys-Cys-Pro-Gly-Cys-Cys, which allows for site-specific labeling and minimal background signal from nonspecific binding within live embryos. This work also represents the first step towards establishing a transgenic mouse model expressing endogenous levels of a trackable variant of ORC4.

4.5 Contributions

Research design: Hieu Nguyen, Nicholas G. James, and W. Steven Ward

Conducted experiments: Hieu Nguyen, Nicholas G. James, and Brandon Nguyen

Contributed to writing: Hieu Nguyen and Nicholas G. James

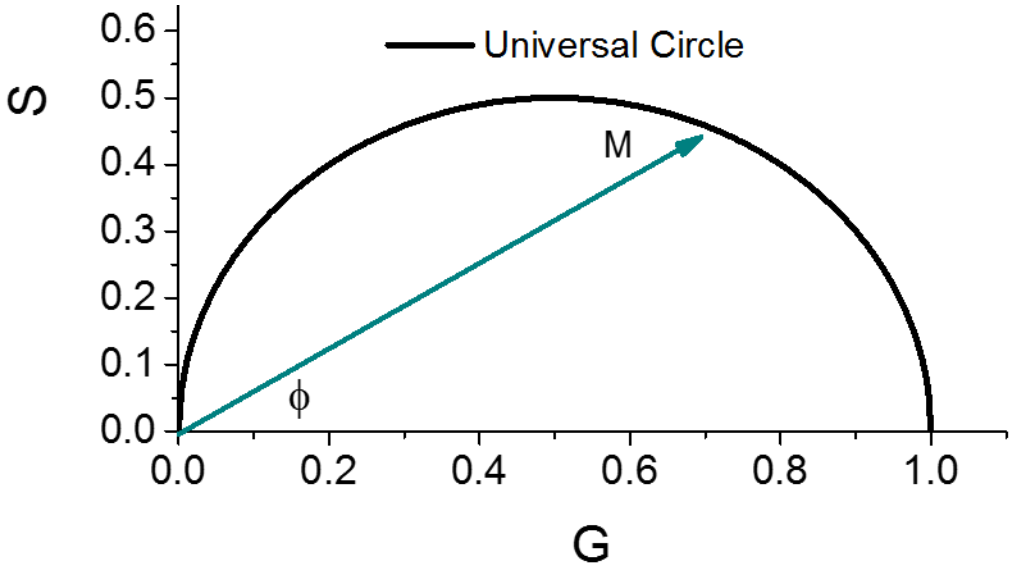

Figure 4.1. Graphical representation of Phasor plot. The phasor point location is a vector with a length equal to the modulation (M) at an angle equal to the phase delay (ϕ). For a fluorophore with a single exponential, this vector describes a semicircle of 0.5 with a center at (0.5, 0); this semicircle is referred to the universal circle.

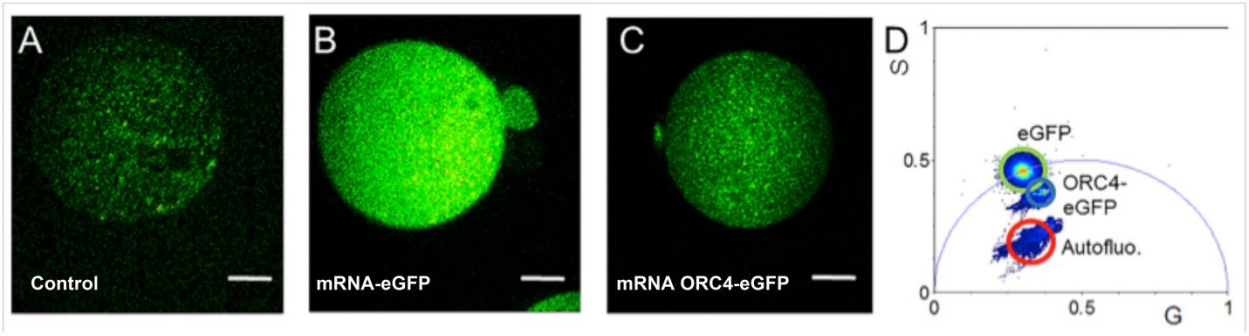

Figure 4.2. Spatial and temporal analysis reveals minimal self-association of ORC4-eGFP in embryos. (A-C) Representative intensity image of non-injected embryos (A; maximum intensity 10 counts at a single pixel), mRNA eGFP injected embryos (B; maximum intensity 100 counts at a single pixel), and ORC4-eGFP mRNA injected embryos (C; maximum intensity 50 counts at a single pixel). Scale bar is 15 microns. (D) Phasor points of reprehensive embryos with no mRNA injected (red), eGFP mRNA injected (green), and ORC4-eGFP mRNA injected (blue).

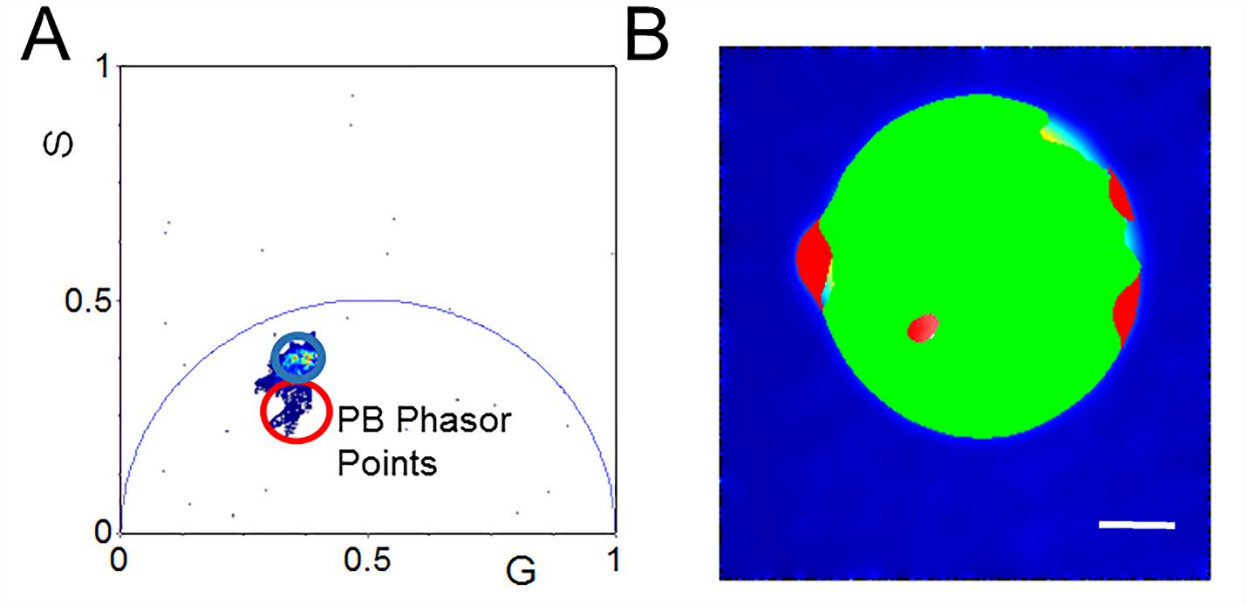

Figure 4.3. FLIM-phasor method demonstrates minimal amount of ORC4-eGFP entering the PB. (A) Phasor plot of an embryo injected with ORC4-eGFP mRNA. The blue circle correlates with Phasor points for ORC4-eGFP while the red points are more indicative of autofluorescence excited state properties. (B) Spatial organization of the phasor points from (A). The green points are found located within the cytosol and the red is located within the areas near the PB. Scale bar is 15 microns.

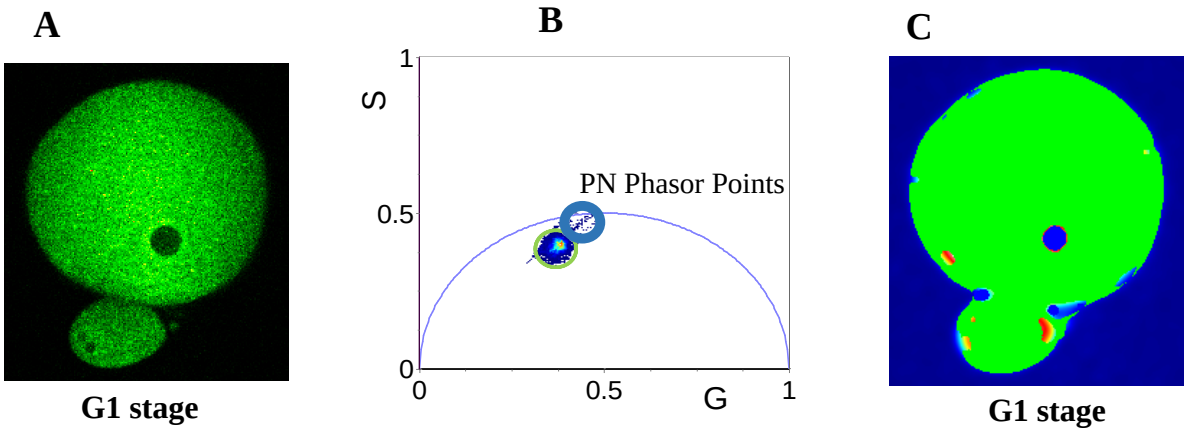

Figure 4.4. FLIM-phasor method during G1 phase indicates that ORC4-eGFP can enter the PN. (A) Intensity image of embryos injected with ORC4-eGFP mRNA during blank phase. Scale bar is 10 microns. (B) Corresponding phasor points from (A). Points circled in blue represent phasor points in similar proximity as those obtained for ORC4-eGFP at previous stages of division while the other circle indicates phasor points that appear in embryos that highlight the PN. (C) Spatial organization of the phasor points from (B) organized within the image from (A). The blue points are found located within the PN and are shown to be shifted away from the phasor point population of ORC4-eGFP within embryos.

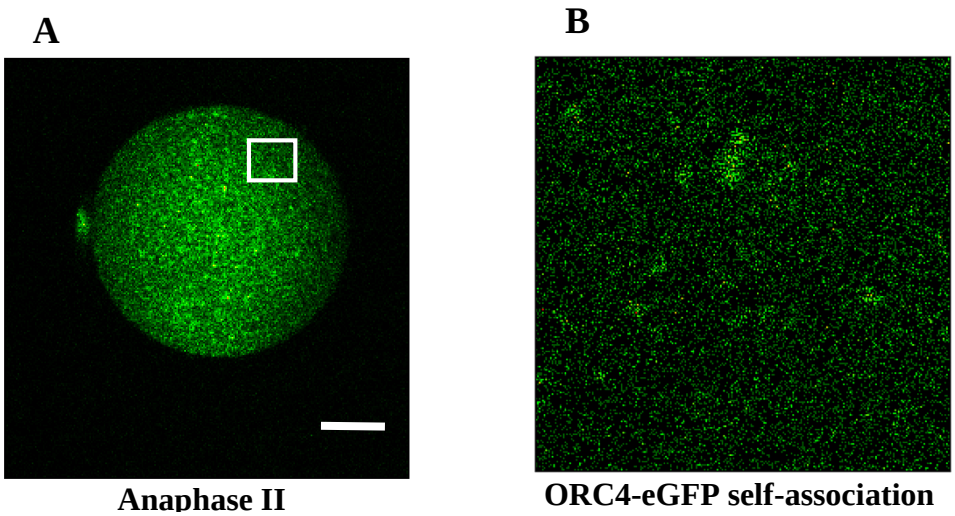

Figure 4.5. Visual observation of ORC4-eGFP self-association in embryos with RICS analysis. The intensity image of embryos injected with ORC4-eGFP mRNA (A) reveals a population wherein ORC4-eGFP is self-associated (B) when the pixel size is set to 50 nms. Scale bar for (A) 10 microns and from (B) is 3 microns.

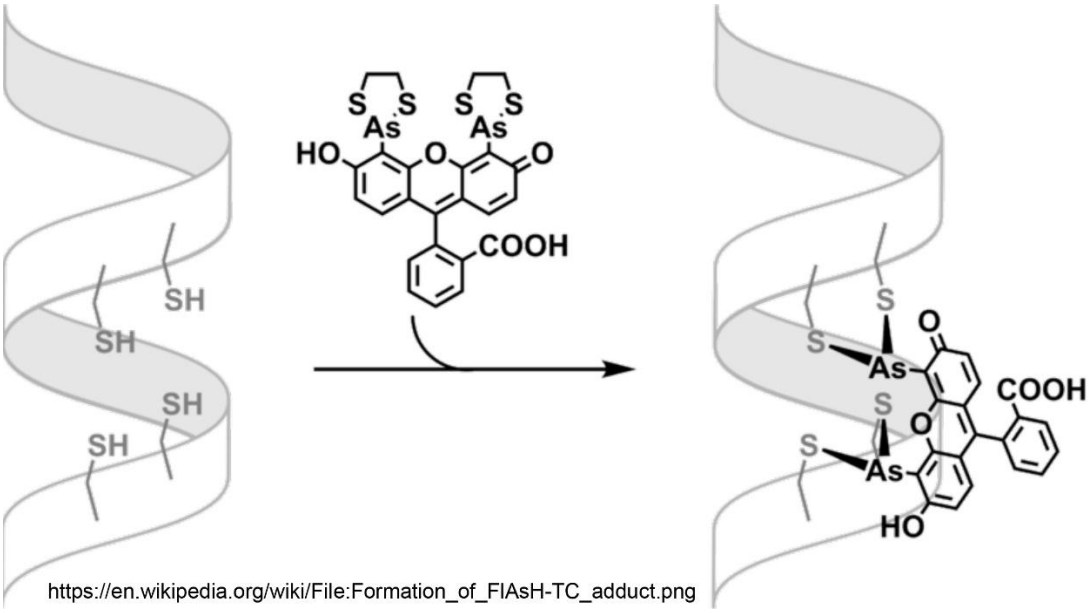

Figure 4.6: Formation of FlAsH-tetracysteine adduct. The stability of FlAsH-EDT_2 has been shown by the binding of cysteine residues to arsenic compounds via strong sulfur-arsenic bond. FlAsH-EDT_2 is a pale yellow color and it becomes fluorescent via the binding of tetracysteine motif.

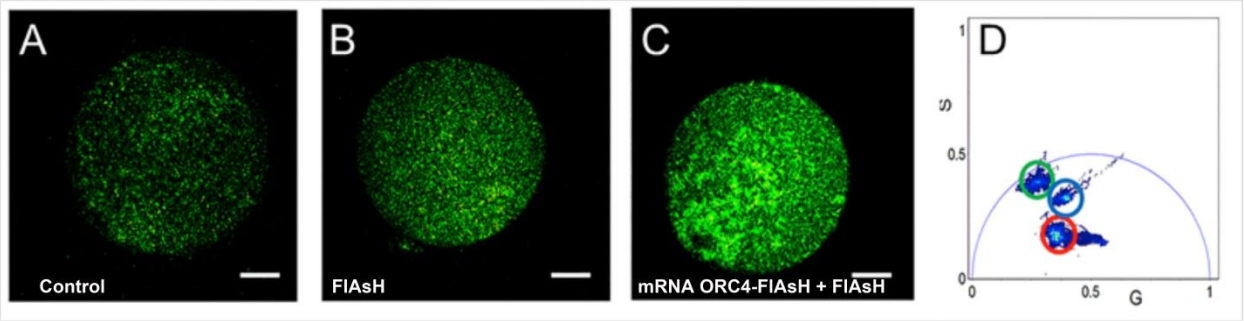

Figure 4.7. ORC4-FlAsH confocal images demonstrate unique structural organizations during cell division. Representative intensity images of embryos with laser excitation at 780 nm. A) No mRNA injected and no FlAsH added. Autofluorescence had a maximum intensity (red pixels) of 6 counts. B) No mRNA injected and FlAsH added. Nonspecific bound FlAsH was found to have a maximum intensity (red pixels) of 15 counts. C) ORC4-FlAsH mRNA injected and FlAsH added. FlAsH was found to have a maximum intensity (red pixels) of 100 counts. Scale bars represent 15 microns. D) Phasor plot showing representative phasor points from embryo Autofluorescence (red), embryos incubated with FlAsH without mRNA injected (green), and embryos incubated with FlAsH and injected with ORC4-FlAsH mRNA.

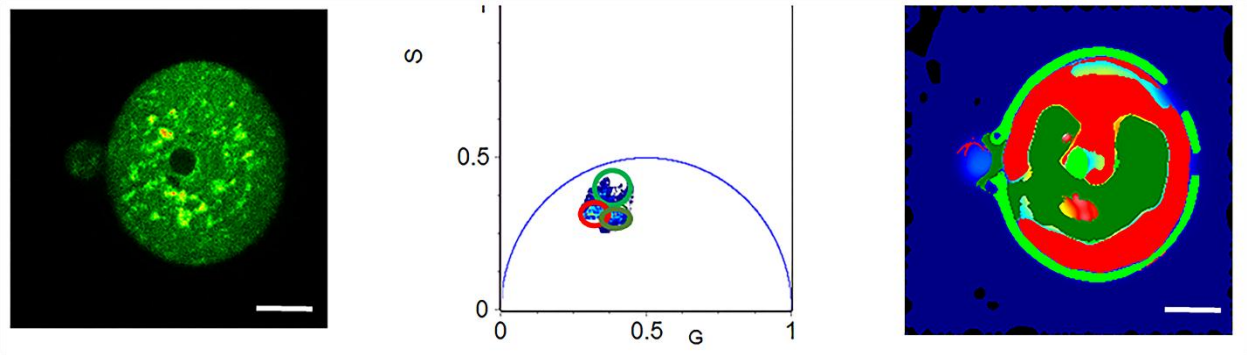

Figure 4.8. ORC4-FlAsH phasor points demonstrate entry within the PN and different properties when bound to the plasma membrane. Spatial distribution of FlAsH lifetime during GI phase. A) Intensity image during blank phase after mRNA injection and Treatment with FlAsH. B) Phasor points of each pixel obtained from FLIM of image A. Circle were created to center around areas with a large number of phasor points as calculated from SimFCS. Green circle highlights PN and the plasma membrane; Red and Dark Green circles highlight pixels within the cytosol. C) Spatial distribution of phasor points overlayed onto A. Scale bars represent 15 microns.

Embryo (920 nm)*	**G**	**S**
Autofluorescence	0.31 (± 0.01)	0.21 (± 0.01)
eGFP	0.31 (± 0.01)	0.45 (± 0.01)
ORC4-eGFP	0.33 (± 0.02)	0.33 (± 0.01)
Embryo (780 nm)*	**G**	**S**
Autofluorescence	0.38 (± 0.01)	0.21 (± 0.01)
FlAsH (no mRNA)	0.23 (± 0.03)	0.39 (± 0.01)
ORC4-FlAsH	0.36 (± 0.02)	0.33 (± 0.02)

Table 4.1. Statistical analysis of Phasor point locations for ORC4-eGFP and ORC4-FlAsH. * N = 10; G and S values are an average from all embryos imaged and represent the area within the phasor plot that contains the highest number of pixels for each condition. Calculations were performed using the FLIM program on SimFCS4.0 (Gratton, UCI).

CHAPTER 5: CONCLUSION

5.1 ORC4 involves in polar body extrusion

The observations described in this dissertation raised the intriguing question that cytoplasmic ORC4 plays a role in the separation of the polar bodies from the oocyte. Contrary to common knowledge of ORC4 and its role in DNA licensing, this unusual behavior of ORC4 lead to my focus for my dissertation, which was to explore the new function of this protein and its role in polar body extrusion. In this section, we would like to summarize evidence we observed through our experiments that suggest ORC4 is involved in polar body extrusion, and to speculate on what it means for the cell biology of meiosis. In our initial work using ICC to observe the ORC4 signals, due to the possibility of off-target effect of the antibodies we were unsure that the ORC4 signal is true. To address this, we expressed the ORC4-HIS protein using mouse ORC4 with histidine tag constructs. This result demonstrated that our prior ICC experiments identified ORC4. As mentioned, the ORC4 surrounds the first and second polar bodies. When we induced a pseudo-polar body using inactivated sperm, an ORC4 cage then formed around the sperm chromatin that was expelled (Fig. 3.6, chapter 3). During normal fertilization sperm chromatin does not extrude a polar body because its chromatin must fuse with maternal chromatin for normal development. This is the reason why we did not observe any ORC4 cage-like structure form around the paternal chromosome. It is only when we induce the paternal chromosomes to develop a pseudo-polar body that we observed the formation of this structure. Following with this result, it is clear that the ORC4 cage is associated with the extruded chromatin or PB, however further investigation was needed to understand it role in polar body extrusion. The most direct evidence that the ORC4 cage is required for PBE is that ORC4 peptides that were injected into the oocyte prevented the formation of the ORC4 cage (Fig. 3.8, chapter 3). Future work will be focused on understanding the mechanisms of how the ORC4 cage coordinates PBE and DNA replication.

5.2 Possible mechanisms that ORC4 may act

We have shown that ORC4 has a new function in polar body extrusion; however, the findings from this research are relatively new, and the exact mechanism of ORC4 plays during polar body extrusion is not yet known. With continued efforts, we hope to understand its role. There are some theories we have regarding its mechanism that we believe should be tested to

determine the exact pathway. The mammalian oocyte undergoes two rounds of asymmetric division to generate a large oocyte in addition to two smaller polar bodies. The asymmetric division results from oocyte polarization including cortical polarity, migration, and spindle position. This process is essential for fertilization and maintenance of maternal genetic information in the early stages of embryo development (91). The asymmetric spindle positioning plays a critical role in polar body formation. In each meiotic division, the meiotic spindle has to be positioned on one particular side of the cortex. After GVBD, the meiotic spindle is located near the cell center and migrates towards one side of the cortex shortly after. The meiotic spindle formation is then completed at metaphase I. The spindle migrates to near cortex and arranges itself perpendicular to the cortex prior to anaphase and cytokinesis. The migration of the spindle to the cortex is necessary for asymmetric division. It is followed by the transition of anaphase I to telophase I. In the mature oocyte, the spindle is arrested in metaphase II. Further process will not proceed prior sperm entry (56) (92). During our observation of ORC4 in two meiotic divisions, the ORC4 cage seems to appear at the same time during which spindle transition occurs. The following question is raised: does the ORC4 play a role in spindle positioning? The BFA, a fungal toxin which is used to inhibit Golgi-based membrane vesicle fusion, has been shown to disrupt spindle position in the mature oocyte. When mature oocyte was treated with BFA, the spindle failed to arrest perpendicular position; additionally, the chromosome separated to develop two half-size oocytes without the formation of PB (20). In our work, when we incubated oocyte in the presence of BFA, we found that BFA inhibits the ORC4 cage-like structure from forming (Fig. 3.4, chapter 3) (79). This hinted toward the theory that the ORC4 might play a role in spindle position. However, to understand whether the ORC4 involves in spindle position, more study is required.

The asymmetric divisions rely on the spindle positioning. This process is also induced by the establishment of cortical polarity which is characterized by an actin domain under the control of a myosin ring. At anaphase, the actin domain protrudes, combining with constriction of the myosin ring that leads to the formation of the two polar bodies (24). The mechanism and role of this cortical polarity model are not completely understood. A recent report has shown that the establishment of cortical polarity depends on chromosome signals. Deng and colleagues have shown that the injected sperm head or DNA-coated beads at the cortex of MII oocytes helped to induce a cortical actin cap that is surrounded by a myosin ring (27). These findings suggest that

the cortical cap formation is regulated by chromatin induction based on a distance between chromatin and the cortex. This model is similar to various factors, such as the Ran guanine nucleotide exchange factors (GEF) and Ran GTPase activating protein, that mediate the chromosome signal to the cortex to induce spindle formation (93), (94). A mutant Ran in MII oocyte disrupts cortical polarization (95). In addition to spindle positioning and cortical polarization, the critical involvement of actin in this system is present in several varieties of species ranging from mouse to human (96), (97). During spindle migration, the actin filaments remained associated with spindle and was able to push the spindle toward the cortex (37). These literature may provide us with a possible explanation as to why ORC4 surrounds only one set of chromosome that will be extruded to form PB. Our unpublished data showed that ORC4 disappeared to be associated with DNA at anaphase I and anaphase II when it was extracted with 100 mM NaCl (Fig. 5.1). This demonstrated that ORC4 does not bind directly to DNA at these stages prior DNA synthesis; rather, ORC4 may bind to actin filaments or the meiotic spindle. When the meiotic spindle arrests and migrates to the cortex, actin polarization is induced. We propose that the ORC4 which plays a new function in PBE may follow this actin-based mechanism; however, this would not explain the phenomena of the ORC4 cage formation surrounding extruded chromatin and PB. Dynamic actin networks have a known function in the processes of cortical flows (98), tissue morphogenesis (99), cell migration (100), and cytoplasmic organization (101). These networks are driven by the vesicles that recruit myosin to reorganize actin filaments (65). Schuh and colleagues showed that vesicles, which are positive for the small GTPase Rab11a, function as cytoskeletal modulators. Asymmetric spindle positioning, the morphology and the polarization of the oocyte were affected by deletion of Rab11a-positive vesicles (65). The Rab11a-positive vesicles were found to interact closely with the exocyst, an 8-protein complex modulating budding in yeast and some types of polarized exocytosis in mammalian cells (102). Moreover, PARD6B, a homolog of par-6 genes and a member of aPCK/par polarity complex along with Par3, aPKC, and CDC42, has been shown to play an important role in cell polarity in many cell types (35). PARD6B is first localized on the spindle microtubules and accumulates at the nearest pole where the cortex is located. It was also found to associate with the spindle during spindle migration and to re-localize on the chromosomes (103). Fogelgren's lab reported that the Par complex interacted with the exocyst complex to guide exocyst-mediated trafficking in some cell types (104). These interesting

findings in the literature might help us to understand and continue our future study the mechanism of ORC4 (Fig. 5.2).

5. 3 Future plans

Based on our results, we can conclude that the licensing protein ORC4 is required for polar body extrusion; however, future research should be conducted to help clarify the exact role of ORC4 on PBE.

Firstly, our preliminary data showed that using immunocytochemistry and peptide disruption strongly support the idea that ORC4 is involved in PBE. We also visualized ORC4-GFP and ORC4 labeled with FlAsH studied on live cells, but the excessive brightness of the ORC4-GFP signals proved to be an obstacle in tracking ORC4 cage formation. We are currently in the process of creating a fusion Hisidine protein with ORC4, IRES and GFP protein in the same plasmid (Fig. 5.3) in addition to a transgenic line by using an eGFP (ORC4-His-IRES-GFP) at the C terminus of ORC4. This should not interfere with its role in DNA replication or in ORC4 cage formation. We use the fusion GFP protein that co-expression with ORC4-His to determine whether the ORC4-His-IRES-GFP will be transfected into mouse based on GFP signals, but we plan to use His tags to target ORC4 due to problems previously inherent in the live ORC4-GFP cells. To better understand the role of ORC4, (1) we will create the ORC4-His-IRES-GFP construct under control of the CAG promoter (Fig. 5.3). This plasmid will then be transfected into HEK cells to determine whether over-expression of ORC4 causes harm to cells that will be used to grow in the future. If the cells survive, we will use this construct to express ORC4-His-IRES-GFP in all transgenic mouse cells. This method will be a useful tool for future studies related to the function of the DNA licensing ORC4. If the HEK cells which will be transfected do not survive, we will conclude that the over-expression of ORC4-His-IRES-GFP is lethal. In this case, we will generate a construct ORC4-His-IRES-GFP under control of ZP3 promoter, a recognized promoter for oocyte specific expression. (2) We will create ORC4-GFP transgenic knock-in mice (Fig. 5.3) to insert this eGFP gene into the last exon 14 of the mouse ORC4 which includes 14 exons. By doing this, we will design a CRISPR guide RNA that targets the stop codon of ORC4 that is found after the first 186 bp of exon 14. A donor template will be synthesized containing a GFP gene flanked by homology arms to facilitate homology directed repair and insertion before the ORC4 stop codon. This will result in GFP fusion to the C-terminal end of endogenous ORC4 in which we expect endogenous ORC4-GFP to be expressed at its

normal levels because it is the endogenous gene. Thus it will not over-express to kill cells as ORC4 has known function on DNA replication. This method will be unlikely to harm the oocyte and will enable examination of ORC4 biology on mouse model.

Secondly, an additional direction to take in the future is to determine the mechanism of ORC4 cage formation on mouse model. Yi et al demonstrated that the mechanism of polar body extrusion on mouse is involved in actin located at the site of cytokinesis, but we propose that the mechanism of the ORC4 cage formation might follow another mechanism related to exocyst. As mentioned above, The Rab11a-positive vesicles interact closely with the exocyst and PARD6B is associated with exocyst-mediated trafficking in some cell types (104), while the mutation of sec, made of exocyst, and has been showed to prevent budding on yeast (102). When we tested PARD6B localization on mouse oocytes via ICC, we found that PARD6B has the same localization where ORC4 localization is on the oocyte during anaphase II and G1 stages (Fig. 5.4). This result led us to propose that the mechanism of ORC4 might follows the mechanism of exocyst-mediated trafficking. To prove this, we will carry out some experiments. (1) We will perform ICC of PARD6B and exocyst proteins at meiosis II stage on mouse oocyte. (2) We will also test whether the siRNA-PARD6B and PARD6B peptides inhibit ORC4 cage formation and PBE. (3) Finally, we will determine the role of the exocyst in PBE by knocking out Pard6b and sec10; one of the proteins is necessary for the formation of the exocyst (104).

Finally, our published data found that the ORC4 surrounds the chromatin that will be extruded in both polar bodies during meiotic I and II on mouse oocyte. This suggests that ORC4 might involve in asymmetric cell divisions on other cell types. The most similar cellular process to PBE that we found is the extrusion of the erythrocyte cell's chromatin during the development of the erythroblast cell. Our preliminary data showed that ORC4 was in the cytoplasm of erythroblast and surrounds the ejected nucleus (Fig. 5.5). This led us to hypothesize that the ORC4 cage mechanism is used in other cell types for chromatin expulsion. To prove this, we will carry out two experiments. (1) We will test whether the ORC4 cage forms during chromatin expulsion by erythroblast, and (2) we will determine the role of ORC4 in erythroblast enucleation using transgenic mice study.

The experiments listed here are all future directions in which we plan to take our experiments. I hope to continue this work during my post-doctoral research.

5.4 Contributions

Theoretical design: Hieu Nguyen, Ben Fogelgren, Stefan Moisyadi, Vernadeth Alarcon, and W. Steven Ward

Contributed to writing: Hieu Nguyen

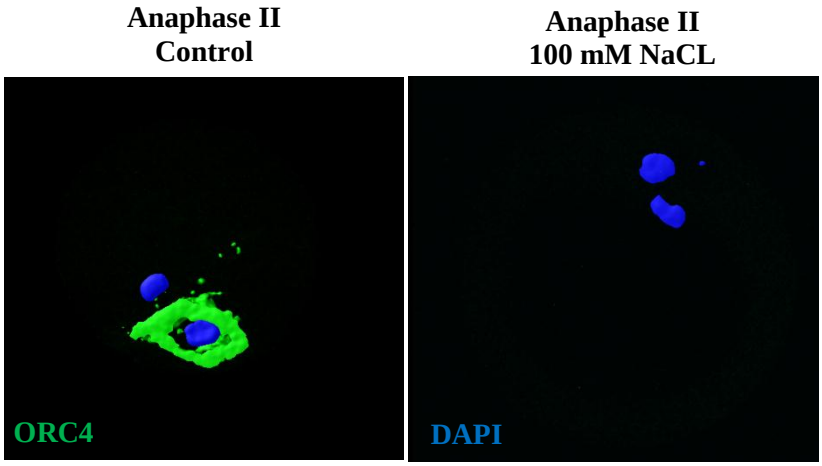

Figure 5.1: ORC4 does not bind directly on DNA at anaphase II. MII oocytes were extracted with 100 mM NaCL to remove soluble ORC4. DAPI (Blue) and ORC4 (Green).

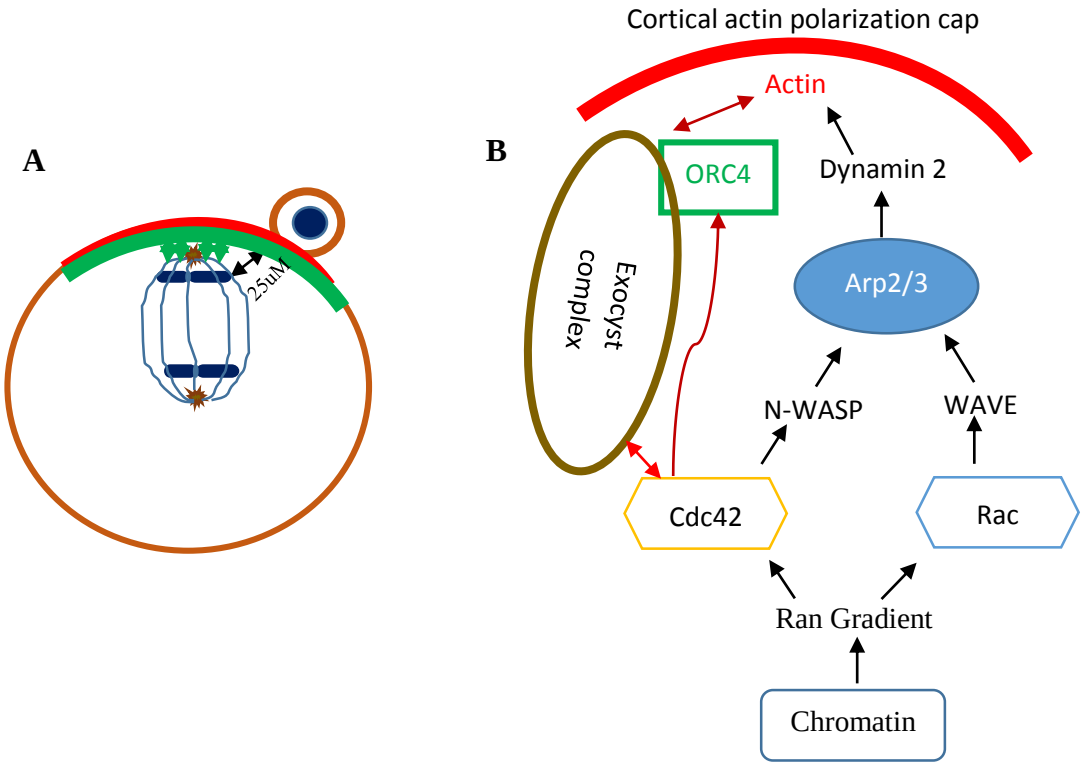

Figure 5.2: A model for ORC4 mechanism in polar body extrusion. (A) A model for Actin and ORC4 interaction in the egg. (B) We suggests that ORC4 may interact with actin via Cdc42 and exocyst complex. Actin (red); ORC4 (green); and Exocyst complex (brown).

Experiment 1: Generation of Transgenic Mice Expressing ORC4-His-GFP

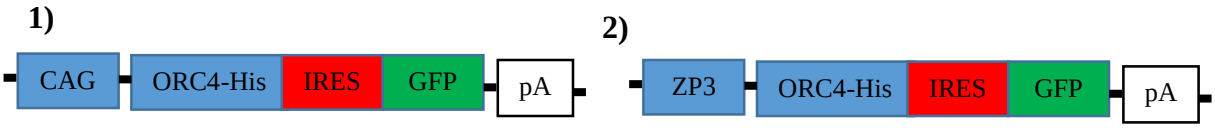

Experiment 2: Generation of Transgenic Mice Expressing Endogenous ORC4-GFP

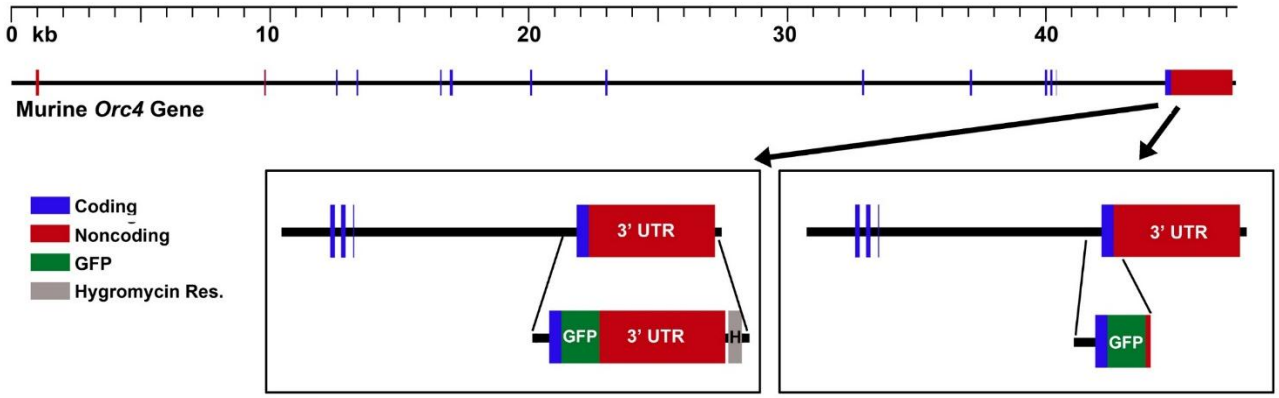

Figure 5.3. Generation of transgenic mouse constructs: In experiment 1, we will generate transgenic mice that overexpress ORC4-His-GFP under control of either the CAG or ZP3 promoters. The full length mRNA-orc4-his fused with eGFP will be transfected into mouse zygotes. In the experiment 2, we will generate transgenic mice that express the endogenous Orc4 fused with eGFP. This construct will knock-in into the last exon of the exon 14th of Orc4 gene.

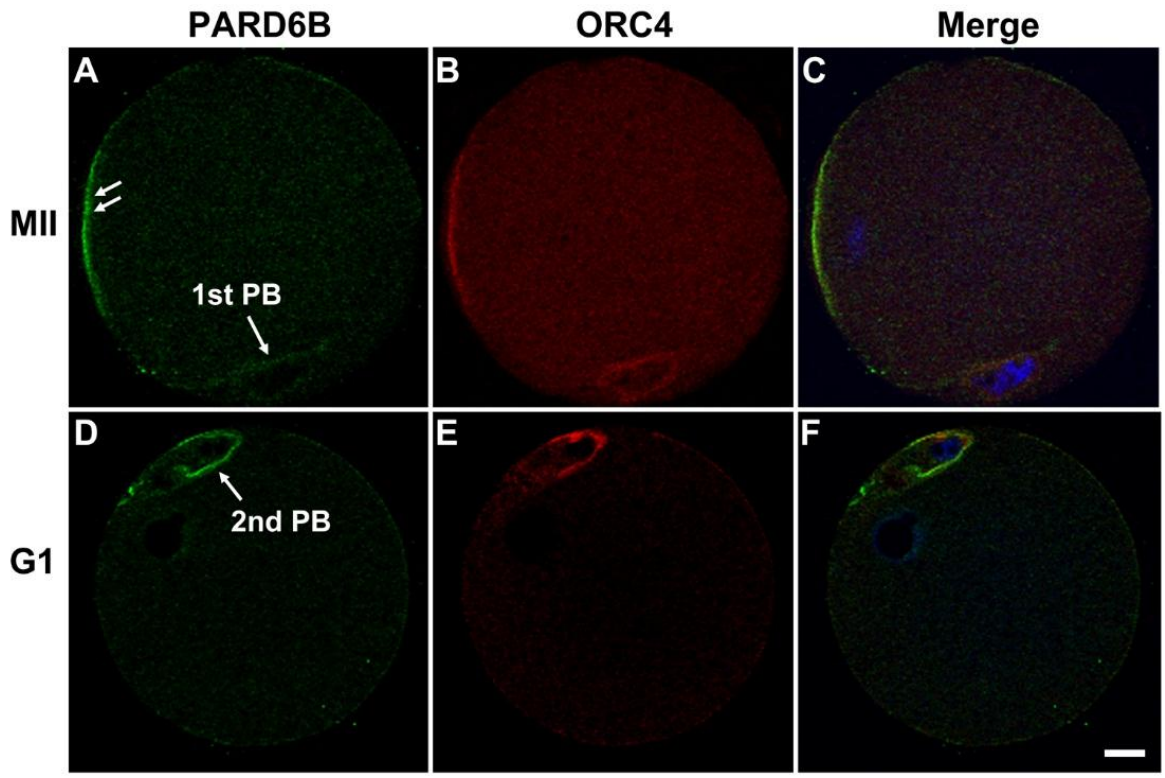

Figure 5.4. PARD6B localization on PBE. An MII oocyte (A-C) and a parthenogenetically activated oocytes (D-F) were stained with PARD6B (green) and ORC4 (red). Both of proteins were found at the site of the cortex where the first and the second polar bodies formed (double arrows). DAPI (Blue). Bar = 10 μm (unpublished data).

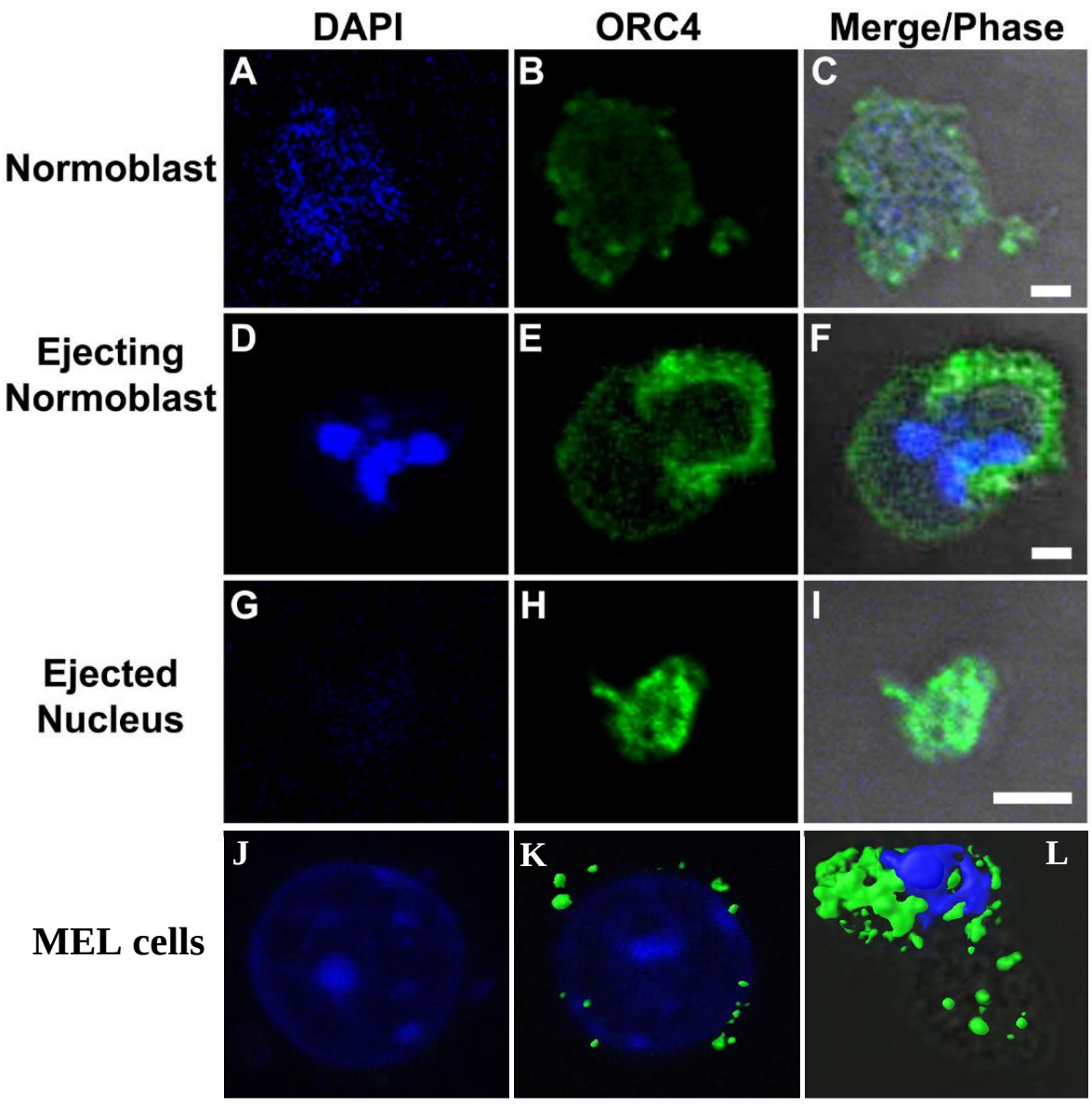

Figure 5.5. ORC4 cage formation on erythroblast chromatin ejection cells. (A-C) Normoblast stage is a stage just before chromatin ejection. (D-F) A normoblast ejecting the chromatin. (G-I) Ejected chromatin capsule. (J) MEL cell. (K-L) Enucleated MEL cell with 15μM Vacuolin-1. Cells were stained with ORC4 (green). DAPI (blue). Bar=2 μm (unpublished data).

REFERENCES

1. Aoki E, Schultz RM. DNA replication in the 1-cell mouse embryo: stimulatory effect of histone acetylation. Zygote. 1999;7(2):165-72.
2. Sonneville R, Querenet M, Craig A, Gartner A, Blow JJ. The dynamics of replication licensing in live Caenorhabditis elegans embryos. The Journal of cell biology. 2012;196(2):233-46. Epub 2012/01/18. doi: jcb.201110080 [pii]10.1083/jcb.201110080. PubMed PMID: 22249291.
3. Yeeles JT, Deegan TD, Janska A, Early A, Diffley JF. Regulated eukaryotic DNA replication origin firing with purified proteins. Nature. 2015;519(7544):431-5. doi: 10.1038/nature14285. PubMed PMID: 25739503.
4. Barlow JH, Nussenzweig A. Replication initiation and genome instability: a crossroads for DNA and RNA synthesis. Cellular and molecular life Sciences. 2014;71(23):4545-59.
5. DePamphilis ML, Blow JJ, Ghosh S, Saha T, Noguchi K, Vassilev A. Regulating the licensing of DNA replication origins in metazoa. Current opinion in cell biology. 2006;18(3):231-9. PubMed PMID: 16650748.
6. Ortega MA, Nguyen H, Ward WS. ORC proteins in the mammalian zygote. Cell and tissue research. 2016;363(1):195-200. doi: 10.1007/s00441-015-2296-3. PubMed PMID: 26453397; PubMed Central PMCID: PMCPMC4703507.
7. Balhorn R, Weston S, Thomas C, Wyrobek AJ. DNA packaging in mouse spermatids. Synthesis of protamine variants and four transition proteins. Experimental cell research. 1984;150(2):298-308.
8. DePamphilis ML. The 'ORC cycle': a novel pathway for regulating eukaryotic DNA replication. Gene. 2003;310:1-15. Epub 2003/06/13. doi: S0378111903005468 [pii]. PubMed PMID: 12801628.
9. Eward KL, Obermann EC, Shreeram S, Loddo M, Fanshawe T, Williams C, Jung HI, Prevost AT, Blow JJ, Stoeber K, Williams GH. DNA replication licensing in somatic and germ cells. Journal of cell science. 2004;117(Pt 24):5875-86. doi: 10.1242/jcs.01503. PubMed PMID: 15522891.
10. Ortega MA, Marh J, Alarcon VB, Ward WS. Unique Pattern of ORC2 and MCM7 Localization During DNA Replication Licensing in the Mouse Zygote. Biology of reproduction. 2012;87:62, 1-9. Epub 2012/06/08. doi: biolreprod.112.101774 [pii]10.1095/biolreprod.112.101774. PubMed PMID: PMID: 22674395 PMCID: PMC3463414.
11. Bicknell LS, Walker S, Klingseisen A, Stiff T, Leitch A, Kerzendorfer C, Martin CA, Yeyati P, Al Sanna N, Bober M, Johnson D, Wise C, Jackson AP, O'Driscoll M, Jeggo PA. Mutations in ORC1, encoding the largest subunit of the origin recognition complex, cause microcephalic primordial dwarfism resembling Meier-Gorlin syndrome. Nature genetics. 2011;43(4):350-5. doi: 10.1038/ng.776. PubMed PMID: 21358633.
12. Lee KY, Bang SW, Yoon SW, Lee SH, Yoon JB, Hwang DS. Phosphorylation of ORC2 protein dissociates origin recognition complex from chromatin and replication origins. The Journal of biological chemistry. 2012;287(15):11891-8. Epub 2012/02/16. doi: M111.338467 [pii]10.1074/jbc.M111.338467. PubMed PMID: 22334659; PubMed Central PMCID: PMC3320937.

13. Cappuccio I, Colapicchioni C, Santangelo V, Sale P, Blandini F, Bonelli M, Niccolini C, Busceti C, Bucci D, Nicoletti F, Melchiorri D. The origin recognition complex subunit, ORC3, is developmentally regulated and supports the expression of biochemical markers of neuronal maturation in cultured cerebellar granule cells. Brain research. 2010;1358:1-10. doi: 10.1016/j.brainres.2010.07.052. PubMed PMID: 20674557.
14. Quintana DG, Hou Z, Thome KC, Hendricks M, Saha P, Dutta A. Identification of HsORC4, a member of the human origin of replication recognition complex. The Journal of biological chemistry. 1997;272(45):28247-51. PubMed PMID: 9353276.
15. Balasov M, Huijbregts RP, Chesnokov I. Functional analysis of an Orc6 mutant in Drosophila. Proceedings of the National Academy of Sciences of the United States of America. 2009;106(26):10672-7. Epub 2009/06/23. doi: 0902670106 [pii]10.1073/pnas.0902670106. PubMed PMID: 19541634; PubMed Central PMCID: PMC2705598.
16. Kusic J, Tomic B, Divac A, Kojic S. Human initiation protein Orc4 prefers triple stranded DNA. Mol Biol Rep. 2010;37(5):2317-22. doi: 10.1007/s11033-009-9735-8. PubMed PMID: 19690980.
17. Nguyen H, Ortega MA, Ko M, Marh J, Ward WS. ORC4 Surrounds Extruded Chromatin in Female Meiosis. J Cell Biochem. 2015;116:778-86. Epub 2014/12/17. doi: 10.1002/jcb.25033. PubMed PMID: PMID: 25502171 PMCID: PMC4355034.
18. Moreno S, Hayles J, Nurse P. Regulation of the cell cycle timing of mitosis. J Cell Sci Suppl. 1989;12:1-8. Epub 1989/01/01. PubMed PMID: 2699733.
19. Alberts B, Johnson A, Lewis J, Raff M, Roberts K, Walter P. Molecular Biology of The Cell. 5 ed. New York NY: Garland Science, Taylor & Francis Group; 2008.
20. Wang L, Wang ZB, Zhang X, FitzHarris G, Baltz JM, Sun QY, Liu XJ. Brefeldin A disrupts asymmetric spindle positioning in mouse oocytes. Developmental biology. 2008;313(1):155-66. Epub 2007/12/07. doi: S0012-1606(07)01433-9 [pii]10.1016/j.ydbio.2007.10.009. PubMed PMID: 18053978.
21. Holt JE, Jones KT. Control of homologous chromosome division in the mammalian oocyte. Molecular human reproduction. 2009;15(3):139-47. doi: 10.1093/molehr/gap007. PubMed PMID: 19179408.
22. Dehapiot B, Carriere V, Carroll J, Halet G. Polarized Cdc42 activation promotes polar body protrusion and asymmetric division in mouse oocytes. Developmental biology. 2013;377(1):202-12. Epub 2013/02/07. doi: S0012-1606(13)00059-6 [pii]10.1016/j.ydbio.2013.01.029. PubMed PMID: 23384564; PubMed Central PMCID: PMC3690527.
23. Perry AC, Verlhac MH. Second meiotic arrest and exit in frogs and mice. EMBO reports. 2008;9(3):246-51. doi: 10.1038/embor.2008.22. PubMed PMID: 18311174; PubMed Central PMCID: PMC2267393.
24. Yi K, Rubinstein B, Li R. Symmetry breaking and polarity establishment during mouse oocyte maturation. Philosophical transactions of the Royal Society of London Series B, Biological sciences. 2013;368(1629):20130002. doi: 10.1098/rstb.2013.0002. PubMed PMID: 24062576; PubMed Central PMCID: PMC3785956.
25. Pollard TD, Cooper JA. Actin, a central player in cell shape and movement. Science. 2009;326(5957):1208-12. doi: 10.1126/science.1175862. PubMed PMID: 19965462; PubMed Central PMCID: PMC3677050.

26. Deng M, Li R. Sperm chromatin-induced ectopic polar body extrusion in mouse eggs after ICSI and delayed egg activation. PloS one. 2009;4(9):e7171. Epub 2009/09/30. doi: 10.1371/journal.pone.0007171. PubMed PMID: 19787051; PubMed Central PMCID: PMC2746308.
27. Deng M, Suraneni P, Schultz RM, Li R. The Ran GTPase mediates chromatin signaling to control cortical polarity during polar body extrusion in mouse oocytes. Developmental cell. 2007;12(2):301-8. Epub 2007/02/06. doi: S1534-5807(06)00513-2 [pii]10.1016/j.devcel.2006.11.008. PubMed PMID: 17276346.
28. Dehapiot B, Halet G. Ran GTPase promotes oocyte polarization by regulating ERM (Ezrin/Radixin/Moesin) inactivation. Cell cycle. 2013;12(11):1672-8. doi: 10.4161/cc.24901. PubMed PMID: 23656777; PubMed Central PMCID: PMC3713125.
29. Halet G, Carroll J. Rac activity is polarized and regulates meiotic spindle stability and anchoring in mammalian oocytes. Developmental cell. 2007;12(2):309-17. doi: 10.1016/j.devcel.2006.12.010. PubMed PMID: 17276347.
30. Rohatgi R, Ma L, Miki H, Lopez M, Kirchhausen T, Takenawa T, Kirschner MW. The interaction between N-WASP and the Arp2/3 complex links Cdc42-dependent signals to actin assembly. Cell. 1999;97(2):221-31. PubMed PMID: 10219243.
31. Sun SC, Wang ZB, Xu YN, Lee SE, Cui XS, Kim NH. Arp2/3 complex regulates asymmetric division and cytokinesis in mouse oocytes. PloS one. 2011;6(4):e18392. doi: 10.1371/journal.pone.0018392. PubMed PMID: 21494665; PubMed Central PMCID: PMC3072972.
32. Wang QC, Liu J, Duan X, Cui XS, Kim NH, Xiong B, Sun SC. The Dynamin 2 inhibitor Dynasore affects the actin filament distribution during mouse early embryo development. The Journal of reproduction and development. 2015;61(1):49-53. doi: 10.1262/jrd.2014-079. PubMed PMID: 25421092; PubMed Central PMCID: PMC4354231.
33. Wei Y, Zhang T, Wang YP, Schatten H, Sun QY. Polar bodies in assisted reproductive technology: current progress and future perspectives. Biology of reproduction. 2015;92(1):19. doi: 10.1095/biolreprod.114.125575. PubMed PMID: 25472922.
34. Poulton J, Chiaratti MR, Meirelles FV, Kennedy S, Wells D, Holt IJ. Transmission of mitochondrial DNA diseases and ways to prevent them. PLoS genetics. 2010;6(8). doi: 10.1371/journal.pgen.1001066. PubMed PMID: 20711358; PubMed Central PMCID: PMC2920841 diseases. Preimplantation genetic diagnosis will be available in the near future. JP takes clinical and diagnostic referrals for the Oxford Centre in the Rare Mitochondrial Disorders Service for Adults and Children (NCG). Further information may be found on http://www.obs-gyn.ox.ac.uk/research/Poulton.
35. Leblanc J, Zhang X, McKee D, Wang ZB, Li R, Ma C, Sun QY, Liu XJ. The small GTPase Cdc42 promotes membrane protrusion during polar body emission via ARP2-nucleated actin polymerization. Molecular human reproduction. 2011;17(5):305-16. doi: 10.1093/molehr/gar026. PubMed PMID: 21511720.
36. Pfender S, Kuznetsov V, Pleiser S, Kerkhoff E, Schuh M. Spire-type actin nucleators cooperate with Formin-2 to drive asymmetric oocyte division. Current biology : CB. 2011;21(11):955-60. doi: 10.1016/j.cub.2011.04.029. PubMed PMID: 21620703; PubMed Central PMCID: PMC3128265.
37. Yi K, Li R. Actin cytoskeleton in cell polarity and asymmetric division during mouse oocyte maturation. Cytoskeleton. 2012;69(10):727-37. doi: 10.1002/cm.21048. PubMed PMID: 22753278.

38. DePamphilis ML. Cell cycle dependent regulation of the origin recognition complex. Cell cycle. 2005;4(1):70-9. PubMed PMID: 15611627.
39. Thomae AW, Pich D, Brocher J, Spindler MP, Berens C, Hock R, Hammerschmidt W, Schepers A. Interaction between HMGA1a and the origin recognition complex creates site-specific replication origins. Proceedings of the National Academy of Sciences of the United States of America. 2008;105(5):1692-7. PubMed PMID: 18234858.
40. Krude T. Initiation of chromosomal DNA replication in mammalian cell-free systems. Cell cycle. 2006;5(18):2115-22. PubMed PMID: 16969109.
41. Takeda DY, Dutta A. DNA replication and progression through S phase. Oncogene. 2005;24(17):2827-43. PubMed PMID: 15838518.
42. Scholefield G, Veening JW, Murray H. DnaA and ORC: more than DNA replication initiators. Trends Cell Biol. 2011;21(3):188-94. Epub 2010/12/03. doi: S0962-8924(10)00235-7 [pii]10.1016/j.tcb.2010.10.006. PubMed PMID: 21123069.
43. Li H, Stillman B. The origin recognition complex: a biochemical and structural view. Sub-cellular biochemistry. 2012;62:37-58. Epub 2012/08/25. doi: 10.1007/978-94-007-4572-8_3. PubMed PMID: 22918579; PubMed Central PMCID: PMC3779782.
44. Springer J, Kneissl M, Putter V, Grummt F. Identification and characterization of MmORC4 and MmORC5, two subunits of the mouse origin of replication recognition complex. Chromosoma. 1999;108(4):243-9. Epub 1999/08/25. doi: 91080243.412 [pii]. PubMed PMID: 10460412.
45. Springer J, Nanda I, Hoehn K, Schmid M, Grummt F. Identification and chromosomal localization of murine ORC3, a new member of the mouse origin recognition complex. Cytogenet Cell Genet. 1999;87(3-4):245-51. Epub 2000/03/07. doi: 15435 [pii]15435. PubMed PMID: 10702681.
46. Kneissl M, Putter V, Szalay AA, Grummt F. Interaction and assembly of murine pre-replicative complex proteins in yeast and mouse cells. J Mol Biol. 2003;327(1):111-28. Epub 2003/03/05. doi: S0022283603000792 [pii]. PubMed PMID: 12614612.
47. Dhar SK, Yoshida K, Machida Y, Khaira P, Chaudhuri B, Wohlschlegel JA, Leffak M, Yates J, Dutta A. Replication from oriP of Epstein-Barr virus requires human ORC and is inhibited by geminin. Cell. 2001;106(3):287-96. Epub 2001/08/18. doi: S0092-8674(01)00458-5 [pii]. PubMed PMID: 11509178.
48. Vashee S, Simancek P, Challberg MD, Kelly TJ. Assembly of the human origin recognition complex. The Journal of biological chemistry. 2001;276(28):26666-73. Epub 2001/04/27. doi: 10.1074/jbc.M102493200M102493200 [pii]. PubMed PMID: 11323433.
49. Ghosh S, Vassilev AP, Zhang J, Zhao Y, DePamphilis ML. Assembly of the human origin recognition complex occurs through independent nuclear localization of its components. The Journal of biological chemistry. 2011;286(27):23831-41. Epub 2011/05/11. doi: M110.215988 [pii]10.1074/jbc.M110.215988. PubMed PMID: 21555516; PubMed Central PMCID: PMC3129165.
50. Nordman J, Orr-Weaver TL. Regulation of DNA replication during development. Development. 2012;139(3):455-64. Epub 2012/01/10. doi: 139/3/455 [pii]10.1242/dev.061838. PubMed PMID: 22223677; PubMed Central PMCID: PMC3252349.

51. Sasaki T, Gilbert DM. The many faces of the origin recognition complex. Current opinion in cell biology. 2007;19(3):337-43. Epub 2007/05/01. doi: S0955-0674(07)00059-2 [pii]10.1016/j.ceb.2007.04.007. PubMed PMID: 17466500.

52. Kimura Y, Yanagimachi R. Intracytoplasmic sperm injection in the mouse. Biology of reproduction. 1995;52(4):709-20.

53. Prasanth SG, Prasanth KV, Siddiqui K, Spector DL, Stillman B. Human Orc2 localizes to centrosomes, centromeres and heterochromatin during chromosome inheritance. The EMBO journal. 2004;23(13):2651-63. Epub 2004/06/25. doi: 10.1038/sj.emboj.76002557600255 [pii]. PubMed PMID: 15215892; PubMed Central PMCID: PMC449767.

54. Pflumm MF, Botchan MR. Orc mutants arrest in metaphase with abnormally condensed chromosomes. Development. 2001;128(9):1697-707. Epub 2001/04/06. PubMed PMID: 11290306.

55. Chen Z, Speck C, Wendel P, Tang C, Stillman B, Li H. The architecture of the DNA replication origin recognition complex in Saccharomyces cerevisiae. Proceedings of the National Academy of Sciences of the United States of America. 2008;105(30):10326-31. Epub 2008/07/24. doi: 0803829105 [pii]10.1073/pnas.0803829105. PubMed PMID: 18647841; PubMed Central PMCID: PMC2480615.

56. Maro B, Verlhac MH. Polar body formation: new rules for asymmetric divisions. Nature cell biology. 2002;4(12):E281-3. Epub 2002/12/04. doi: 10.1038/ncb1202-e281ncb1202-e281 [pii]. PubMed PMID: 12461532.

57. Maro B, Johnson MH, Webb M, Flach G. Mechanism of polar body formation in the mouse oocyte: an interaction between the chromosomes, the cytoskeleton and the plasma membrane. J Embryol Exp Morphol. 1986;92:11-32. Epub 1986/03/01. PubMed PMID: 3723057.

58. Longo FJ, Chen DY. Development of cortical polarity in mouse eggs: involvement of the meiotic apparatus. Developmental biology. 1985;107(2):382-94. Epub 1985/02/01. doi: 0012-1606(85)90320-3 [pii]. PubMed PMID: 4038667.

59. Leader B, Lim H, Carabatsos MJ, Harrington A, Ecsedy J, Pellman D, Maas R, Leder P. Formin-2, polyploidy, hypofertility and positioning of the meiotic spindle in mouse oocytes. Nature cell biology. 2002;4(12):921-8. Epub 2002/11/26. doi: 10.1038/ncb880ncb880 [pii]. PubMed PMID: 12447394.

60. Yamauchi Y, Shaman JA, Boaz SM, Ward WS. Paternal Pronuclear DNA Degradation Is Functionally Linked to DNA Replication in Mouse Oocytes. Biology of reproduction. 2007;77:407-15. PubMed PMID: PMID: 17494913.

61. Usui N, Ogura A, Kimura Y, Yanagimachi R. Sperm nuclear envelope: breakdown of intrinsic envelope and de novo formation in hamster oocytes or eggs. Zygote. 1997;5(1):35-46.

62. Chuang RY, Kelly TJ. The fission yeast homologue of Orc4p binds to replication origin DNA via multiple AT-hooks. Proceedings of the National Academy of Sciences of the United States of America. 1999;96(6):2656-61. Epub 1999/03/17. PubMed PMID: 10077566; PubMed Central PMCID: PMC15824.

63. A D, R R, A J, H M, S S. Recurrent Patellar Instabilty Culminating in a Vertically Rotated and a Locked Patellar Dislocation - A Rare Entity. Journal of orthopaedic case

reports. 2016;6(2):95-7. doi: 10.13107/jocr.2250-0685.456. PubMed PMID: 27703948; PubMed Central PMCID: PMC5040587.

64. Schuh M, Ellenberg J. Self-organization of MTOCs replaces centrosome function during acentrosomal spindle assembly in live mouse oocytes. Cell. 2007;130(3):484-98. Epub 2007/08/19. doi: S0092-8674(07)00792-1 [pii]10.1016/j.cell.2007.06.025. PubMed PMID: 17693257.

65. Holubcova Z, Howard G, Schuh M. Vesicles modulate an actin network for asymmetric spindle positioning. Nature cell biology. 2013;15(8):937-47. Epub 2013/07/23. doi: ncb2802 [pii]10.1038/ncb2802. PubMed PMID: 23873150; PubMed Central PMCID: PMC3797517.

66. Wakayama T, Hayashi Y, Ogura A. Participation of the female pronucleus derived from the second polar body in full embryonic development of mice. Journal of reproduction and fertility. 1997;110(2):263-6. Epub 1997/07/01. PubMed PMID: 9306980.

67. Wakayama T, Yanagimachi R. The first polar body can be used for the production of normal offspring in mice. Biology of reproduction. 1998;59(1):100-4. Epub 1998/07/23. PubMed PMID: 9674999.

68. Takeda DY, Shibata Y, Parvin JD, Dutta A. Recruitment of ORC or CDC6 to DNA is sufficient to create an artificial origin of replication in mammalian cells. Genes & development. 2005;19(23):2827-36. PubMed PMID: 16322558.

69. Mohar I, Szczygiel MA, Yanagimachi R, Ward WS. Sperm Nuclear Halos Can Transform Into Normal Chromosomes After Injection Into Oocytes. Molecular reproduction and development. 2002;62:416-20. PubMed PMID: PMID: 12112607.

70. Szczygiel M, Yanagimachi R. Intracytoplasmic sperm injection. In: Nagy A, Gertsenstein M, Vintersten K, Behringer R, editors. Manipulation of the Mouse Embryo - A Laboratory Manual. New York: Cold Spring Harbor Laboratory Press 2003. p. 585-97.

71. Yamauchi Y, Riel JM, Ward MA. Paternal DNA damage resulting from various sperm treatments persists after fertilization and is similar before and after DNA replication. Journal of andrology. 2012;33(2):229-38. Epub 2011/05/07. doi: jandrol.111.013532 [pii]10.2164/jandrol.111.013532. PubMed PMID: 21546611; PubMed Central PMCID: PMC3331785.

72. Nishioka N, Inoue K, Adachi K, Kiyonari H, Ota M, Ralston A, Yabuta N, Hirahara S, Stephenson RO, Ogonuki N, Makita R, Kurihara H, Morin-Kensicki EM, Nojima H, Rossant J, Nakao K, Niwa H, Sasaki H. The Hippo signaling pathway components Lats and Yap pattern Tead4 activity to distinguish mouse trophectoderm from inner cell mass. Developmental cell. 2009;16(3):398-410. doi: 10.1016/j.devcel.2009.02.003. PubMed PMID: 19289085.

73. Diez-Roux G, Banfi S, Sultan M, Geffers L, Anand S, Rozado D, Magen A, Canidio E, Pagani M, Peluso I, Lin-Marq N, Koch M, Bilio M, Cantiello I, Verde R, De Masi C, Bianchi SA, Cicchini J, Perroud E, Mehmeti S, Dagand E, Schrinner S, Nurnberger A, Schmidt K, Metz K, Zwingmann C, Brieske N, Springer C, Hernandez AM, Herzog S, Grabbe F, Sieverding C, Fischer B, Schrader K, Brockmeyer M, Dettmer S, Helbig C, Alunni V, Battaini MA, Mura C, Henrichsen CN, Garcia-Lopez R, Echevarria D, Puelles E, Garcia-Calero E, Kruse S, Uhr M, Kauck C, Feng G, Milyaev N, Ong CK, Kumar L, Lam M, Semple CA, Gyenesei A, Mundlos S, Radelof U, Lehrach H, Sarmientos P, Reymond A, Davidson DR, Dolle P, Antonarakis SE, Yaspo ML, Martinez S, Baldock

RA, Eichele G, Ballabio A. A high-resolution anatomical atlas of the transcriptome in the mouse embryo. PLoS biology. 2011;9(1):e1000582. doi: 10.1371/journal.pbio.1000582. PubMed PMID: 21267068; PubMed Central PMCID: PMCPMC3022534.
74. Longo FJ. Reorganization of the egg surface at fertilization. Int Rev Cytol. 1988;113:233-69. PubMed PMID: 3068182.
75. Jedrusik A, Ajduk A, Pomorski P, Maleszewski M. Mouse oocytes fertilised by ICSI during in vitro maturation retain the ability to be activated after refertilisation in metaphase II and can generate Ca2+ oscillations. BMC Dev Biol. 2007;7:72. Epub 2007/06/23. doi: 1471-213X-7-72 [pii]10.1186/1471-213X-7-72. PubMed PMID: 17584490; PubMed Central PMCID: PMC1913504.
76. Stefanovic D, Kusic J, Divac A, Tomic B. Formation of noncanonical DNA structures mediated by human ORC4, a protein component of the origin recognition complex. Biochemistry. 2008;47(33):8760-7. doi: 10.1021/bi800684f. PubMed PMID: 18652488.
77. Ji P, Jayapal SR, Lodish HF. Enucleation of cultured mouse fetal erythroblasts requires Rac GTPases and mDia2. Nature cell biology. 2008;10(3):314-21. doi: 10.1038/ncb1693. PubMed PMID: 18264091.
78. Keerthivasan G, Small S, Liu H, Wickrema A, Crispino JD. Vesicle trafficking plays a novel role in erythroblast enucleation. Blood. 2010;116(17):3331-40. doi: 10.1182/blood-2010-03-277426. PubMed PMID: 20644112; PubMed Central PMCID: PMCPMC2995360.
79. Nguyen H, James NG, Nguyen L, Nguyen TP, Vuong C, Ortega MA, Jameson DM, Ward WS. Higher order oligomerization of the licensing ORC4 protein is required for polar body extrusion in murine meiosis. J Cell Biochem. 2017;In Press. doi: 10.1002/jcb.25949. PubMed PMID: 28230328.
80. Hinde E, Digman MA, Hahn KM, Gratton E. Millisecond spatiotemporal dynamics of FRET biosensors by the pair correlation function and the phasor approach to FLIM. Proceedings of the National Academy of Sciences of the United States of America. 2013;110(1):135-40. doi: 10.1073/pnas.1211882110. PubMed PMID: 23248275; PubMed Central PMCID: PMC3538204.
81. Byers CE, Barylko B, Ross JA, Southworth DR, James NG, Taylor CAt, Wang L, Collins KA, Estrada A, Waung M, Tassin TC, Huber KM, Jameson DM, Albanesi JP. Enhancement of dynamin polymerization and GTPase activity by Arc/Arg3.1. Biochimica et biophysica acta. 2015;1850(6):1310-8. doi: 10.1016/j.bbagen.2015.03.002. PubMed PMID: 25783003; PubMed Central PMCID: PMC4398645.
82. Jameson DM, Ross JA, Albanesi JP. Fluorescence fluctuation spectroscopy: ushering in a new age of enlightenment for cellular dynamics. Biophysical reviews. 2009;1(3):105-18. doi: 10.1007/s12551-009-0013-8. PubMed PMID: 21547245; PubMed Central PMCID: PMC3086800.
83. Nienhaus G, Wiedenmann J. Structure, dynamics and optical properties of fluorescent proteins: perspectives for marker development. Chemphyschem. 2009;10(9-10): 1369-79.
84. Lelek M, Di Nunzio F, Zimmer C. FlAsH-PALM: super-resolution pointillist imaging with FlAsH-tetracysteine labeling. Mrthods Mol Biol. 2014;1171:183-93.
85. Jameson DM, James NG, Albanesi JP. Fluorescence fluctuation spectroscopy approaches to the study of receptors in live cells. Methods in enzymology. 2013;519:87-113. doi: 10.1016/B978-0-12-405539-1.00003-8. PubMed PMID: 23280108.

86. Adams S, Tsien R. Preparation of the membrane-permeant biarsenicals FlAsH-EDT2 and ReAsH-EDT2 for fluorescent labeling of tetracysteine-tagged proteins. Nat Protoc. 2008;3(9):1527-34.
87. Balzarotti F, Eilers Y, Gwosch KC, Gynna AH, Westphal V, Stefani FD, Elf J, Hell SW. Nanometer resolution imaging and tracking of fluorescent molecules with minimal photon fluxes. Science. 2017;355(6325):606-12. doi: 10.1126/science.aak9913. PubMed PMID: 28008086.
88. Levi V, Gratton E. Exploring dynamics in living cells by tracking single particles. Cell biochemistry and biophysics. 2007;48(1):1-15. PubMed PMID: 17703064.
89. Ranjit S, Dvornikov A, Dobrinskikh E, Wang X, Luo Y, Levi M, Gratton E. Measuring the effect of a Western diet on liver tissue architecture by FLIM autofluorescence and harmonic generation microscopy. Biomedical optics express. 2017;8(7):3143-54. doi: 10.1364/BOE.8.003143. PubMed PMID: 28717559; PubMed Central PMCID: PMC5508820.
90. Arcangeli C, Yu W, Cannistraro S, Gratton E. Two-photon autofluorescence microscopy and spectroscopy of Antarctic fungus: new approach for studying effects of UV-B irradiation. Biopolymers. 2000;57(4):218-25. doi: 10.1002/1097-0282(2000)57:4<218::AID-BIP3>3.0.CO;2-G. PubMed PMID: 10861386.
91. Sun SC, Kim NH. Molecular mechanisms of asymmetric division in oocytes. Microscopy and microanalysis : the official journal of Microscopy Society of America, Microbeam Analysis Society, Microscopical Society of Canada. 2013;19(4):883-97. doi: 10.1017/S1431927613001566. PubMed PMID: 23764118.
92. Kim HC, Jo YJ, Kim NH, Namgoong S. Small molecule inhibitor of formin homology 2 domains (SMIFH2) reveals the roles of the formin family of proteins in spindle assembly and asymmetric division in mouse oocytes. PloS one. 2015;10(4):e0123438. doi: 10.1371/journal.pone.0123438. PubMed PMID: 25837661; PubMed Central PMCID: PMC4383420.
93. Kalab P, Heald R. The RanGTP gradient - a GPS for the mitotic spindle. Journal of cell science. 2008;121(Pt 10):1577-86. doi: 10.1242/jcs.005959. PubMed PMID: 18469014.
94. Caudron M, Bunt G, Bastiaens P, Karsenti E. Spatial coordination of spindle assembly by chromosome-mediated signaling gradients. Science. 2005;309(5739):1373-6. doi: 10.1126/science.1115964. PubMed PMID: 16123300.
95. Yi K, Unruh JR, Deng M, Slaughter BD, Rubinstein B, Li R. Dynamic maintenance of asymmetric meiotic spindle position through Arp2/3-complex-driven cytoplasmic streaming in mouse oocytes. Nature cell biology. 2011;13(10):1252-8. doi: 10.1038/ncb2320. PubMed PMID: 21874009; PubMed Central PMCID: PMC3523671.
96. Kim E, Miller CJ, Reisler E. Polymerization and in vitro motility properties of yeast actin: a comparison with rabbit skeletal alpha-actin. Biochemistry. 1996;35(51):16566-72. doi: 10.1021/bi9623892. PubMed PMID: 8987991.
97. Tremoleda JL, Schoevers EJ, Stout TA, Colenbrander B, Bevers MM. Organisation of the cytoskeleton during in vitro maturation of horse oocytes. Molecular reproduction and development. 2001;60(2):260-9. doi: 10.1002/mrd.1086. PubMed PMID: 11553927.
98. Munro E, Nance J, Priess JR. Cortical flows powered by asymmetrical contraction transport PAR proteins to establish and maintain anterior-posterior polarity in the early C. elegans embryo. Developmental cell. 2004;7(3):413-24. doi: 10.1016/j.devcel.2004.08.001. PubMed PMID: 15363415.

99. Lecuit T, Lenne PF, Munro E. Force generation, transmission, and integration during cell and tissue morphogenesis. Annual review of cell and developmental biology. 2011;27:157-84. doi: 10.1146/annurev-cellbio-100109-104027. PubMed PMID: 21740231.
100. Gardel ML, Schneider IC, Aratyn-Schaus Y, Waterman CM. Mechanical integration of actin and adhesion dynamics in cell migration. Annual review of cell and developmental biology. 2010;26:315-33. doi: 10.1146/annurev.cellbio.011209.122036. PubMed PMID: 19575647; PubMed Central PMCID: PMC4437624.
101. Field CM, Lenart P. Bulk cytoplasmic actin and its functions in meiosis and mitosis. Current biology : CB. 2011;21(19):R825-30. doi: 10.1016/j.cub.2011.07.043. PubMed PMID: 21996509.
102. Pleskot R, Cwiklik L, Jungwirth P, Zarsky V, Potocky M. Membrane targeting of the yeast exocyst complex. Biochimica et biophysica acta. 2015;1848(7):1481-9. doi: 10.1016/j.bbamem.2015.03.026. PubMed PMID: 25838123.
103. Vinot S, Le T, Maro B, Louvet-Vallee S. Two PAR6 proteins become asymmetrically localized during establishment of polarity in mouse oocytes. Current biology : CB. 2004;14(6):520-5. doi: 10.1016/j.cub.2004.02.061. PubMed PMID: 15043819.
104. Polgar N, Lee AJ, Lui VH, Napoli JA, Fogelgren B. The exocyst gene Sec10 regulates renal epithelial monolayer homeostasis and apoptotic sensitivity. American journal of physiology Cell physiology. 2015;309(3):C190-201. doi: 10.1152/ajpcell.00011.2015. PubMed PMID: 26040895; PubMed Central PMCID: PMC4525081.